이학박사학위논문

Bioinformatic Study of Microbes in Aquatic Environment using DNA metabarcoding

DNA metabarcoding을 이용한 수생환경에서의 생물정보학적 연구

2020년 **8**월

서울대학교 대학원

생명과학부

김 희 수

Bioinformatic Study of microbes in Aquatic Environment using DNA metabarcoding

DNA metabarcoding을 이용한 수생환경에서의 생물정보학적 연구

지도교수 김 원

이 논문을 이학박사 학위논문으로 제출함

2020년 7월

서울대학교 대학원

생명과학부

김 희 수

김희수의 이학박사 학위논문을 인준함

2020년 7월

위 원 장 이건수 (인)

부 위 원 장 김 원 (인)

위 원 원 정영운 (인)

위 원 원 이상구 (인)

위 원 원 오승윤

Bioinformatic Study of microbes in Aquatic Environment using DNA metabarcoding

A dissertation submitted in partial fulfillment
of the requirement for the degree of

DOCTOR OF PHILOSOPHY
TO THE FACULTY OF THE
SCHOOL OF BIOLOGICAL SCIENCE
at
SEOUL NATIONAL UNIVERSITY
by

Heesoo Kim

Date Approved:
24 June 2020

Abstract

Bioinformatic Study of Microbes in Aquatic Environment using DNA metabarcoding

Heesoo Kim
School of Biological Sciences
The Graduate School
Seoul National University

The development of next-generation sequencing technology has led to the advent of DNA metabarcoding that identify many organisms in the mixture or environmental samples at once. This approach enables the efficient acquisition of large amounts of biological data, and has the ability to evaluate the biodiversity and community structure of ecosystems. With the importance of DNA metabarcoding recognized, many research projects are already actively underway in other countries.

However, compared with the research trends of DNA metabarcoding around the world, researches of DNA metabarcoding in Korea are more basic and limited in scope. This

dissertation reports three case studies of the aquatic environments that were conducted using DNA metabarcoding to compensate for the drawbacks of domestic research trends in DNA metabarcoding. The final objective of this study is to apply DNA metabarcoding approach to various case studies in aquatic environments. Based on this, it is to understand and explain the biological phenomena of aquatic environments with metadata produced DNA metabarcoding. Each chapter of the dissertation was organized according to the case study.

In Chapter 1, DNA metabarcoding was newly applied along with the traditional morphological identification to establish a method for zooplankton community survey in the Marine and Coastal National Park areas of Korea. By comparing the results of these two identification methods, the strengths and limitations of DNA metabarcoding were verified with the zooplankton communities appearing in these areas. The sensitive detection capability of DNA metabarcoding enabled the identification of potential bioindicator taxa associated with external factors in these national parks. I propose the use of metabarcoding for efficient surveys of mesozooplankton communities in the Marine and Coastal National Parks to establish monitoring of bioindicator taxa. It is also necessary to continuously search for taxa with high research value in these national parks using metabarcoding. Establishing an ongoing monitoring system that employs this approach can provide an effective tool for managing marine ecosystems in the Marine and Coastal National Parks.

In Chapter 2, the association between family of crabs and feeding behavior on their intestinal microbiomes of Korean crabs was confirmed using DNA metabarcoding. With the metadata of the intestinal microbiome in the crabs, the controversial phylogenetic

relationship between the superfamilies Ocypodoidea and Grapsoidea was newly interpreted. It was confirmed that the intestinal microbiome differed according to the family of crabs and specific microbial operational taxonomic units (OTUs) related to the evolution of Malacostraca were indentified. Intestinal microbial biodiversity and community were found to differ according to the feeding behavior. The function and role of intestinal microbiomes associated with the feeding behavior were predicted. These results were inferred to be related to the type of food available to hosts and its nutritional characteristics.

In Chapter 3, as a case study, microeukaryotic biodiversity and community structures of car bonnet and pig carcass were investigated to determine the applicability of DNA metabarcoding in drowning case. Pig carcass was used to simulate the decomposing process of drowning bodies. As a control, car bonnet was used to confirm the general process of succession occurring in aquatic environments. Using DNA metabarcoding, I confirmed that the microeukaryotic biodiversity in pig carcass was relevantly lower than that in car bonnet. Also, some taxa were related to the decomposition. The relative abundances of these taxa varied with the decomposition period. It is expected that the change pattern of these taxa may be used as a good indicator for estimating the postmortem submersion interval (PMSI) of drowning cases.

This dissertation includes manuscripts that were submitted to peer-reviewed journals during my Ph.D. course.

Key words: DNA metabarcoding, biodiversity, community structure, mesozooplankton, bioindicator, crab, intestinal microbiome, postmortem submersion interval, drowning

Student number: 2016-27480

Contents

List of Figures

List of Tables

General introduction

General introduction

DNA barcoding, which was proposed and standardized by Hebert *et al.* (2003), is being used as an essential tool for identifying species (Cristescu, 2014). The principle of DNA barcoding is to identify species of organisms precisely through short DNA sequences in a manner similar to barcodes at convenience stores. Because the target gene regions for each kingdom are well established, DNA barcodes as a short sequence allow for relatively fast and accurate species identification (e.g., cytochrome oxidase c subunit I (COI) – animals; nuclear internal transcribed spacer (ITS) – fungi; rbcL and matK chloroplast genes – plants) (Hebert *et al.*, 2003; Group *et al.*, 2009; Schoch *et al.*, 2012; Kress *et al.*, 2015; Shokralla *et al.*, 2015). With these standardized markers, voucher sequences were extracted from morphologically identified specimens, which were then collected to establish public DNA barcode databases (e.g., BoLD) (Ratnasingham and Hebert, 2007; Comtet *et al.*, 2015). The deployment of these databases laid the foundation on which DNA barcoding could be applied to various fields of biology (Wallace *et al.*, 2012; Decaëns *et al.*, 2013; Dormontt *et al.*, 2018). However, DNA barcoding faces several constraints. Sanger sequencing for obtaining DNA barcodes demands a relatively high concentration and high-quality DNA template (Polz and Cavanaugh, 1998). This characteristic makes it difficult to acquire sequence data for old specimens (Van Houdt *et al.*, 2010). In a similar vein, it is not possible to use DNA barcoding from bulk samples that are contaminated or mixed. Using DNA barcoding, a single sequence can be obtained from a single sample. Given the fact that most species around the world have not been found (86% of existing species on Earth), the establishment of a complete DNA barcode database also seems to require sequence data of

organisms in highly diversified environmental samples (Janzen *et al.*, 2009; Mora *et al.*, 2011; Shokralla *et al.*, 2015). In the field of ecology, in particular, DNA barcoding can only provide taxonomic aspects of making a list of species that exist in the ecosystem. These limitations have been addressed to some extent by the development of next-generation sequencing (NGS) technology (Coissac *et al.*, 2012).

With the development of NGS technology since the 2000s, large quantities of sequence data can be produced simultaneously. Sanger sequencing produces up to 96 reads in a single run. However, in case of Illumina MiSeq sequencing, which is mainly used for DNA metabarcoding, up to 25 million sequences can be obtained at a time (Unno, 2015). These high-throughput DNA sequencing technology has further upgraded DNA-based research methods. DNA metabarcoding was devised to identify various taxa in a mixed or environmental sample. It allows large amounts of biological data to be obtained quickly at a relatively low cost and has the potential to enable the assessment of biodiversity and community structure in ecosystems (Taberlet *et al.*, 2012a; Taberlet *et al.*, 2012b; Thomsen *et al.*, 2012; Yoccoz *et al.*, 2012; Cristescu, 2014; Valentini *et al.*, 2016).

As the importance of DNA metabarcoding has been recognized, many research projects are already actively underway in other countries. In 2007, the National Institutes of Health (NIH) established the Human Microbiome Project (HMP) to form the largest pan-national-level research group. The research team established standardized pipelines to analyze and explain the correlations between human health and disease by identifying all the microbes present in humans and their specific functions using metagenomics (Gevers *et al.*, 2012). The Earth Microbiome Project (EMP) is also an international project for identifying microbial communities in environmental samples throughout the globe,

including seawater, soil, and sewage. This research group also presented standardized protocols and bioinformatics analysis methods (Gilbert *et al.*, 2014). Using standardized protocols and analysis methods based on these projects, large-scale studies using DNA metabarcoding are being conducted across the entire field of biology. Especially in the ecology and forensic fields related to this dissertation, DNA metabarcoding is applied to wide range of studies such as environmental monitoring, diet analysis, detection of illegal trade, and food fraud (Yang *et al.*, 2014; Ruppert *et al.*, 2019). However, compared with the research trends of DNA metabarcoding worldwide, researches in Korea are more basic and limited in scope.

This dissertation reports three case studies of the aquatic environments that were conducted using DNA metabarcoding to compensate for the drawbacks of domestic research trends in DNA metabarcoding. The final objective of this study is to apply DNA metabarcoding approach to various case studies in aquatic environments. Based on this, it is to understand and explain the biological phenomena of aquatic environments with metadata produced DNA metabarcoding. Each chapter of the dissertation was organized according to the case study. In Chapter 1, DNA metabarcoding was newly applied along with the traditional morphological identification to establish a method for zooplankton community survey in the Marine and Coastal National Park areas of Korea. By comparing the results of these two identification methods, the strengths and limitations of metabarcoding were verified with the zooplankton communities appearing in these areas. Based on this results, I discussed the potential of metabarcoding analysis as an efficient method to monitor the zooplankton community in the Marine and Coastal National Park areas. In Chapter 2, the association between family of crabs and feeding behavior on their

intestinal microbiomes of Korean crabs was confirmed using DNA metabarcoding. With the metadata of intestinal microbiome in the Korean crabs, biodiversity and community structure were compared according to the family of crabs and the feeding groups. Based on the intestinal microbiome data, the families, as well as the controversial phylogenetic relationship between the superfamilies Ocypodoidea and Grapsoidea, were observed from a new perspective. In addition, the functional profile was predicted in the intestinal microbiome and the roles of the intestinal microbes that significantly affect their family of crabs and their feeding behavior was inferred. In Chapter 3, biodiversity and microeukaryotic community structures of car bonnet and pig carcass were investigated to determine the applicability of DNA metabarcoding in drowning cases. To assume the drowning case, a drowning experiment was carried out in a reservoir with pig and car bonnet. Pig carcass was used to simulate the decomposing process of drowning bodies. As a control, car bonnet was used to confirm the general process of succession occurring in aquatic environments. Through these results, I determined whether biodiversity and community structure of microeukaryotes could be used to infer PMSI for drowning cases. The general contents of each chapter were tabulated (Table 1).

Table 1. Summary of each chapter in the dissertation.

	Chapter1	Chapter2	Chapter3
Target organism	Mesozooplankton	Intestinal microbes	Microeukaryotes
Target region	18S rDNA v8-v9	16S rDNA v4	18S rDNA v1-v2
Purpose	▪ Verifying the strengths and limitations of metabarcoding by comparing the results with those obtained by morphological identification. ▪ Identifying bioindicator taxa associated with spatial and environmental characteristics based on the metabarcoding analysis.	▪ Investigating the association between intestinal microbiomes and family of crabs, feeding behavior. ▪ Interpreting phylogenetic relationship between superfamilies Ocypodoidea and Grapsoidea using intestinal microbiome data. ▪ Identification of microbes associated with the divergence of crabs ▪ Predicting the function and role of intestinal microbiome related to the family of crabs and feeding behavior.	▪ Confirming the correlation between decomposition and biodiversity ▪ Detecting aquatic organisms related to the decomposition ▪ Identifying potential indicator organisms for determining PMSI depending on the decomposition period.
Final objective	▪ Applying DNA metabarcoding approach to various case studies in aquatic environments ▪ Understanding and explaining biological phenomena of aquatic environments with metadata produced DNA metabarcoding		

Chapter 1

Biodiversity and community structure of mesozooplankton in the Marine and Coastal National Park areas of Korea

1.1 Introduction

Marine ecosystems are changing as a result of global climate change and industrialization in coastal areas. Unlike terrestrial ecosystems, marine ecosystems can be difficult to access and are influenced by a unique set of external factors, including the degree of light transmission, oxygen concentration, water masses, currents, and salinity, which complicate assessments and predictions. As marine ecosystems change, bioindicators respond by changing their morphological or cellular structure, metabolic processes, behaviors, and communities (Bortone *et al.*, 1989; Bongers and Ferris, 1999; Sánchez *et al.*, 2000). Due to these characteristics, studying bioindicators that can confirm and monitor the changes in the marine ecosystem is becoming important worldwide (Kuklina *et al.*, 2013; Parmar *et al.*, 2016).

Zooplankton represent the primary and secondary consumers in the aquatic food chain and are some of the most abundant and ubiquitous taxa in aquatic ecosystems (Richardson, 2008; Ward *et al.*, 2012; Pochon *et al.*, 2013). The spatial and temporal distribution of zooplankton communities fluctuate in response to environmental changes in marine ecosystems, such as variations in temperature and salinity (Sabatés *et al.*, 1989; Purushothama *et al.*, 2011). Therefore, zooplankton are useful bioindicators for detecting environmental changes in the marine ecosystem (Zheng and Li, 1989; Hsieh *et al.*, 2004; Thierstein *et al.*, 2004; Casé *et al.*, 2008; Chen *et al.*, 2011; Chen and Liu, 2015). However, the investigation of zooplankton communities using traditional morphological identification requires high taxonomic knowledge as well as considerable time and labor (Sawaya *et al.*, 2019). Additionally, it can be difficult to identify the lowest taxonomic

ranks (i.e., genus and species) as some zooplankton have ambiguous morphological characteristics, particularly in the larval stages (Heimeier *et al.*, 2010). The development of next-generation sequencing (NGS) technology led to the advent of DNA metabarcoding, a method that can quickly and simultaneously detect any taxa within the database (Rusch *et al.*, 2007; Caporaso *et al.*, 2012). Thus, large-scale marine ecological surveys were made possible with bulk-sample DNA metabarcoding (Taberlet *et al.*, 2012b; Bucklin *et al.*, 2016; Dormontt *et al.*, 2018; Adamowicz *et al.*, 2019). As these advantages were revealed, many researchers conducted comparative studies to confirm that DNA metabarcoding was effective for ecological surveys when compared to traditional morphological identification. Most previous studies report that DNA metabarcoding detects more taxa than morphological identification methods. Additionally, differences in communities can be distinguished and identified more efficiently. However, it is still difficult to achieve accurate biodiversity and species composition surveys with DNA metabarcoding because of the potential for distortion of species abundance as a result of technical biases and false negatives (Cowart *et al.*, 2015; Zimmermann *et al.*, 2015; Clare *et al.*, 2016; Kim *et al.*, 2019; Serrana *et al.*, 2019).

The national parks of South Korea are designated as regions that represent the natural ecosystems or the natural and cultural landscapes of Korea. According to the Korea National Park Service website (http://www.knps.or.kr), a total of 22 national parks have been designated in South Korea. Among these, only four are marine and coastal national parks. Taeanhaean National Park and the Byeonsan-bando National Park, are situated along the Yellow Sea coast. Dadohaehaesang National Park includes areas of both the Yellow Sea coast and Southern Sea coast of Korea and Hallyeohaesang National Park is located on

the Southern Sea coast of Korea. The Marine and Coastal National Parks aim to preserve the valuable and highly diverse ecosystems within them. As such, ecological study and efficient management of the Marine and Coastal National Parks are essential.

In this chapter, DNA metabarcoding was newly applied along with traditional morphological identification to establish a method for zooplankton community surveys in the Marine and Coastal National Park areas of Korea. Mesozooplankton (>200 μm) were selected as the target organisms because there were many previous studies conducted using regular zooplankton surveys at the Marine and Coastal National Park areas, thus allowing for comparison of the identification results of DNA metabarcoding with those of morphological identification. The mesozooplankton communities in the Marine and Coastal National Park areas were compared and analyzed according to sea area and location because the two areas (Yellow Sea and Southern Sea of Korea) and four locations (Taean, Byeonsan, Dadohae, and Hallyeo areas) included representative diverse marine environments with variations in depth, topography, effects of currents, and inflow of freshwater (Pang and Hyun, 1998; Cheng *et al.*, 2004; Go *et al.*, 2009). The main objective of this study was to perform a DNA metabarcoding analysis of the biodiversity and community structure of mesozooplankton communities in the Marine and Coastal National Park areas. First, I verified the strengths and limitations of DNA metabarcoding by comparing the results with those obtained by morphological identification. Second, bioindicator taxa associated with spatial and environmental characteristics were identified based on the DNA metabarcoding analysis. Finally, I discussed the potential of DNA metabarcoding analysis as an efficient method to monitor the zooplankton community.

1.2 Materials and Methods

Mesozooplankton samples and spatial and environmental data collection

Mesozooplankton samples were obtained from a spring season survey during "A Survey on Marine Ecosystems of the Marine and Coastal National Park Areas of Korea" conducted by the Marine Research Center of the Korea National Park Service from May to June 2019.

Sampling was conducted at 58 sampling stations, including the sampling stations in the four Marine and Coastal National Parks and adjacent sea areas (Figure 1). The sampling points consisted of one to four points depending on the location of each district, and the distance between the points was at least 10 km in consideration of the velocity of tidal current (https://www.knps.or.kr/). All sampling stations were designated categories according to the sea area and location. The study area was divided into two sea areas and four locations (Taean, Byeonsan, Dadohae, and Hallyeo areas) based on the standard line drawn at 225° from Haenamgak (34°17'33.09" N, 126°31'26.02" E) of the Korea Hydrographic and Oceanographic Agency and areas under the jurisdictions in the Marine and Coastal National Parks, respectively. A 200 μm mesh conical net with a 60 cm diameter mouth was lowered vertically to the bottom of each sampling station and then raised at a rate of 1 m/s. A flowmeter (Hydrobios, 438115) was attached to the entrance of the net to measure the amount of seawater filtered. Sampling was performed in duplicate at each sampling point; one of the obtained samples was stored in 4% formalin solution for morphological identification and the other in 99% ethanol for DNA extraction and molecular identification.

Spatial and environmental data were also obtained to verify the relationships with the zooplankton community structure and distribution (Appendix 2). At each sampling station, spatial data were obtained using longitude and latitude data from a global positioning system (GPS). Environmental parameters, such as water temperature and salinity, and depth were measured at each sampling station using a SBE 9plus conductivity-temperature-depth (CTD) instrument (Sea-Bird Electronics Inc., Bellevue, Washington, USA). Chlorophyll samples were collected at each sampling station by filtering both the surface and benthic seawater through glass fiber filters (GF/F; Ø 25 mm, pore size 0.7 μm, Whatman, Maidstone, England) for chlorophyll *a* analysis. The filter papers were then placed in light-resistant containers with 90% acetone and frozen until the chlorophyll *a* was extracted. The extracted chlorophyll samples were transferred to test tubes, and chlorophyll *a* concentration measured using a fluorophotometer (10AU, Turner Designs, Sunnyvale, CA, USA). The environmental variables at each sampling station were measured from the surface to the benthic layer and then averaged.

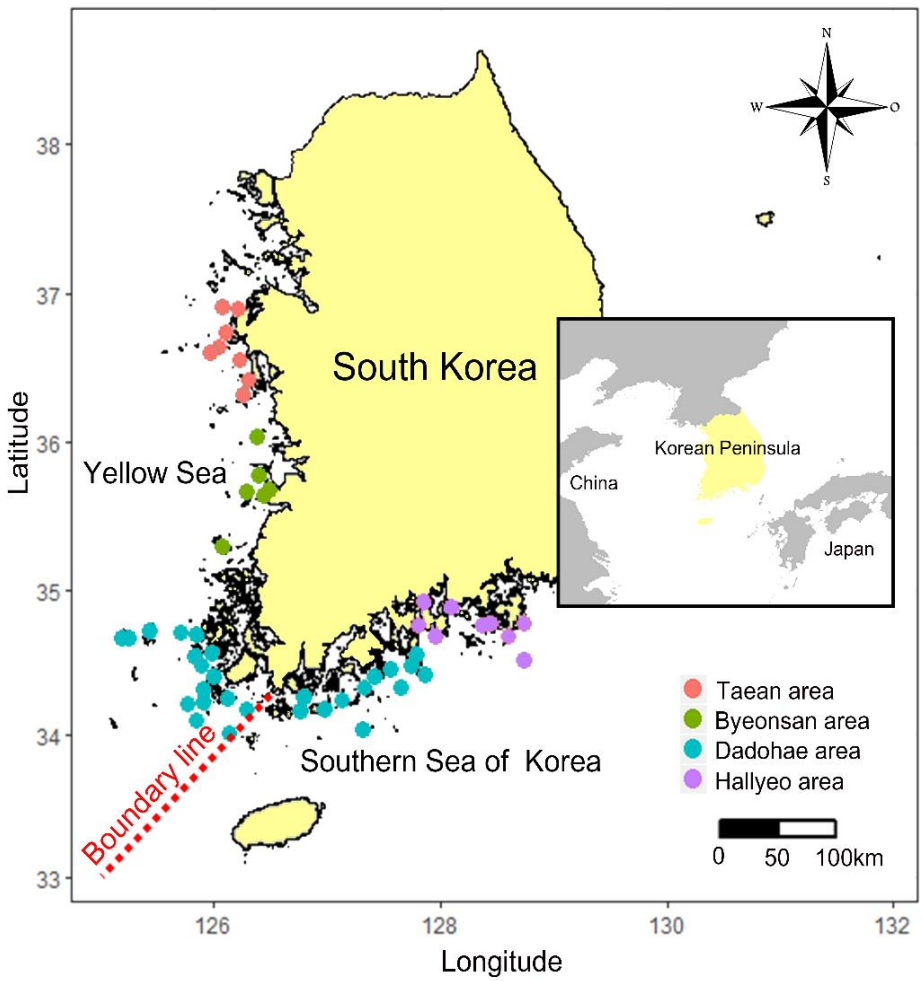

Figure 1. Sampling stations in Marine and Coastal National Park areas of Korea.

Morphological identification and DNA metabarcoding process

Formalin-fixed mesozooplankton samples were transported to the laboratory for species identification and counting. In the laboratory, mesozooplankton samples were divided into subsamples of 500 - 1,000 individuals using a Folsom zooplankton splitter. Each subsample was counted and identified in a Bogorov counting chamber under a Leica M165C stereomicroscope (Leica Microsystems, Wetzlar, Germany). Taxonomy experts identified most of the copepods to the species level but some individuals that were difficult to identify at the species level were classified to the lowest possible taxonomic level (Appendix 3).

The samples for DNA extraction were vortexed at maximum speed and then centrifuged for 5 min at 13,000 rpm. Subsequently, the supernatant was removed and incubated at room temperature until ethanol had completely evaporated. DNA was extracted from the pellets using a Qiagen DNeasy Blood & Tissue Kit (Qiagen, Valencia, CA, USA) following the manufacturer's instructions. In the last step, each eluted DNA sample was recombined according to the sampling station. Three PCR replicates were performed for DNA amplification and each DNA sample was diluted by 1:10. I chose a primer set to target the V9 region of the 18S ribosomal DNA, because it has the ability to detect the whole of zooplankton communities. Also, it is one of the most commonly used to investigate zooplankton using DNA metabarcoding (Amaral-Zettler *et al.*, 2009; Pearman *et al.*, 2014; De Vargas *et al.*, 2015; Albaina *et al.*, 2016; Bucklin *et al.*, 2016; Abad *et al.*, 2017; Djurhuus *et al.*, 2018; Stefanni *et al.*, 2018). The 18S ribosomal DNA (rDNA) V9 variable region was amplified using the 1391F (5′-GTACACACCGCCCGTC-3′) and EukBr (5′-TGATCCTTCTGCAGGTTCACCTAC-3′) primers (Amaral-Zettler *et*

al., 2009). The PCR amplification was performed as follows: 3 min at 94°C, 35 cycles of 45 s at 94°C, 45 s at 65°C, 30 s at 57°C, and a final extension step of 10 min at 72°C. The amplified PCR products were confirmed via electrophoresis and pooled together for each sample. The amplified PCR products were then purified using the QIAquick PCR Purification Kit (Qiagen, Valencia, CA, USA) and paired-end sequencing was performed at Macrogen Inc. (Seoul, Korea) on the Illumina MiSeq platform.

The 18S rDNA sequencing data produced by Illumina MiSeq was analyzed using the custom python script "DNA_metabarcoding_analysis.py" based on the Querial Insights Into Microbial Ecology (QIIME) v 1.9.1. (Caporaso *et al.*, 2010) (Appendix 1). Forward and reverse sequences were concatenated into one read using PEAR with the default parameters (Zhang *et al.*, 2013). Short (< 200 bp) or low-quality assembled reads (Q < 30) were discarded and only the assembled reads were included in the bioinformatics analysis. Detection of chimeric sequences and operational taxonomic unit (OTU) clustering were performed using VSEARCH (Rognes *et al.*, 2016). Chimeric sequences and singleton sequences were excluded from the analysis. All OTUs were clustered with 97% similarity and the most abundant sequence was selected in each OTU. These representative sequences were assigned taxonomic information by comparing the 18S rDNA eukaryotic database from the NCBI GenBank parsed using Biopython (http://www.biopython.org). In cases where the assigned taxonomic information of OTUs was unclear (e.g., uncultured/environmental sample sequences), it was inferred with the taxonomic information of the closest assigned species, considering lowest similarity thresholds for copepod taxonomic resolution (more than 96% for identification to family level; 85% or

more to phlyum level) (Wu *et al.*, 2015). To revise the number of reads distorted by the technical bias problem, rarefaction for biodiversity analysis was conducted considering a minimum number of reads.

All bioinformatics and statistical analyses were conducted and visualized with plots using ggplot2, Phyloseq, ggplot2, vegan, pairwise Adonis, dunn.test, rcompanion, and ade4 packages in R v 3.5.1 (Dray *et al.*, 2007; Oksanen *et al.*, 2007; McMurdie and Holmes, 2013; Team, 2014; Wickham, 2016; Dinno and Dinno, 2017; Mangiafico and Mangiafico, 2017; Martinez Arbizu, 2017). All p-value adjustments were applied as the false discovery rate (FDR) (Benjamini and Hochberg, 1995). Taxonomic information and species counts (read counts) obtained using the morphological identification and DNA metabarcoding were converted to Biological Observation Matrix (BIOM) format for the analysis of biodiversity and community structure, respectively. The indices of richness (observed species (OTUs) and Chao1), diversity (Shannon's diversity), and evenness (equitability) for each BIOM file were calculated using QIIME script (alpha_diversity.py). Statistical significances in the biodiversity indices for the sea area variables were determined by the Wilcoxon rank sum test. The Kruskal-Wallis test and pairwise comparisons were conducted to identify significant differences among the location variables, with the Dunn's test as a post hoc test.

To examine the differences between mesozooplankton community structures, the unweighted pair group method with arithmetic averages (UPGMA) was analyzed based on Bray-Curtis dissimilarities. To test the similarity in the zooplankton community structure identified by the two methods, two UPGMA cluster trees were compared with formed

zooplankton communities. Procrustes analysis was conducted with 1,000 permutations using the protest function. Constrained analysis of principal coordinates (CAP) was also performed to identify the relationships between zooplankton community structures and the following categories: sea area (Yellow Sea and Southern Sea of Korea), location (Taean, Byeonsan, Dadohae, and Hallyeo areas), and spatial, environmental variables (latitude, longitude, water temperature, salinity, and chlorophyll *a* concentration). Statistical differences from the CAP analysis and among community structures were evaluated using ANOVA and the pairwise Adonis with the test of 999 random permutations, respectively. The taxonomic compositions of the mesozooplankton communities identified with the two methods were compared based on the phylum level and the most frequently detected family level.

1.3 Results

Environmental characteristics in the Marine and Coastal National Park areas in Korea

During the survey period, the environmental data collected from of the Marine and Coastal National Park areas were compared according to the sea area and location (Table 2). Among the sampling stations, the average water temperature was higher in the Southern Sea of Korea than the Yellow Sea. The salinity of the Taean and Byeonsan areas was lower than that of Dadohae and Hallyeo areas. The average chlorophyll *a* concentration in the Yellow Sea was higher compared with that in the Southern Sea of Korea. The average depth was the greatest in the Hallyeo area and the lowest in the Byeonsan area. The deepest individual sampling point was N2 (76.05 m) in the Dadohae area and the shallowest was H2 (3.29 m) in the Dadohae area.

Mesozooplankton biodiversity analysis

I performed a comparison between the number of species identified by the morphological identification and the number of OTUs based on the similarities of sequences in DNA metabarcoding (Table 3). This is an indirect comparison because the 97% similarity distance measures used for the OTU clustering have insufficient resolution to distinguish between zooplankton species. With morphological identification, a total of 79 taxa were identified in mesozooplankton samples from the Marine and Coastal National Park areas. Fifty-five taxa were found in the Yellow Sea, 73 taxa were found in the Southern Sea of Korea, and 52 taxa were shared by both sea areas. The number of taxa identified in each

location was as follows: 37 in the Taean area, 30 in the Byeonsan area, 57 in the Dadohae area, and 61 in the Hallyeo area. Using Illumina MiSeq sequencing, 18S rDNA sequencing data were produced from 51 of the 58 mesozooplankton samples. A total of 15,108,829 zooplankton sequences were obtained and after filtration and elimination of low quality and chimeric sequences, 6,201,616 sequences remained. There were 629 OTUs detected in the Yellow Sea and 728 OTUs in the Southern Sea of Korea. Of these, 476 OTUs were present in both sea areas. For the location variables, the number of OTUs detected was 336 in the Taean area, 244 in the Byeonsan area, 730 in the Dadohae area, and 522 in the Hallyeo area. All Good's coverage values for all 18S rDNA sequencing data were greater than 0.99, which means that there is a sufficient number of sequences for all zooplankton samples. In taxonomic categorical ranks, morphological identification identified of 10 phyla, 18 classes, 27 orders, 36 families, and 43 genera of zooplankton individuals; DNA metabarcoding detected 20 phyla, 38 classes, 86 orders, 187 families, and 230 genera of zooplankton individuals.

The biodiversity indices were compared by sea area and location (Figures 2 and 3, Tables 4 and 5). The results of morphological identification and DNA metabarcoding showed similar pattern in biodiversity indices according to the sea area. Although the diversity indices calculated from the two methods were slightly different, the richness and evenness of the zooplankton communities were the same (Figure 2, and Table 4). In contrast, the pattern of all biodiversity indices calculated among locations was completely different when using the morphological identification and DNA metabarcoding (Figure 3, and Table 5). The zooplankton richness of the Hallyeo area using the morphological identification

was high compared to other areas but when the DNA metabarcoding approach was used, there were no statistical differences among locations. Comparing the diversity indices and evenness of zooplankton between the two methods, these biodiversity indices were distinctly lower in the Byeonsan area than the Dadohae area when calculated using the morphological identification results. However, these biodiversity indices calculated using DNA metabarcoding were significantly higher in the Hallyeo area than the Dadohae area.

Table 2. Average water temperature, salinity, chlorophyll *a* concentration, and depth according to the sea area and location in the Marine and Coastal National Park areas of Korea. The average values of the environmental variables according to the sea area are presented as means with standard deviation.

Sea area / Location	Water temperature	Salinity	Chlorophyll *a*	Depth
Yellow Sea	13.25 (1.94)	32.35 (0.80)	1.77 (1.28)	24.86 (18.44)
Southern Sea of Korea	17.39 (1.86)	33.30 (0.66)	0.87 (0.47)	25.00 (18.03)
Taean area	12.13 (1.80)	31.79 (0.08)	1.57 (0.80)	21.73 (20.12)
Byeonsan area	15.56 (0.99)	31.64 (0.17)	3.31 (1.36)	13.16 (3.89)
Dadohae area	14.94 (2.64)	33.05 (0.77)	1.18 (0.95)	26.74 (16.65)
Hallyeo area	17.94 (1.31)	33.44 (0.39)	0.84 (0.29)	29.0 (23.78)

Table 3. The number of taxa analyzed by morphological identification and DNA metabarcoding with mesozooplankton samples collected in the Marine and Coastal National Park areas of Korea.

Variables		Morphological identification	DNA metabarcoding
Sea area	Yellow Sea	55	629
	Southern Sea of Korea	73	728
Location	Taean area	37	336
	Byeonsan area	30	244
	Dadohae area	57	730
	Hallyeo area	61	522
Taxonomic rank	Phylum	10	20
	Class	18	38
	Order	27	86
	Family	36	187
	Genus	43	230

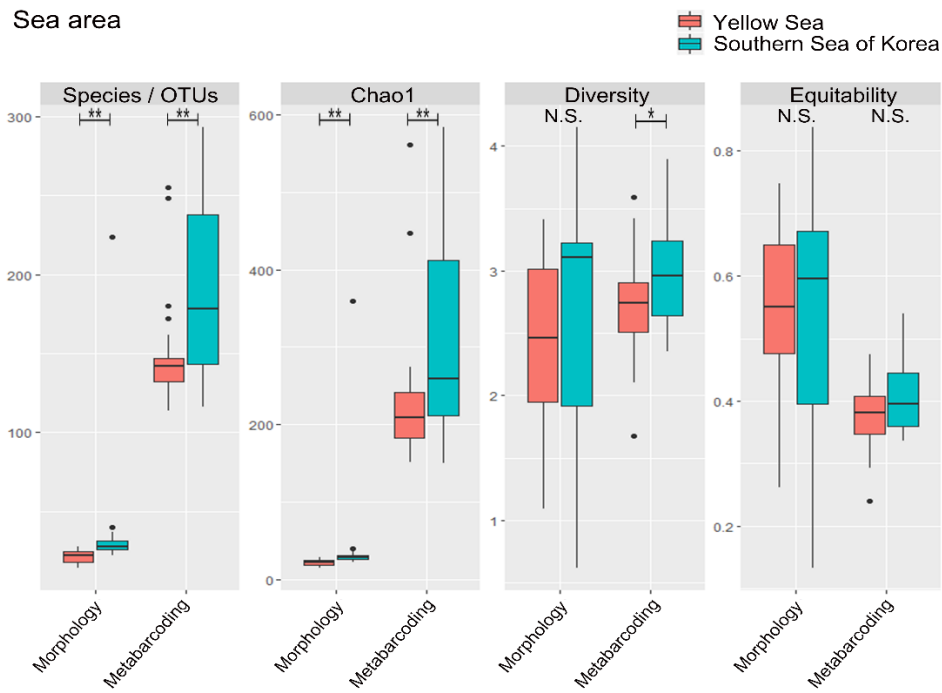

Figure 2. Boxplots for the mesozooplankton biodiversity indices were calculated using morphological identification and DNA metabarcoding results according to the sea area. Statistical differences in the biodiversity indices according to the sea area were calculated using the Wilcoxon rank sum test. As a post hoc analysis, all p-values were corrected using the Benjamini-Hochberg procedure (** $P < 0.01$, * $P < 0.05$, N.S. no significance).

Table 4. Statistical differences in zooplankton biodiversity according to sea area between morphological identification and DNA metabarcoding. Statistical significances in biodiversity indices for sea area variables were calculated with the Wilcoxon rank sum test. All P-value adjustments were applied as False Discovery Rate (FDR) suggested by Benjamini-Hochberg (**: P < 0.01, *: P < 0.05, N.S.: no significance).

Method	Biodiversity index	Post hoc test	adjusted *P*	Significance
Morphological identification	Species	Yellow Sea - Southern Sea of Korea	< 0.001	**
	Chao1	Yellow Sea - Southern Sea of Korea	< 0.001	**
	Shannon's diversity	Yellow Sea - Southern Sea of Korea	0.280	
	equitability	Yellow Sea - Southern Sea of Korea	0.870	
DNA metabarcoding	OTUs	Yellow Sea - Southern Sea of Korea	< 0.001	**
	Chao1	Yellow Sea - Southern Sea of Korea	< 0.001	**
	Shannon's diversity	Yellow Sea - Southern Sea of Korea	0.020	*
	equitability	Yellow Sea - Southern Sea of Korea	0.180	

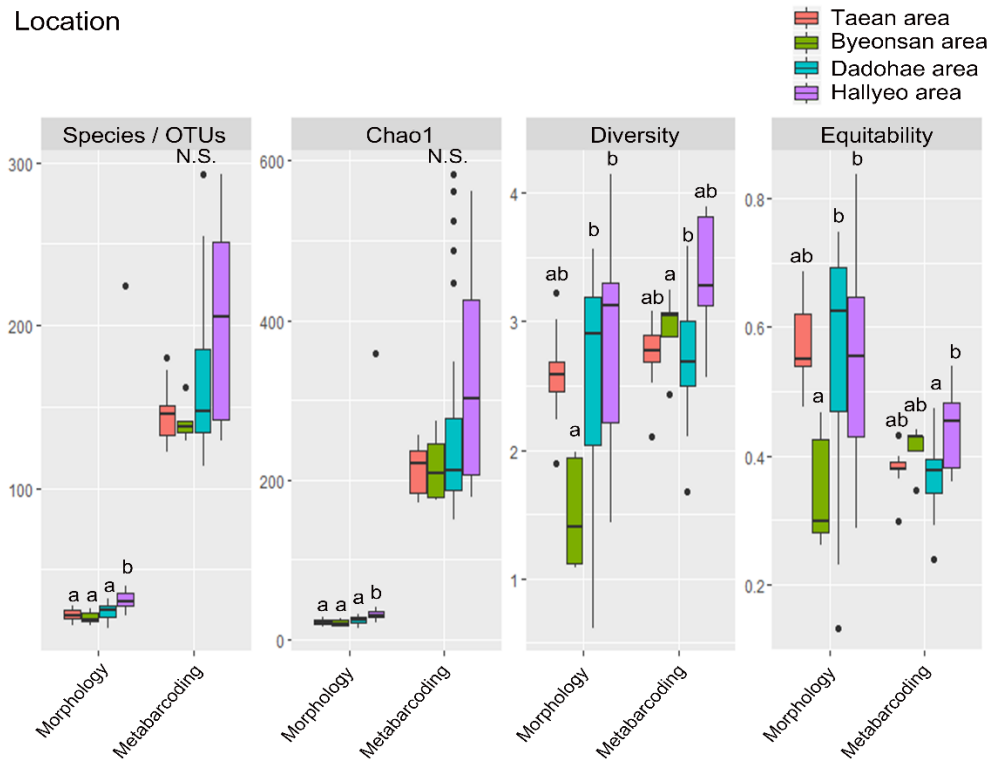

Figure 3. Boxplots for the mesozooplankton biodiversity indices were calculated using morphological identification and DNA metabarcoding results according to the location. The significances of biodiversity indices were calculated using the Kruskal-Wallis test. As a post hoc analysis, pairwise comparisons were conducted using Dunn's test. The results for Dunn's test were marked using the same letter for values that were not significantly different from each other (N.S. no significance).

Table 5. Statistical differences in zooplankton biodiversity according to the location between morphological identification and DNA metabarcoding. Statistical values among location variables were calculated with Kruskal-Wallis and pairwise comparisons were performed using Dunn's test, as a post hoc test. All P-value adjustments were applied as False Discovery Rate (FDR) suggested by Benjamini-Hochberg (**: $P < 0.01$, *: $P < 0.05$, N.S.: no significance).

Method	Biodiversity index	Pairwise comparison	adjusted *P*	Significance
Morphological identification	Species ($P < 0.01$)	Taean area - Byeonsan area	0.567	N.S.
		Taean area - Dadohae area	0.298	N.S.
		Taean area - Hallyeo area	0.013	*
		Byeonsan area - Dadohae area	0.175	N.S.
		Byeonsan area - Hallyeo area	0.017	*
		Dadohae area - Hallyeo area	0.036	*
	Chao1 ($P < 0.01$)	Taean area - Byeonsan area	0.567	N.S.
		Taean area - Dadohae area	0.298	N.S.
		Taean area - Hallyeo area	0.013	*
		Byeonsan area - Dadohae area	0.175	N.S.
		Byeonsan area - Hallyeo area	0.017	*
		Dadohae area - Hallyeo area	0.036	*
	Shannon's diversity ($P < 0.05$)	Taean area - Byeonsan area	0.064	N.S.
		Taean area - Dadohae area	0.735	N.S.
		Taean area - Hallyeo area	0.868	N.S.
		Byeonsan area - Dadohae area	0.038	*
		Byeonsan area - Hallyeo area	0.027	*
		Dadohae area - Hallyeo area	0.877	N.S.
	equitability ($P < 0.05$)	Taean area - Byeonsan area	0.058	N.S.
		Taean area - Dadohae area	0.918	N.S.
		Taean area - Hallyeo area	0.949	N.S.
		Byeonsan area - Dadohae area	0.022	*
		Byeonsan area - Hallyeo area	0.076	N.S.
		Dadohae area - Hallyeo area	0.801	N.S.

Table 5. Continued.

Method	Biodiversity index	Pairwise comparison	adjusted *P*	Significance
DNA metabarcoding	OTUs ($P = 0.13$)	Taean area - Byeonsan area	0.593	N.S.
		Taean area - Dadohae area	0.557	N.S.
		Taean area - Hallyeo area	0.184	N.S.
		Byeonsan area - Dadohae area	0.350	N.S.
		Byeonsan area - Hallyeo area	0.206	N.S.
		Dadohae area - Hallyeo area	0.232	N.S.
	Chao1 ($P = 0.369$)	Taean area - Byeonsan area	0.930	N.S.
		Taean area - Dadohae area	0.552	N.S.
		Taean area - Hallyeo area	0.721	N.S.
		Byeonsan area - Dadohae area	0.500	N.S.
		Byeonsan area - Hallyeo area	0.483	N.S.
		Dadohae area - Hallyeo area	0.624	N.S.
	Shannon's diversity ($P < 0.05$)	Taean area - Byeonsan area	0.461	N.S.
		Taean area - Dadohae area	0.944	N.S.
		Taean area - Hallyeo area	0.023	*
		Byeonsan area - Dadohae area	0.517	N.S.
		Byeonsan area - Hallyeo area	0.335	N.S.
		Dadohae area - Hallyeo area	0.008	**
	equitability ($P < 0.05$)	Taean area - Byeonsan area	0.361	N.S.
		Taean area - Dadohae area	0.727	N.S.
		Taean area - Hallyeo area	0.137	N.S.
		Byeonsan area - Dadohae area	0.209	N.S.
		Byeonsan area - Hallyeo area	0.728	N.S.
		Dadohae area - Hallyeo area	0.030	*

Mesozooplankton community analysis

In both methods, mesozooplankton communities in the Marine and Coastal National Park areas were grouped into three clusters (Figure 4). Although there were some differences in the mesozooplankton samples that belonged to the cluster, there were similar pattern: Cluster 1 mainly contained the zooplankton samples from the Dadohae area; Cluster 2 tended to consist of zooplankton samples from the Hallyeo area, in addition to samples from the eastern parts of the Dadohae area; and the zooplankton samples of the Yellow Sea (included in the Taean and Byeonsan areas) formed Cluster 3. Through the Procrustes analysis, I confirmed that there was a significant correlation between the mesozooplankton communities formed by the morphological identification and DNA metabarcoding (m12 squared = 0.80; correlation value = 0.44; p-value = 0.001) (Figure 5).

Using CAP analysis, the mesozooplankton communities in the Marine and Coastal National Park areas detected using the two methods were significantly different according to the sea area (morphological identification: p-value = 0.001, explanatory power = 16.6%; DNA metabarcoding: p-value = 0.001, explanatory power = 29.0%) and location (morphological identification: p-value = 0.001, explanatory power = 25.0%; DNA metabarcoding: p-value = 0.001, explanatory power = 40.1%) (Figure 6). According to the pairwise Adonis test, all mesozooplankton communities formed by the CAP analysis were significantly different (Table 6). In the contrast, taxonomic compositions between mesozooplankton communities differed depending on the identification method. At the phylum level, the identification results of the morphological identification and DNA metabarcoding confirmed that Arthropoda was the largest taxon in the Marine and Coastal

National Park areas (Figures 7A and 7B). However, while more Myzozoa were identified using morphological identification than DNA metabarcoding, Cnidaria were conspicuously detected using DNA metabarcoding. Interestingly, Rotifera were detected only by the DNA metabarcoding method. Myzozoa and Cnidaria were found more prominently in the Hallyeo area compared with other locations, while Rotifers were detected more in the Taean and Byeonsan areas. Differences in the taxonomic composition of taxa identified using the two methods were more apparent when compared at the major family level (Figures 7C and 7D). The proportions of Acartiidae, Corycaeidae, Noctilucaceae, Oikopleuridae, and Podonidae identified applying the morphological identification were higher than when applying DNA metabarcoding. In contrast, more Calanidae, Centropagidae, Diphyidae, Euphausiidae, Mysidae, Paracalanidae, and Sagittidae were detected with DNA metabarcoding. Based on the results of the two identification methods, the taxonomic compositions of mesozooplankton communities in the Marine and Coastal National Park areas were compared according to the sea area and location. In the Taean area, both Centropagidae and Podonidae were more dominant compared to the other areas, and in the Byeonsan area, Acartiidae was more abundant compared to other areas. Paracalanidae was often observed in samples from the Southern Sea of Korea (Dadohae and Hallyeo areas). Oithonidae was also more common in two areas of the Southern Sea of Korea compared to the other areas. Calanidae, Euphausiidae, and Mysidae were identified more in the Dadohae area than in other areas. In the Hallyeo area, Notilucaceae accounted for nearly half of the mesozooplankton community when identified using the morphological identification, while Diphyidae and Sagittidae were also detected using DNA metabarcoding.

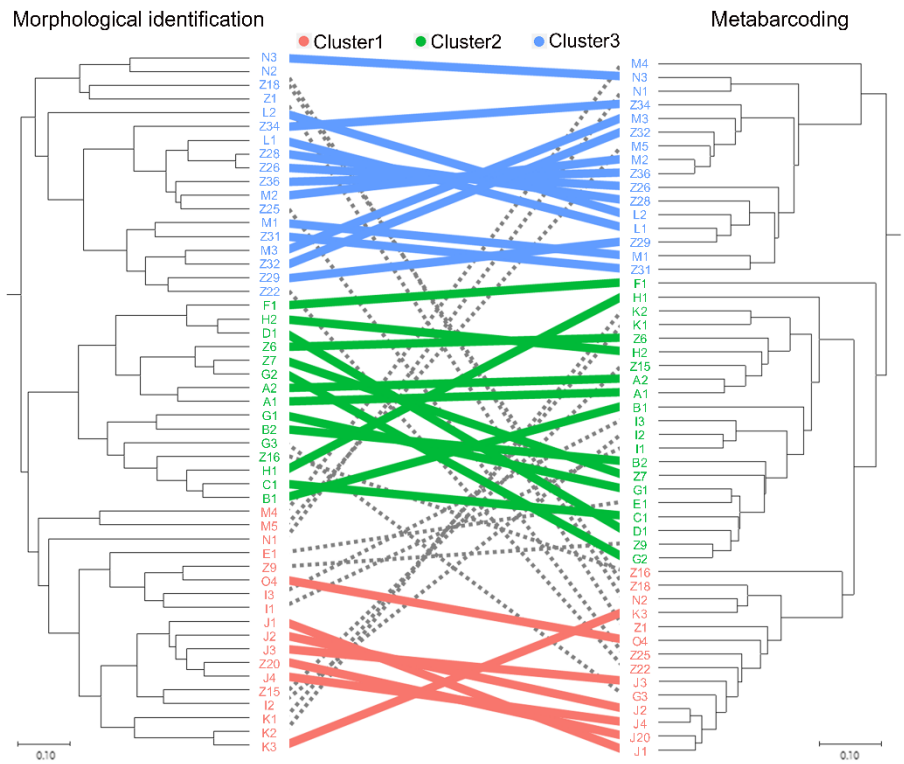

Figure 4. Comparison of UPGMA cluster trees for zooplankton communities between morphological identification and DNA metabarcoding using Bray-Curtis dissimilarities.

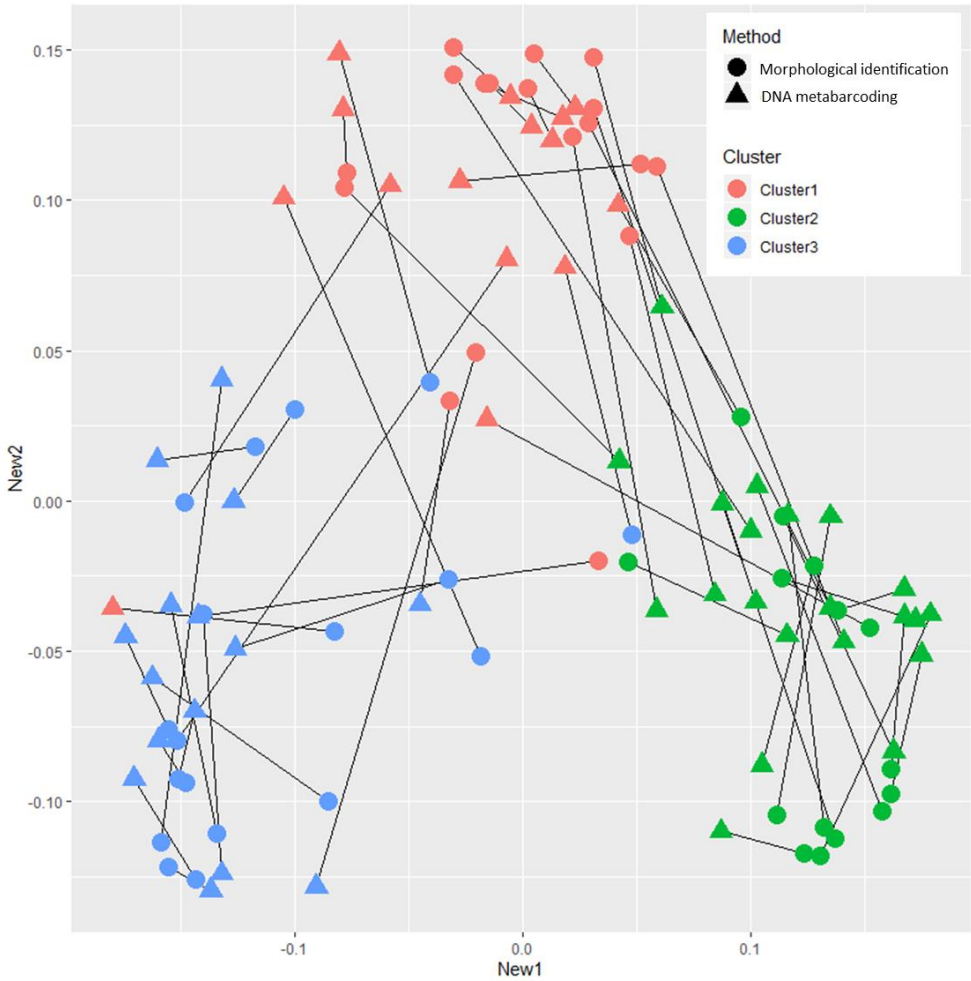

Figure 5. Procrustes analysis based on Bray-Curtis dissimilarities for zooplankton communities between morphological identification and DNA metabarcoding. All samples are represented by morphological identification (circle) and DNA metabacoding (triangle), and are wired between the corresponding Sample ID.

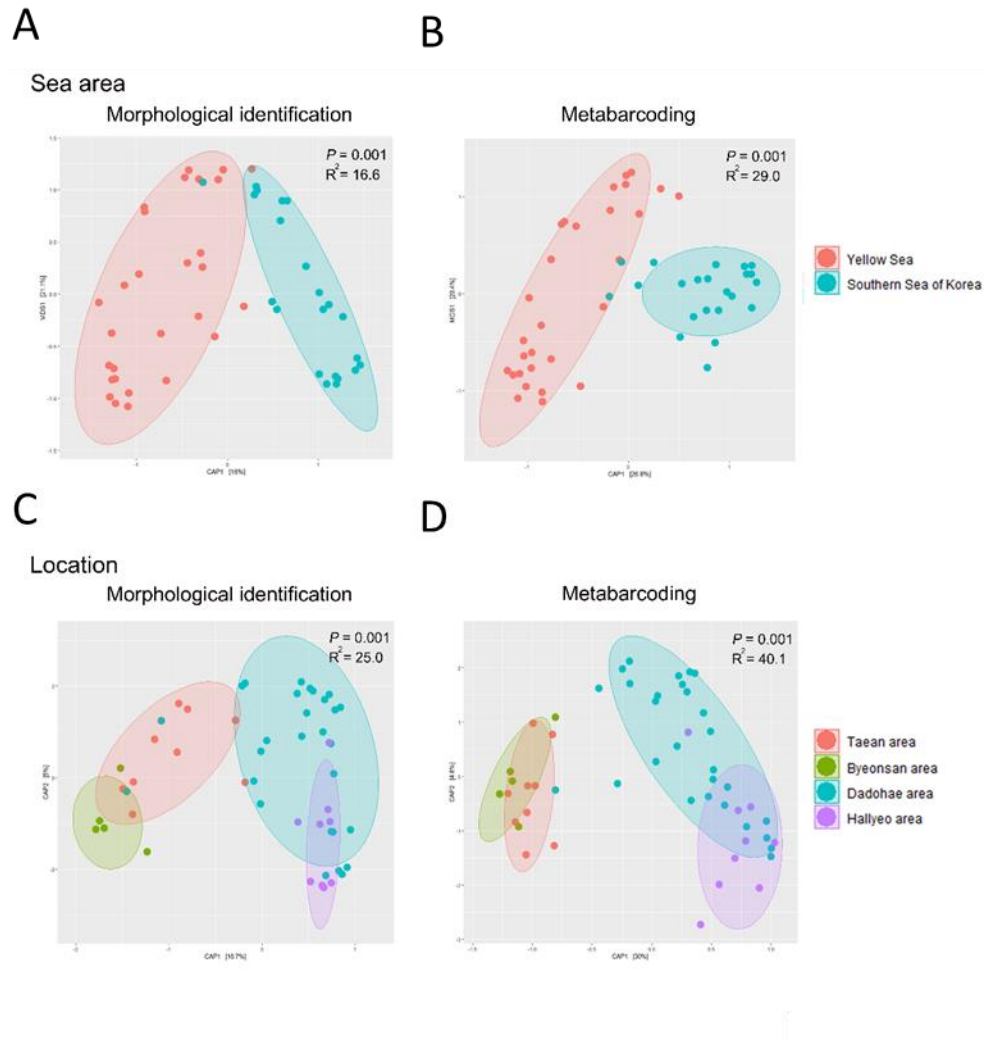

Figure 6. CAP plots for mesozooplankton communities identified using the morphological identification and DNA metabarcoding methods. CAP analysis for mesozooplankton communities based on Bray–Curtis dissimilarities according to each category and identification method: (A) sea area and morphological identification, (B) sea area and DNA metabarcoding, (C) location and morphological identification, and (D) location and DNA metabarcoding.

Table 6. Statistical differences in mesozooplankton communities for the sea area and location between morphological identification and DNA metabarcoding. Statistical significances in zooplankton communities based on Bray-Curtis dissimilarities by the sea area and location variables were calculated using pairwise Adonis test. All p-value adjustments were applied as the false discovery rate (FDR) suggested by Benjamini-Hochberg (**: $p < 0.01$, *: $p < 0.05$, N.S.: no significance).

Method	Variable	Pairwise comparison	adjusted *p*	Significance
Morphological identification	Sea area	Yellow Sea - Southern Sea of Korea	0.001	**
	Location	Taean area - Byeonsan area	0.018	*
		Taean area - Dadohae area	0.002	**
		Taean area - Hallyeo area	0.002	**
		Byeonsan area - Dadohae area	0.002	**
		Byeonsan area - Hallyeo area	0.002	**
		Dadohae area - Hallyeo area	0.014	*
DNA metabarcoding	Sea area	Yellow Sea - Southern Sea of Korea	0.001	**
	Location	Taean area - Byeonsan area	0.027	*
		Taean area - Dadohae area	0.002	**
		Taean area - Hallyeo area	0.002	**
		Byeonsan area - Dadohae area	0.002	**
		Byeonsan area - Hallyeo area	0.002	**
		Dadohae area - Hallyeo area	0.006	**

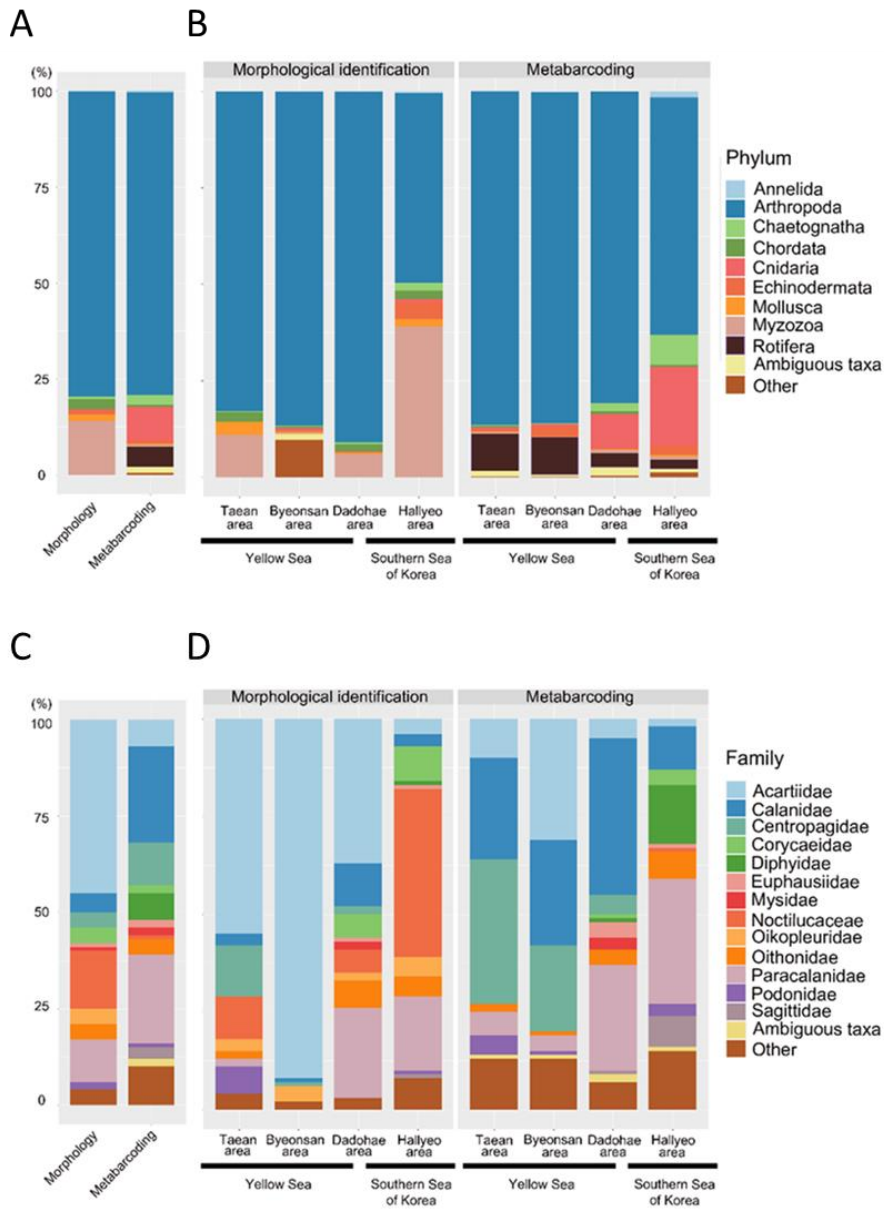

Figure 7. Taxonomic composition of mesozooplankton communities. Bar plots show phylum level proportions according to (A) the identification method and (B) the sea area and location using morphological identification and DNA metabarcoding; Bar plots show major family level proportions according to (C) the identification method and (D) the sea area and location using morphological identification and DNA metabarcoding.

Potential indicator taxa detection using DNA metabarcoding

Morphological identification and DNA metabarcoding were compared to identify potential bioindicator taxa reflecting spatial and environmental characteristics in the Marine and Coastal National Park areas. A CAP analysis revealed that the associations between mesozooplankton communities and all variables produced similar results using both methods. The mesozooplankton communities identified by both methods were significantly affected by all spatial and environmental variables (morphological identification: p-value = 0.001, explanatory power = 36.7%; DNA metabarcoding: p-value = 0.001, explanatory power = 49.8%) (Figures 8A and 8B). Each mesozooplankton community cluster exhibited significant differences when using both methods (p-values = 0.001 for all clusters). Of the three community clusters formed, Cluster 1 exhibited no correlation between the external variables I obtained and the mesozooplankton community. In contrast, Cluster 2 and Cluster 3 were related to spatial and environmental variables. Cluster 2 was correlated with longitude, water temperature, and salinity; latitude and chlorophyll a concentration were correlated with Cluster 3. The taxonomic compositions between mesozooplankton community clusters formed by constraining spatial and environmental variables was shown in CAP analysis (Figures 8C and 8D). Paracalanidae, which was dominant in the Southern Sea of Korea, was more abundant in Cluster 1 and Cluster 2 compared to Cluster 3. A larger number of Calanidae were identified in Cluster 1 by both methods. Oikopleuridae and Oithonidae were frequently observed through morphological identification in Cluster 1, while Euphausiidae and Mysidae were detected more in Cluster 1 with DNA metabarcoding. Notilucaceae, Diphyidae, and Sagittidae, which were associated with the Hallyeo area, were more common in Cluster 2 than other mesozooplankton clusters using both methods.

The phylum Rotifera included in Other with Acartiidae, Podonidae, and Centropagidae, which were more dominant in the Yellow Sea, were identified more in Cluster 3 by DNA metabarcoding.

Depending on the DNA metabarcoding results, the dominant or uniquely identified taxa were considered as potential bioindicator taxa that characterize the mesozooplankton cluster (Figure 7B). Paracalanidae, Diphyidae, and Sagittidae, and Noctilucaceae, which were common in Cluster 2, could be associated with high water temperature, salinity, and topography. Acartiidae, Podonidae, Rotifera, and Centropagidae, which were more dominant in Cluster 3, could be bioindicators for inflow of freshwater and chlorophyll *a* concentration.

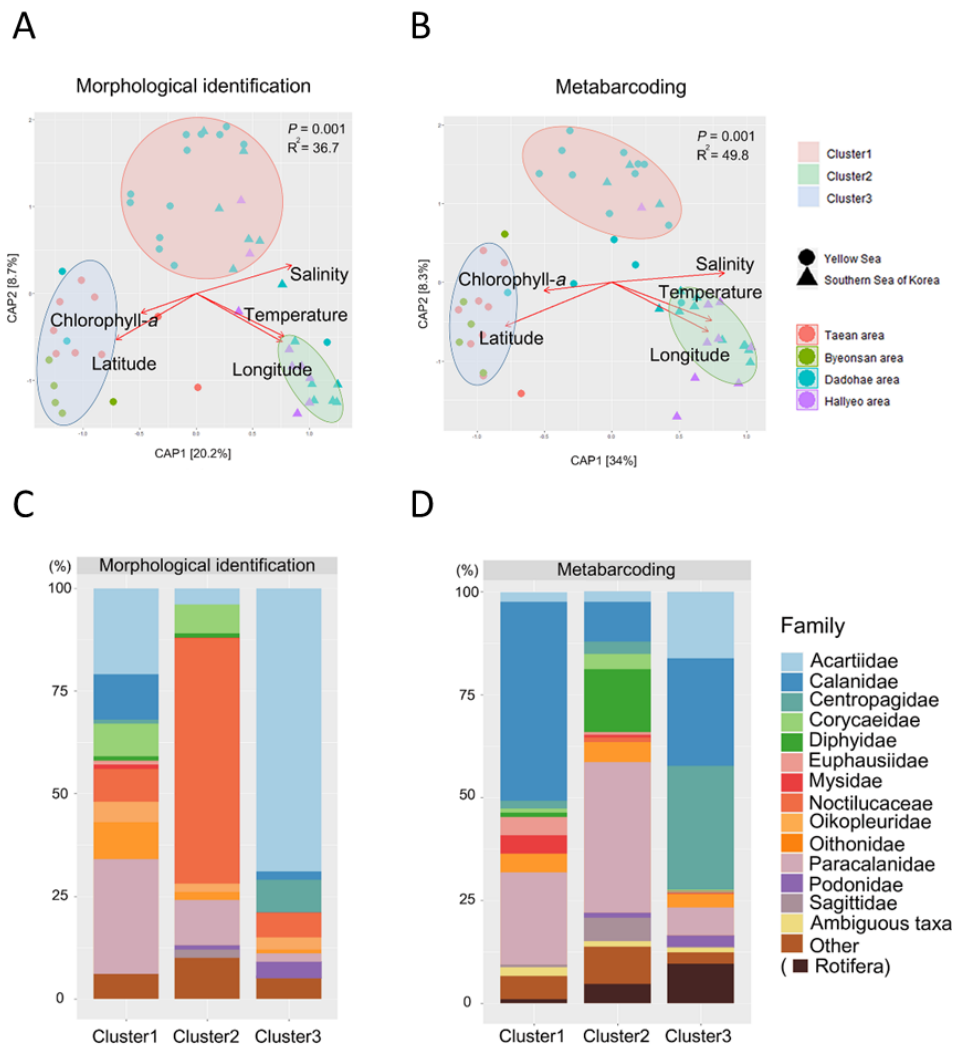

Figure 8. The association between spatial, environmental characteristics and mesozooplankton communities. CAP analysis for zooplankton communities based on Bray–Curtis dissimilarities according to each category and identification method: (A) spatial and environmental variables, and morphological identification; (B) spatial and environmental variables, and DNA metabarcoding. The arrows on the CAP plots in (A) and (B) indicate the patterns in response to the spatial and environmental variables for the zooplankton community clusters. Bar plots between zooplankton community clusters formed using (C) morphological identification and (D) DNA metabarcoding according to spatial and environmental variables in CAP analysis.

1.4 Discussion

Comparison between the morphological identification and DNA metabarcoding results

In this study, the efficiency of DNA metabarcoding was verified by comparing it with the results of morphological identification. Therefore, I could validate the use of DNA metabarcoding for investigation of the mesozooplankton community of the Marine and Coastal National Park areas.

Consistent with the results of previous studies comparing the efficiency of morphological identification and DNA metabarcoding, my results demonstrated that DNA metabarcoding was able to detect much more zooplankton taxa than morphological identification (Table 3). Additionally, mesozooplankton community structures clustered in similar pattern when the results of both methods were compared. The morphological identification method may overlook small-sized zooplankton species and premature or cryptic species that are difficult to distinguish morphologically. In contrast, the sensitive detection capability of DNA metabarcoding is likely to detect small, immature, and cryptic individuals, which cannot be detected by the naked eye. In my results, many individuals of the phylum Rotifera, that were not morphologically identified, were detected by DNA metabarcoding (Figures 7A and 7B). There is less interest in Rotifera compared to other taxa and domestic taxonomic experts of Rotifera are rare.

In addition, through species identification using DNA barcoding, it was confirmed that there are many cryptic species in this phylum. As such, ecological studies of Rotifera have limitations (Gabaldón *et al.*, 2017). However, they are important for understanding

the aquatic ecosystem as this taxon represents an important food source for large aquatic organisms such as crustaceans and fishes (Oh *et al.*, 2020). These results reveal that DNA metabarcoding may be more useful than morphological identification for the detection of Rotifera. Additionally, DNA metabarcoding brought the presence of the taxon to our attention, so I will be more aware of Rotifera when morphologically examining zooplankton communities in the Marine and Coastal National Parks.

My results also revealed some limitations of the DNA metabarcoding method that were previously reported. Consistent with the results of previous studies, I found that the biodiversity and taxonomic composition of mesozooplankton communities were different between the morphological identification and DNA metabarcoding methods. In particular, the abundance of Calanidae, which was relatively large compared to other taxa, tended to be overestimated by DNA metabarcoding (Figures 7C and 7D). Among the copepods collected from my results, Calanidae individuals generally have a larger body size (up to 3 mm) than Acartiidae, Centropagidae, and Paracalanidae. The large body size of these organisms may contribute to the amount of DNA extracted from a sample, resulting in an overestimate (Aylagas *et al.*, 2016; Schiebelhut *et al.*, 2017; Lamb *et al.*, 2019). The underestimated abundance of the dinoflagellate *Noctiluca scintillans* in DNA metabarcoding appears to be due to the low efficiency of DNA extraction compared to other zooplankton taxa. The DNA extraction efficiency for dinoflagellates varies according to the protocol (Yuan *et al.*, 2015). It is inferred that a relatively small amount of DNA was extracted from Noctiluca scintillans due to the use of a zooplankton-focused method of DNA extraction. These technical biases, including DNA extraction and PCR biases, distort the actual number of sequences (Pochon *et al.*, 2013; Andruszkiewicz *et al.*, 2017; Borrell

et al., 2017; Wurzbacher *et al.*, 2017; Lacoursière-Roussel *et al.*, 2018; Doi *et al.*, 2019). Additionally, Oikopleuridae, which was among the most frequently detected family levels, was not detected with DNA metabarcoding. Considering the results of previous studies, which detected Oikopleuridae in the stomach of fish using the same primer (Albaina *et al.*, 2016; Kodama *et al.*, 2017), it is expected that the lack of detection of Oikopleuridae may have been caused by the technical biases generated during the sampling or experimental processes.

Potential bioindicator taxa in the Marine and Coastal National Park areas of Korea in spring

Zooplankton taxa can provide early detections of global climate change due to their sensitivity to environmental changes. DNA metabarcoding has a sensitive detection capability, which can identify potential indicator taxa in bulk samples or communities (Xiong *et al.*, 2020). Using DNA metabarcoding, I identified the characteristics of three clusters divided according to spatial and environmental variables (Figure 8B). In addition, using the results from both identification methods, I determined found potential bioindicator taxa that were related to the characteristics of Cluster 2 and Cluster 3.

Cluster 1 was unable to identify any correlations between the cluster of mesozooplankton communities and the spatial and environmental variables (Figure 8B). This indistinctness may be attributed to the diverse geographical characteristics and extensive range of the Dadohae area. The sampling stations in the Dadohae area are distributed in both the Yellow Sea and the Southern Sea of Korea; therefore, these sampling

stations are affected by the environmental characteristics of both sea areas. In addition, due to the seasonal changes of the Kuroshio currents and the southward movement of freshwater in the Yellow Sea by wind, the zooplankton habitat here changes more frequently than in other areas (Oscar, 1982; Lee *et al.*, 2011). Using DNA metabarcoding, Calanidae, Euphausiidae, and Mysidae, were found more in this cluster compared with others (Figure 8D). However, I was not able to identify the common characteristics of these taxa that reflect the characteristics of Cluster 1 in this study.

Cluster 2 was associated with longitude, water temperature, and salinity (Figure 8B). This distinct clustering could be a result of the environmental characteristics of the Kuroshio Current and topographical characteristics of the Southern Sea of Korea. Paracalanidae, Diphyidae, and Sagittidae, detected in high abundance by DNA metabarcoding, appear to be associated with high temperature and salinity, which are characteristics of the Kuroshio Current (Figure 8D). The Kuroshio Current has relatively high temperature and salinity compared with other currents affecting the Korean Peninsula (Lie and Cho, 2016). The Genus *Paracalanus* belonging to Paracalanidae is one of the common copepods on the coast of Korea., which are reportedly correlated with high water temperature or salinity (Kang, 1996; Araujo, 2006; Kang and Kim, 2008; Jang *et al.*, 2012). Diphyidae can be easily moved through ocean surface currents and thrive explosively upon encountering a preferred environment (Mackie *et al.*, 1988; Blackett *et al.*, 2014). Most jellyfish are known to prefer high water temperature and salinity in marine environments (Buecher, 1999). In addition, Chaetognatha, a phylum that includes Sagittidae, is moved by the Kuroshio Current and its distribution is closely related to the physical and environmental characteristics (e.g., high water temperature and salinity) of these currents

(Johnson and Terazaki, 2003; Noblezada and Campos, 2008; Grossmann and Lindsay, 2013). Noctilucaceae was also detected more in Cluster 2 than others when DNA metabarcoding was used, although not as much as the result of morphological confirmation. The hydrographical characteristics of the Hallyeo area and high salinity of the Kuroshio Current may also contribute to this result, as the most widely known of Noctilucaceae species, *Noctiluca scintillans*, is widely distributed globally and is one of the red tide forming species (Dela-Cruz *et al.*, 2003; Miyaguchi *et al.*, 2006). The distribution of *Noctiluca scintillans* in Cluster 2 appears to be affected by unique hydrographical characteristics (e.g., topography) in the Hallyeo area. The Hallyeo and part of the Dadohae areas in Cluster 2 are well developed partially enclosed bays. This topography has the characteristic of accumulating buoyant cells of *Noctiluca scintillans*, causing large bloom (Miyaguchi *et al.*, 2006). In addtion, previous studies reported that salinity is positively correlated with the number of *Noctiluca scintillans* individuals in Gwangyang Bay, a nearby sea area of Hallyeohaesang National Park. Thus, *Noctiluca scintillans* are likely well-adapted to high salinity conditions (Kang, 2010; Baek *et al.*, 2013).

The DNA metabarcoding identification results revealed that the proportions of Acatiidae, Podonidae, Rotifera, and Centropagidae were found to be higher in Cluster 3 than in other clusters (Figure 8D). This cluster consisted mostly of samples from the Taean and Byeonsans area in the Yellow Sea, which is associated with the inflow of freshwater and high concentrations of chlorophyll *a*. The Taean area and Byeonsan area, in the Yellow Sea, have freshwater inflows from the Geum River, Mankyung River, and Dongjin River. In addition, these areas have constructed artificial seawalls to prevent the inflow of seawater to the land due to large tidal differences. To improve the water quality of the lake

created by the artificial seawall, a large quantity of freshwater is released into the sea through floodgates. This inflow of freshwater appears to have created a habitat for coastal species of zooplankton that are adapted to the low level of salinity. This release of freshwater can causes a change in the zooplankton assemblage (Williams, 1998; Yoo *et al.*, 2006; Gao *et al.*, 2008; Lee *et al.*, 2009; Paturej and Gutkowska, 2015). For example, as salinity decreases in the surrounding marine environment, high-salinity tolerant species are replaced by low-salinity tolerant species with similar functions in the marine ecosystems (Lee *et al.*, 2003). In my results, a high proportion of Acartiidae was found in Cluster 3 with the DNA metabarcoding method. Using morphological identification, Acartiidae were identified to the species level as *Acartia hongi, Acartia hudsonica, Acartia ohtsukai, and Acartia omorii*. Podonidae, which were abundant in the Taean area, were identified morphologically as *Pleopis polyphemoides*. This species has the characteristic of preferring brackish water and river estuary areas and is known as being highly resistant to low salinity (Ueda, 1982; Shim and Choi, 1996; Soh and Suh, 2000; Põllupüü *et al.*, 2010; Moon *et al.*, 2012). The phylum Rotifera also consist of freshwater invertebrates that play a pivotal role in freshwater and marine ecosystems, as mentioned above (Segers, 2007). With the inflow of freshwater, it can be inferred that the proportions of Acartiidae, Podonidae, and Rotifera, which prefer low salinity were higher in Cluster 3 than in other mesozooplankton community clusters. The occurrence of a highly detected Centropagidae species appears to be closely related to the chlorophyll *a* concentration. As mentioned above, the average chlorophyll *a* concentration was higher in the Yellow Sea compared with that of the Southern Sea of Korea. A Centropagidae species detected using DNA metabarcoding was identified as *Centropages abdominalis* and verified by morphological identification.

Similar to my results, Kang and Kim (2008) also found that the occurrence of *Centropages abdominalis* is positively related to the concentration of chlorophyll *a*, and the amount of phytoplankton greatly affects its growth and development.

Chapter 2

Association between host traits and the intestinal microbiome of Korean crabs

2.1 Introduction

Many previous studies using experimental and molecular methods have reported that various factors of hosts relate to the diversity and community structure of their intestinal microbiomes (Youngblut *et al.*, 2019). Among them, host traits such as host taxon and feeding behavior account for a large proportion of the diversity of the intestinal microbiome (Faith *et al.*, 2011; Groussin *et al.*, 2017). With the development of next-generation sequencing (NGS) technology, metagenomic analysis using the 16S ribosomal DNA (16S rDNA) regions of symbiotic microbes has been made possible (Ju and Zhang, 2015; Youngblut *et al.*, 2019). Based on this, it has also been revealed to some extent how host traits affect the symbiotic microbiome in model organisms such as humans, primates, and mice (Moeller *et al.*, 2013; Wang *et al.*, 2015; Clayton *et al.*, 2018).

In the case of marine organisms, the association between host traits and gut microbiome has been studied, with a focus on fish speices. The divergence in fish species is associated with the formation of evolutionary forces that have intestinal microbiomes (Sullam *et al.*, 2015; Tarnecki *et al.*, 2017). In addition, diet and feeding bahavior are formed differently to the intestinal microbiome (Miyake *et al.*, 2015; Talwar *et al.*, 2018). However, in the case of other aquatic organismss, there have few studies into the relationships between these factors. The associations are difficult to clearly identify because the host and its prey constantly make contact with the aquatic environment (Li *et al.*, 2012; Tzeng *et al.*, 2015). In addition, intestinal microbiomes differ significantly in biodiversity and community structure depending on the organisms and its characteristics (O'Brien *et al.*, 2019). For example, the Hawaiian bobtail squid has a simple microbial

community with only a single microbe that emits light from its body. Corals and sponges, conversely, have high microbial diversity and complex microbial communities. However, coral is sensitive to seasonal and regional factors, while sponges are comparably more resistant to these factors (McFall-Ngai, 2008; Littman *et al.*, 2009; Rader and Nyholm, 2012; Thomas *et al.*, 2016; Webster and Thomas, 2016; O'Brien *et al.*, 2019). For these reasons, the relationship between host evolutionary history, diet and intestinal microbiome in marine organisms remains unclear.

Brachyuran crabs are one of the most dominant species of crustaceans and have high morphological diversity (Warner and Warner, 1977; Bertini *et al.*, 2004; Tsang *et al.*, 2014). The evolutionary history of brachyuran crabs is as complex as its morphological diversity. The phylogenetic relationship between the two superfamilies, Ocypodoidea and Grapsoidea, which are most commonly seen in the intertidal zone, remains controversial (Ji *et al.*, 2014; Chen *et al.*, 2018). From a traditional morphological perspective, these two superfamilies have been interpreted as one monophyletic clade due to their common characteristic of gonopores; however, molecular phylogenetic studies have revealed that they are paraphyletic. (Kitaura *et al.*, 2002; Tsang *et al.*, 2014; Wang *et al.*, 2020). In addition, Brachyuran crabs have high ecological diversity: they are opportunistic omnivores that use a variety of foods as energy sources (Lee, 2015). However, they have various feeding behaviors (e.g., deposit-feeding, herbivory, and carnivory), according to morphological characteristics such as the claw shape, body size, and structure of the digestive system (Heeren and Mitchell, 1997; Schenk and Wainwright, 2001; Buck *et al.*, 2003). They also change their feeding behaviors according to their habitat and the size of their prey. Currently, studies into the microbiome of crabs have focused on edible resource

species, such as *Eriocheir sinensis*, and the correlation between host and microbiome. The association between crab microbiome and habitat, health status, and diet type has been elucidated.

In this chapter, the association between the intestinal microbiome of crabs according to the family of crabs and feeding behavior was investigated using 16S rDNA amplicons on the Illumina MiSeq. The intestinal microbial biodiversity and community structures of crab samples were compared according to the family of crabs and feeding groups. The family variables were divided to five groups: Leucosiidae, Dotillidae, Macrophthalmidae, Sesarmidae, and Varunidae according to the taxonomic rank of the crab samples. Based on the previous studies related to the ecology of crabs (Kobayashi, 2013; Lee, 2015), the feeding behavior variables were divided into three groups: carnivore, deposit-feeder, and detritivore. Based on the intestinal microbiome data, the families, as well as the controversial phylogenetic relationship between the superfamilies Ocypodoidea and Grapsoidea, were observed from a new perspective. In addition, the functional profile was predicted in the intestinal microbiome and the roles of the intestinal microbes that significantly affect their family of crabs and their feeding behavior was inferred.

2.2 Materials and Methods

Sample collection

A total of 80 brachyuran crabs were collected from the intertidal zones of five sites (Boryeong, Ganghwado Island, Shinan, Yeosu, and Yeongjongdo Island) located on the western and southern coasts of South Korea in September, 2018 and April, 2019 (Table 7). To gain high-quality DNA from the intestinal microbiomes of the collected crabs, all samples were brought into the laboratory alive. Only male crabs were selected, due to the microbiome differences between the sexes. The crabs were washed thoroughly with distilled water and sterilized with 70% ethanol for 5 minutes. For DNA extraction of the intestinal microbiome, each crab was dissected immediately after washing. Genomic DNA was extracted from the dissected intestine and muscle tissue of the crab using DNeasy DNA Micro Kit and DNeasy Blood & Tissue Kit (Qiagen, Valencia, CA, USA), respectively, according to the manufacturer's instructions. The total DNA extracts were frozen and stored at -80°C until further analysis. The species of the crab was initially identified based on their morphological characteristics. The species was then cross-checked with the DNA sequences of the cytochrome oxidase c subunit I (COI) region obtained from the each muscle tissues. These sequences were identified based on the closest BLAST result in the NCBI nucleotide database.

Host phylogenetic analysis

To construct a phylogenetic tree of the crab samples, the DNA sequences of mitochondrial 12S, 16S rDNA, and COI gene of each species was obtained using several primer sets

(Simon *et al.*, 1994; Ivanova *et al.*, 2007; Radulovici *et al.*, 2009; Tsang *et al.*, 2009) (Table 8). All sequences were aligned using MUSCLE with the L-INS-i algorithm and maximum likelihood (ML) analysis was performed with RAxML 8.0.2 (Katoh and Standley, 2013; Stamatakis, 2014). The GTRGAMMA model of nucleotide substitution was used with 1000 bootstrap replication. In the multigene analysis, alignments of three genes were concatenated and partitioned by gene region.

Intestinal microbiome analysis

For detection of the intestinal microbiome of the crab samples, the 16S rDNA V4 variable region was amplified using 515F-Y and 806RB universal primer sets (Apprill *et al.*, 2015; Parada *et al.*, 2016). PCR conditions were as follow: 3 min at 94 °C; 35 cycles of 45 s at 94 °C, 1 min at 50 °C, and 1 min 30s at 72 °C, and a final extension step of 10 min at 72 °C. PCR products were purified using a QIAquick PCR Purification Kit (QIAGEN, Germany) and sequenced using the Illumina MiSeq sequencing platform at Macrogen Inc. (Seoul, Korea).

Raw data of the intestinal microbiome in each crab sample were processed with the custom python script "DNA_metabarcoding_analysis.py" based on the Querial Insights Into Microbial Ecology (QIIME) v 1.9.1. (Caporaso *et al.*, 2010) (Appendix 1). Forward and reverse reads from each raw data were merged into single contig using PEAR with the default settings (Zhang *et al.*, 2013). Short (< 200 bp) or low-quality assembled contigs (Q < 30) were excluded from the bioinformatics analysis. *De novo* chimera detection and operational taxonomic unit (OTU) clustering were conducted using VSEARCH and the detected chimeric sequences and singleton sequences were discarded from the analysis (Rognes *et al.*, 2016). All OTUs were clustered with 97% similarity and the taxonomic

categorical rank was assigned to the most abundant sequence in each clustered OTU based on 16S rDNA database in SILVA. Non-bacteria (e.g., archaea and arthropods), chloroplasts, and mitochondrial sequences were also excluded from the analysis. Normalization was performed considering sequence depths among the crab samples. The normalized data of the intestinal microbiomes of the crab samples were analyzed according to the family of crabs and feeding behavior variables. Intestinal microbial biodiversity indices (Phylogenetic distance, Chao1, Shannon's diversity, and equitability) were calculated using the QIIME command "alpha_diversity.py". Constrained analysis of principal coordinates (CAP) based on weighted UniFrac distance and unweighted UniFrac distance was conducted to confirm the differecnes in intestinal microbial communities according to the family of crabs and feeding behavior variables. Additionally, the taxonomic compositions of the intestinal microbiomes were analyzed at the most frequently detected bacteria family level.

All statistical values were calculated using several R packages, including vegan, pairwise Adonis, dunn.test, rcompanion, and ade4 (Dray *et al.*, 2007; Oksanen *et al.*, 2010; Dinno and Dinno, 2017; Mangiafico and Mangiafico, 2017; Martinez Arbizu, 2017). Bioinformatics and statistical analysis were visualized by plots containing ggplot2 and Phyloseq in R (McMurdie and Holmes, 2013; Team, 2014; Wickham, 2016). All P-values were calibrated using the false discovery rate (FDR) presented by Benjamini and Hochberg (Benjamini and Hochberg, 1995). To identify significant differences between intestinal microbial biodiversity indices for family of crabs and feeding behavior, Kruskal-Wallis test was conducted and the Dunn's test was performed for pairwise comparisons as a post hoc

test. The statistical differences between the intestinal microbial communities from the CAP analysis were determined by ANOVA with 999 permutations.

Investigation into the relationship between intestinal microbiome and host phylogeny

To investigate the phylogenetic relationship between the two superfamilies of Ocypodoidea and Grapsoidea and their intestinal microbiomes, CAP analysis was constrained to the superfamily variables of crabs (e.g., Leucosioidea, Ocypodoidea, and Grapsoidea) by two hypotheses: 1) two superfamilies in one monophyletic clade or 2) two superfamilies in a non-monophyletic clade (different groups). To confirm the association between the family of crabs and their intestinal microbiomes, the intestinal microbes associated with the family of crabs were selected using Clade-based taxonomic units (ClaaTU) algorithm (Gaulke *et al.*, 2018). Based on the phylogenetic tree of the intestinal microbiome constructed from the OTU representative sequences, the OTU matrix was converted into clade taxonomic unit (CTU) matrix. Each clade of this phylogenetic tree was assigned taxonomic information, and statistical differences were confirmed according to the family of crabs. Using this algorithm, the conserved microbes were identified in all crab samples and the significant microbes according to the family of crabs. To track the shift of the potential intestinal microbes related to evolution, a presence-absence mapping matrix of these microbes was created. The OTUs of potential intestinal microbes involved in the divergence of crabs were considered rare if their abundance was less than 1% and their appearance frequency was less than 25% in each crab species. Using Count V. 10.04, OTUs gains and losses according to the family of crabs were determined by asymmetrical Wagner parsimony with gain and loss penalties of 3 and 1, respectively.

Functional profile prediction of intestinal microbes

Phylogenetic Investigation of Communities by Reconstruction of Unobserved States (PICRUSt) v. 2 was used to predict the functional profiles of intestinal microbes according to the feeding behavior of crabs (Douglas *et al.*, 2020). PICRUSt analysis was performed according to the tutorial instructions on the PICRUSt website. To evaluate the accuracy of the prediction results, the nearest-sequenced taxon index (NSTI) values were calculated and OTUs with a NSTI value above 2.0 were excluded from the analysis. For the analysis of OTUs of each intestinal microbe (e.g, microbes associated with family of crabs or feeding hebavior), the metagenome prediction was analyzed with the option "--per_sequence_contrib". Through this analysis step, the CountContributedByOTU value calculated for each OTU was added according to the bacterial taxonomy and compared for each taxonomic rank. In the case of family of crabs, the top five predicted functional profiles for each intestinal microbe were identified. In the case of the feeding behavior, the statistical values for the predicated functional profiles and the relative frequency for each feeding group were calculated using STAMP (Parks *et al.*, 2014). The functional profiles satisfied the statistical analysis and post hoc test (using Kruskal-Wallis test and the Tukey test). The predicted functional profiles resulting from the PICRUSt analysis were assigned functions based on the MetaCyc pathway database (Caspi *et al.*, 2007)

Table 7. Information of collected crabs.

Superfamily	Family	Genus	Species	Feeding behavior	Location	Samples
Leucosioidea	Leucosiidae	Pyrhila	*Pyrhila pisum*	Carnivore	Yeongjongdo Island	7
Ocypodoidea	Dotillidae	Ilyoplax	*Ilyoplax pingi*	Deposit-feeder	Ganghwado Island	1
		Scopimera	*Scopimera longidactyla*		Yeongjongdo Island	10
Grapsoidea	Sesarmidae	Sesarma	*Chiromantes dehaani*	Detritivore	Shinan	2
		Parasesarma	*Parasesarma pictum*		Shinan	1
			Parasesarma erythodactylum		Yeosu	1
Ocypodoidea	Macrophthalmidae	Macrophthalmus	*Macrophthalmus japonica*	Deposit-feeder	Ganghwado Island Shinan Yeosu	12
Grapsoidea	Varunidae	Gaetice	*Gaetice depressus*	Detritivore	Boryeong	5
			Hemigrapsus sanguineus		Shinan	2
		Hemigrapsus	*Hemigrapsus takanoi*		Shinan Ganghwado Island Shinan Yeosu Yeongjongdo Island	23
			Hemigrapsus penicillatus		Yeosu	7
		Helicana	*Helice tridens*		Yeosu	9

Table 8. Sequences of primer sets used for host phylogenetic analysis.

Primer	Sequence (5' to 3')	Source
COI		
FF2d	TTC TCC ACC AAC CAC AAR GAY ATY GG	Ivanova et al. (2007)
CrustDF1	GGT CWA CAA AYC ATA AAG AYA TTG G	Radulovici et al. (2009)
FR1d	CAC CTC AGG GTG TCC GAA RAA YCA RAA	Ivanova et al. (2007)
CrustDR1	TAA ACY TCA GGR TGA CCR AAR AAY CA	Radulovici et al. (2009)
12S		
12SFB	GTG CCA GCA GCT GCG GTT A	Tsang et al. (2009)
Crab 12S-F1	TAT TTG TGC CAG CAG C	This study
Crab 12S-F2	GCT GCG GTT ATA CTT TRA G	This study
12SR2	CCT ACT TTG TTA CGA CTT ATC TC	Tsang et al. (2009)
Crab 12S-R1	GCG ATA TGT ACA YRA TTT AG	This study
Crab 12S-R2	RAT GAA AGC GAC GGG CG	This study
16S		
16Sar	CGC CTG TTT ATC AAA AAC AT	Simon et al. (1994)
Crab 16S-F1	TAT TTG TGC CAG CAG C	This study
Crab 16S-F2	GCT GCG GTT ATA CTT TRA G	This study
16Sbr	CCG GTC TGA ACT CAG ATC ACG T	Simon et al. (1994)
Crab 16S-R1	GCG ATA TGT ACA YRA TTT AG	This study
Crab 16S-R2	RAT GAA AGC GAC GGG CG	This study

2.3 Results

A total of 15,108,829 intestinal microbial sequences were produced using Illumina MiSeq sequencing, of which 13,531,089 sequences were retained after the filtering process. The number of microbial OTUs from the crab samples was 7,725, consisting of 54 phyla, 163 classes, 247 orders, 404 families, and 807 genera. All coverage values in raw data exceeded 0.98, indicating that the number of sequences was sufficient to analyze biodiversity.

Association between the family of crabs and intestinal microbiome

Intestinal microbial biodiversity indices (Phylogenetic distance, Chao1, Shannon's diversity and equitability) of the crab samples were compared according to the family of crabs (Figure 9 and Table 9). As a result, the specific change pattern of biodiversity indices was not found according to the family of crabs.

Using CAP analysis, intestinal microbial communities from the crab samples based on unweighted UniFrac and weighted UniFrac distances were compared according to the family of crabs. As a result, all families had a significant influence on the clustering of communities (unweighted UniFrac: P = 0.001, explanatory power = 11.2 %; weighted UniFrac: P = 0.001, explanatory power = 20.1 %) (Figure 10). All pairwise comparisons of intestinal microbial communities based on unweighted UniFrac distance were also confirmed to have statistical differences (Table 10). However, pairwise comparisons of intestinal microbial communities among families of crabs based on weighted UniFrac distance did not show any significant differences between some families (Dotillidae and Sesarmidae, Sesarmidae and Macrophthalmidae, and Sesarmidae and Varunidae). The relative abundances of the intestinal microbiomes were also different depending on the

family of crabs (Figure 11). Mycoplasmataceae, which is reported to be linked to the evolution of the class Malacostraca, were more dominant in Macrophthalmidae, Varunidae, and Sesarmidae than in Leucosiidae and Dotillidae.

To confirm the phylogenetic relationship between the superfamilies Ocypodoidea and Grapsoidea using intestinal microbiomes, CAP analysis was performed by constraining two types of superfamily. When performing CAP analysis with two superfamilies of different groups based on unweighted UniFrac and weighted UniFrac distances, the values of R^2 were slightly higher than when two superfamilies were analyzed with one group (Table 11).

Using the ClaaTU algorithm, 92 clades of intestinal microbes were identified that were conserved across all crab samples (all the group *P* values for the clades were < 0.05). All the conserved clades belonged to the phylum Proteobacteria (Figure 12). The predicted major functional profiles of these conserved microbes were dominant in the order of nucleoside and nucleotide biosynthesis, amino acid biosynthesis, fatty acid and lipid biosynthesis, carbohydrate biosynthesis, and cofactor, carrier, and vitamin biosynthesis. In addition, 153 clades of intestinal microbes were identified that were conserved according to the family of crabs. Among these clades, it was confirmed that the intestinal microbes of Mycoplasmataceae were significantly conserved in Sesarmidae, Macrophthalmidae, and Varunidae. To identify the OTUs that were conserved in the host, the OTUs that were deemed to have been detected by chance were removed according to the relative abundance and appearance. As a result, seven Mycoplasmataceae OTUs were identified that were potentially associated with the phylogeny of crabs (Figure 13). Of these, four OTUs were assigned taxonomic information as *Candidatus* Bacilloplasma. In addition, under the

assumption that microbes in Mycoplasmataceae are inherited according to crab divergence, it was inferred that the shift of these microbes progressed during divergence by mapping their OTUs to the phylogenetic tree of the crab samples (Figure 14). Using asymmetrical Wagner parsimony, it was inferred that OTU_10 and OTU_38 existed when Leucosiidae and other families of crabs diverged. OTU_1590 was identified as specific Mycoplasmaceae in Sesarmidae. OTU_3260, OTU_21293, and OTU_5 were only significantly found in the Macrophthalmidae. OTU_8 was found uniquely in the crab samples of the genus *Hemigrapsus*. These Mycoplasmataceae OTUs are predicted to perform the major functions of nucleic acid metabolism (e.g., nucleoside and nucleotide biosynthesis and degradation), lipid metabolism (e.g., fatty acid and lipid biosynthesis) and pentose phosphate pathways (Figure 15 and Table 12).

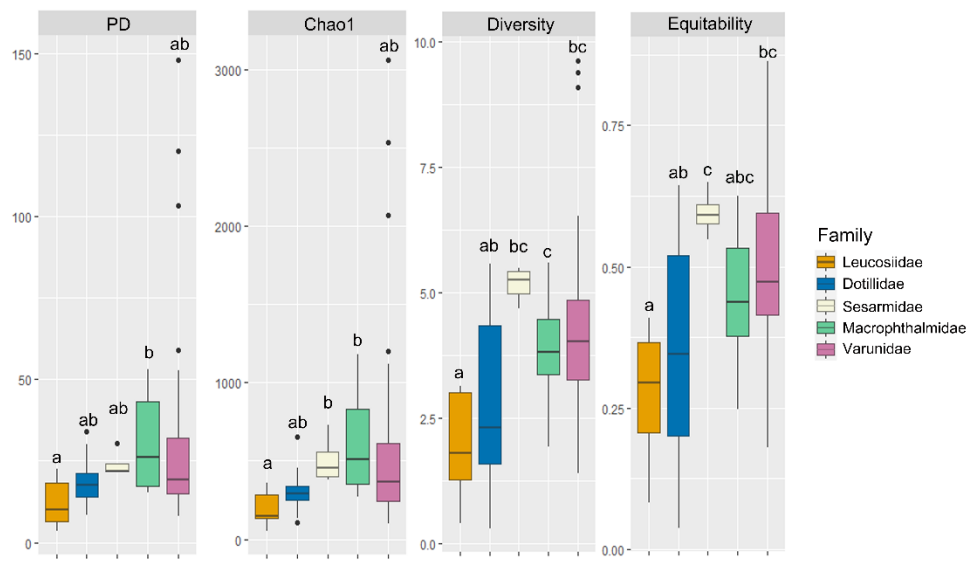

Figure 9. Biodiversity indices for the intestinal microbiomes according to the family of crabs. Statistical differences of the biodiversity indices according to the family of crabs were marked in alphabet, and groups sharing the same alphabet were not significantly different from each other. More detailed statistical values were given in Table 9.

Table 9. Statistical differences in intestinal microbial biodiversity according to the family of crabs. Statistical significances among families of crabs were calculated with Kruskal-Wallis and pairwise comparisons were performed using Dunn's test, as a post hoc test. All P-value adjustments were applied as False Discovery Rate (FDR) suggested by Benjamini-Hochberg (**: $P < 0.01$, *: $P < 0.05$, N.S.: no significance).

Biodiversity index	Pairwise comparison	adjusted *P*	Significance
Phylogenetic distance ($P < 0.05$)	Leucosiidae - Dotillidae	0.292	N.S.
	Leucosiidae - Sesarmidae	0.101	N.S.
	Leucosiidae - Macrophthalmidae	0.018	*
	Leucosiidae - Varunidae	0.073	N.S.
	Dotillidae - Sesarmidae	0.301	N.S.
	Dotillidae - Macrophthalmidae	0.076	N.S.
	Dotillidae - Varunidae	0.312	N.S.
	Sesarmidae - Macrophthalmidae	0.833	N.S.
	Sesarmidae - Varunidae	0.533	N.S.
	Macrophthalmidae - Varunidae	0.261	N.S.
Chao1 ($P < 0.01$)	Leucosiidae - Dotillidae	0.272	N.S.
	Leucosiidae - Sesarmidae	0.036	*
	Leucosiidae - Macrophthalmidae	0.011	*
	Leucosiidae - Varunidae	0.051	N.S.
	Dotillidae - Sesarmidae	0.260	N.S.
	Dotillidae - Macrophthalmidae	0.059	N.S.
	Dotillidae - Varunidae	0.260	N.S.
	Sesarmidae - Macrophthalmidae	0.926	N.S.
	Sesarmidae - Varunidae	0.322	N.S.
	Macrophthalmidae - Varunidae	0.207	N.S.

Table 9. Continued.

Biodiversity index	Pairwise comparison	adjusted *P*	Significance
Shannon's diversity ($P < 0.01$)	Leucosiidae - Dotillidae	0.203	N.S.
	Leucosiidae - Sesarmidae	0.002	**
	Leucosiidae - Macrophthalmidae	0.023	*
	Leucosiidae - Varunidae	0.002	**
	Dotillidae - Sesarmidae	0.015	*
	Dotillidae - Macrophthalmidae	0.195	N.S.
	Dotillidae - Varunidae	0.051	N.S.
	Sesarmidae - Macrophthalmidae	0.109	N.S.
	Sesarmidae - Varunidae	0.082	N.S.
	Macrophthalmidae - Varunidae	0.629	N.S.
equitability ($P < 0.01$)	Leucosiidae - Dotillidae	0.229	N.S.
	Leucosiidae - Sesarmidae	0.005	**
	Leucosiidae - Macrophthalmidae	0.075	N.S.
	Leucosiidae - Varunidae	0.003	**
	Dotillidae - Sesarmidae	0.031	*
	Dotillidae - Macrophthalmidae	0.390	N.S.
	Dotillidae - Varunidae	0.075	N.S.
	Sesarmidae - Macrophthalmidae	0.188	N.S.
	Sesarmidae - Varunidae	0.188	N.S.
	Macrophthalmidae - Varunidae	0.284	N.S.

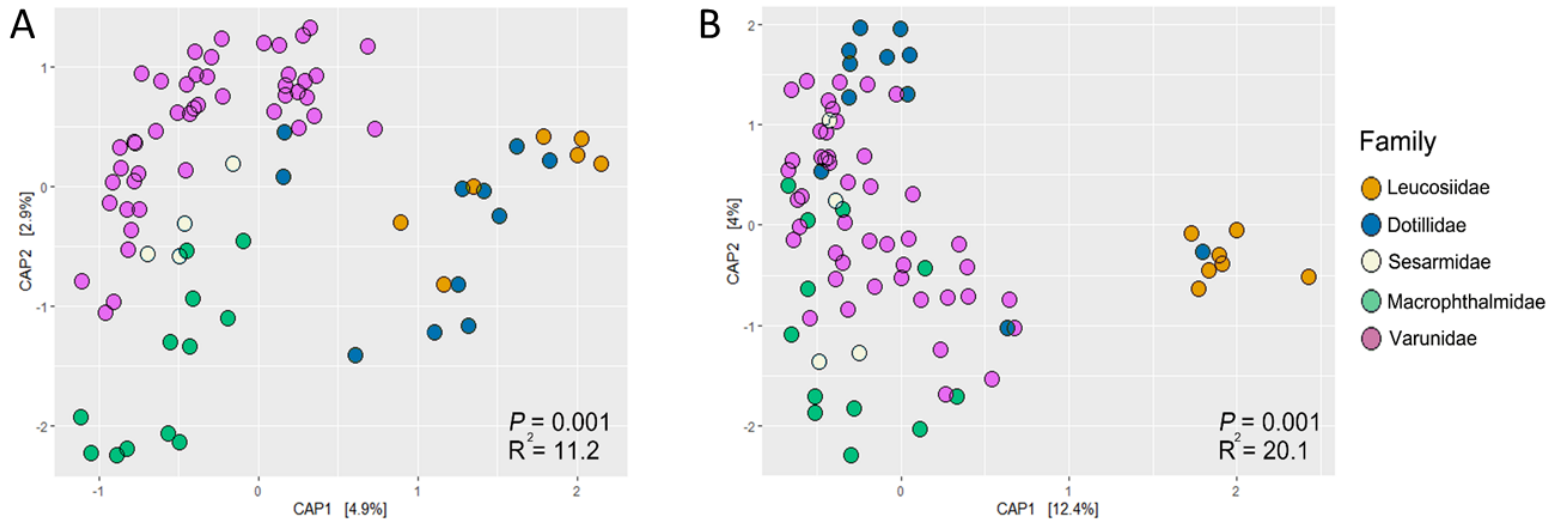

Figure 10. Intestinal microbial communities of crab samples according to the family of crabs. CAP analysis for intestinal microbial communities based on (A) unweighted UniFrac and (B) weighted UniFrac distances.

Table 10. Statistical differences in intestinal microbial communities of crab samples based on unweighted UniFrac and weighted UniFrac distances according to the family of crabs. Statistical significance by family of crabs was calculated with Kruskal-Wallis and pairwise comparisons were performed using Dunn's test, as a post hoc test. All P-value adjustments were applied as False Discovery Rate (FDR) suggested by Benjamini-Hochberg (**: $P < 0.01$, *: $P < 0.05$, N.S.: no significance).

Distance	Pairwise comparison	adjusted *P*	Significance
unweighted UniFrac distance	Leucosiidae - Dotillidae	0.041	*
	Leucosiidae - Sesarmidae	0.008	**
	Leucosiidae – Macrophthalmidae	0.005	**
	Leucosiidae - Varunidae	0.005	**
	Dotillidae - Sesarmidae	0.006	**
	Dotillidae - Macrophthalmidae	0.005	**
	Dotillidae - Varunidae	0.005	**
	Sesarmidae - Macrophthalmidae	0.013	*
	Sesarmidae - Varunidae	0.041	*
	Macrophthalmidae - Varunidae	0.003	**

Table 10. Continued.

Distance	Pairwise comparison	adjusted *P*	Significance
weighted UniFrac distance	Leucosiidae - Dotillidae	0.003	**
	Leucosiidae - Sesarmidae	0.008	**
	Leucosiidae – Macrophthalmidae	0.003	**
	Leucosiidae - Varunidae	0.003	**
	Dotillidae - Sesarmidae	0.24	N.S.
	Dotillidae - Macrophthalmidae	0.003	**
	Dotillidae - Varunidae	0.003	**
	Sesarmidae - Macrophthalmidae	0.34	N.S.
	Sesarmidae - Varunidae	0.49	N.S.
	Macrophthalmidae - Varunidae	0.003	**

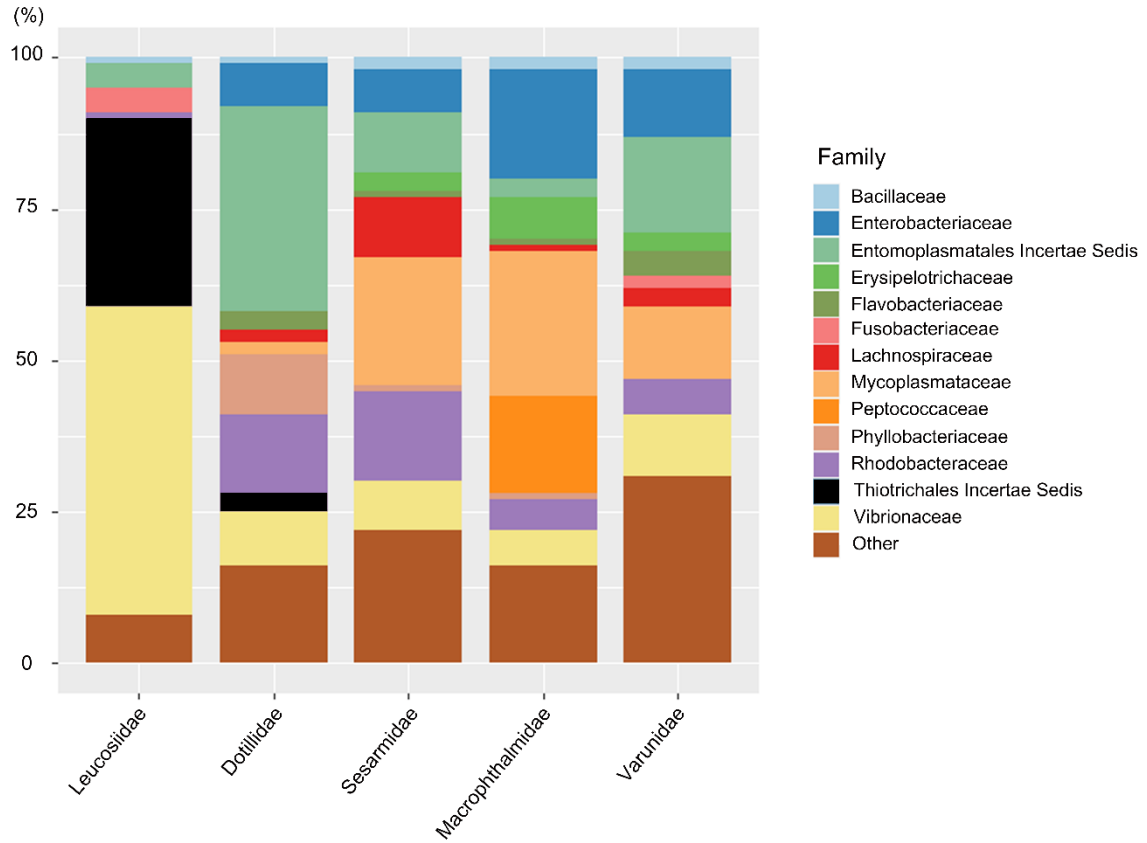

Figure 11. The relative abundance of intestinal microbiomes of the crab samples according to the family of crabs. Bar plots of bacteria family level proportions according to the family of crabs.

Table 11. The values of R^2 for phylogenetic relationship of two superfamilies based on the intestinal microbiomes. The relationship between these two superfamilies was confirmed by considering both the abundance (unweighted UniFrac distance) and their presence or absence (weighted UniFrac distance) of their intestinal microbiome.

Hypothesis	unweighted UniFrac distance	weighted UniFrac distance
Two superfamilies in monophyletic clade	3.2	10.1
Two superfamilies in non-monophyletic clade	6.3	14.6

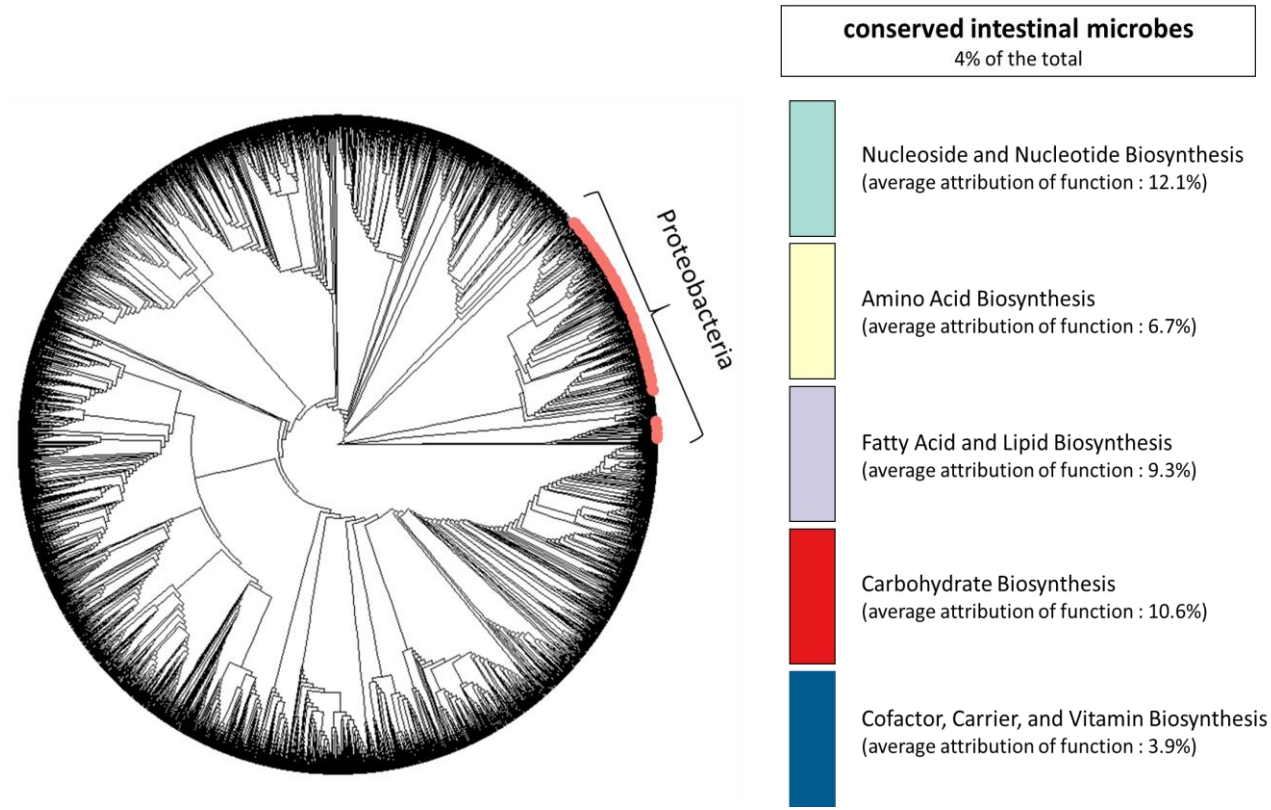

Figure 12. The conserved intestinal microbes across the crab samples. Using the Claatu algorithm, the conserved intestinal microbes were identified across the crab samples and marked with red dots only on the conserved taxa.

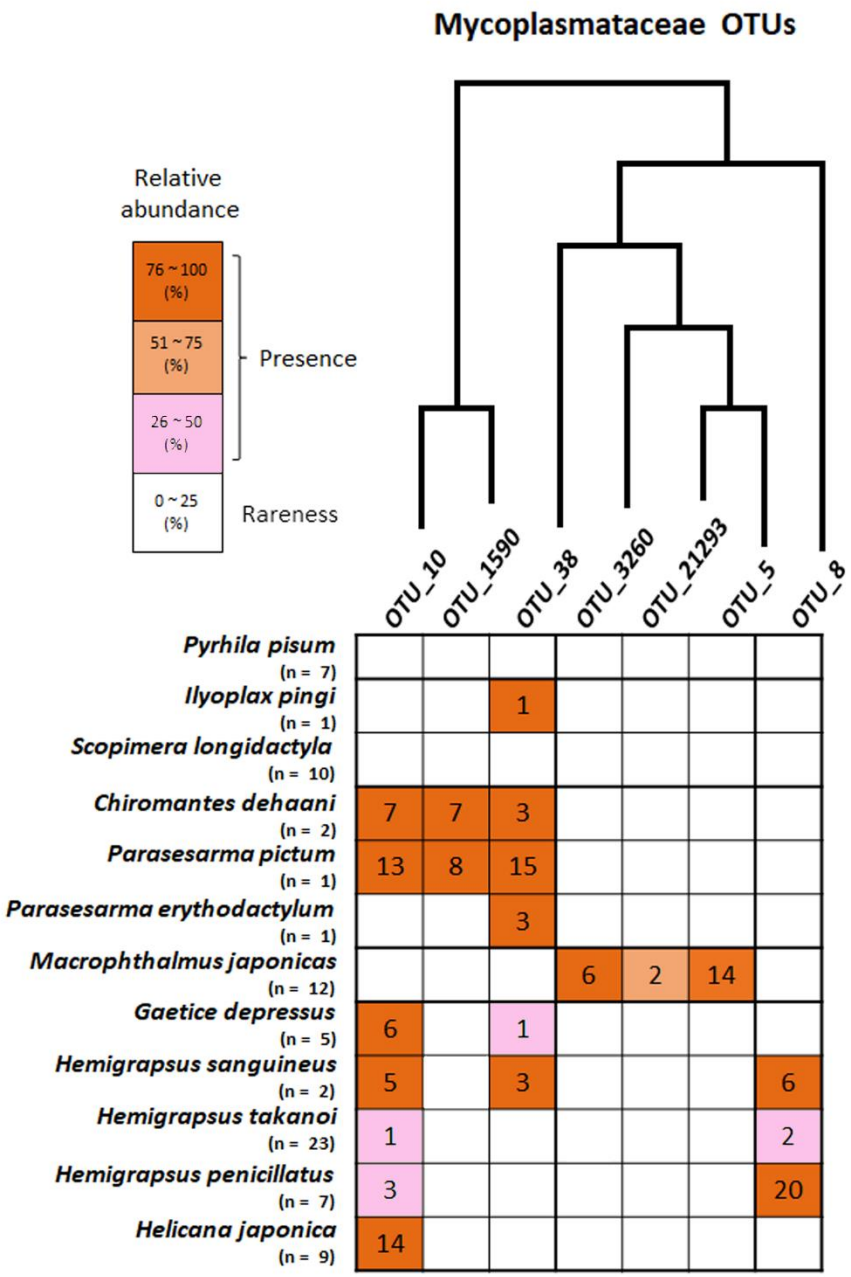

Figure 13. Mycoplasmataceae profiles according to the crab species. This heat map represents the proportion of the crab samples per species of crabs with a bacterial taxon in >1% abundance.

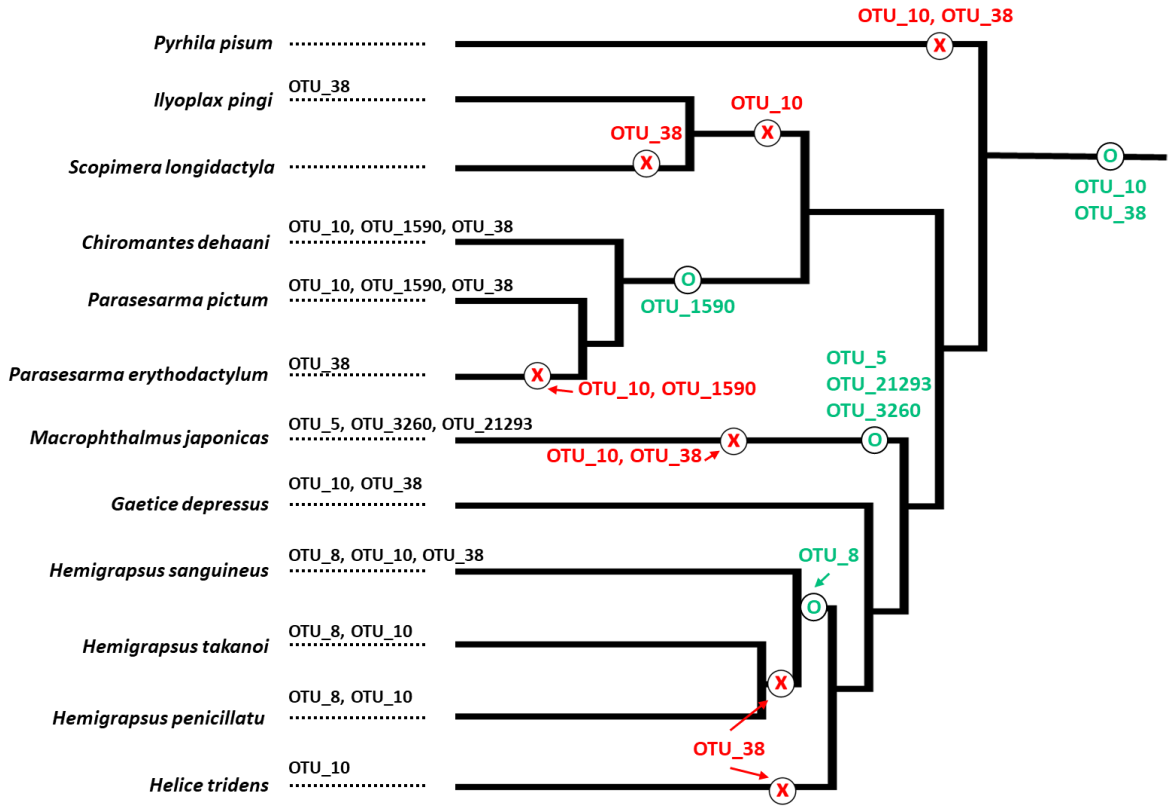

Figure 14. Shifts of Mycoplasmataceae OTUs according to the crab species. Only gains and losses of the Mycoplasmataceae OTUs are labelled. OTUs with <1% abundance and <25% appearance frequency are considered loss.

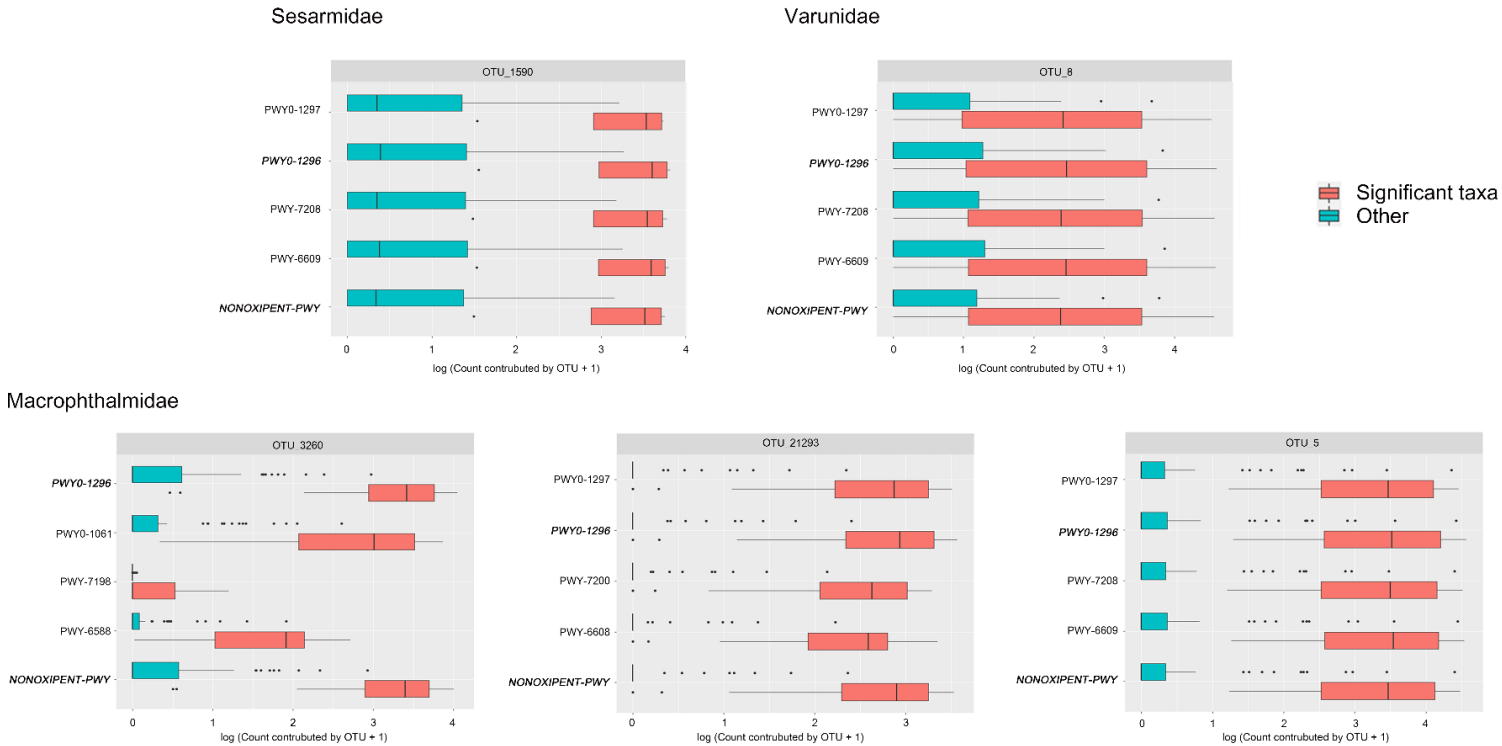

Figure 15. Major functional profiles of Mycoplasmataceae that are particularity identified according to family of crabs.

Table 12. List of major functional profiles that were significantly abundant in specific crab taxa.

OTUs	Profile	Function	Specific taxa
OTU_1590	PWY0-1297	Superpathway of purine deoxyribonucleosides degradation	
OTU_1590	PWY0-1296	Purine ribonucleosides degradation	
OTU_1590	PWY-7208	Superpathway of pyrimidine nucleobases salvage	Sesarmidae
OTU_1590	PWY-6609	Adenine and adenosine salvage III	
OTU_1590	NONOXIPENT-PWY	Pentose phosphate pathway (non-oxidative branch)	
OTU_3260	PWY0-1296	Purine ribonucleosides degradation	
OTU_3260	PWY0-1061	Superpathway of L-alanine biosynthesis	
OTU_3260	PWY-7198	Pyrimidine deoxyribonucleotides de novo biosynthesis IV	
OTU_3260	PWY-6588	Pyruvate fermentation to acetone	
OTU_3260	NONOXIPENT-PWY	Pentose phosphate pathway (non-oxidative branch)	
OTU_21293	PWY0-1297	Superpathway of purine deoxyribonucleosides degradation	
OTU_21293	PWY0-1296	Purine ribonucleosides degradation	
OTU_21293	PWY-7200	Superpathway of pyrimidine deoxyribonucleoside salvage	Macrophthalmidae
OTU_21293	PWY-6608	Guanosine nucleotides degradation III	
OTU_21293	NONOXIPENT-PWY	Pentose phosphate pathway (non-oxidative branch)	
OTU_5	PWY0-1297	Superpathway of purine deoxyribonucleosides degradation	
OTU_5	PWY0-1296	Purine ribonucleosides degradation	
OTU_5	PWY-7208	Superpathway of pyrimidine nucleobases salvage	
OTU_5	PWY-6609	Adenine and adenosine salvage III	
OTU_5	NONOXIPENT-PWY	Pentose phosphate pathway (non-oxidative branch)	
OTU_8	PWY0-1297	Superpathway of purine deoxyribonucleosides degradation	
OTU_8	PWY0-1296	Purine ribonucleosides degradation	
OTU_8	PWY-7208	Superpathway of pyrimidine nucleobases salvage	*Hemigrapsus*
OTU_8	PWY-6609	Adenine and adenosine salvage III	
OTU_8	NONOXIPENT-PWY	Pentose phosphate pathway (non-oxidative branch)	

Association between feeding behavior and intestinal microbiome

Regarding feeding behaviors, all intestinal microbial biodiversity indices showed statistical differences ($P < 0.01$ for the Phylogenetic distance and Chao1 indices; $P < 0.05$ for Shannon's diversity and equitability indices) (Figure 16 and Table 13). The Phylogenetic distance and Chao1 indices of deposit-feeders and detritivores were higher than that of carnivores. Shannon's diversity and equitability indices were the highest in the following order: detritivore, deposit-feeder, and carnivore.

Using CAP analysis, the intestinal microbial communities of the crab samples based on unweighted UniFrac and weighted UniFrac distances were compared according to the feeding behavior. As a result, all feeding groups had a significant influence on the clustering of communities (unweighted UniFrac: $P = 0.001$, explanatory power = 6.3 %; weighted UniFrac: $P = 0.001$, explanatory power = 15.3 %) (Figure 17 and Table 14). All pairwise comparisons of intestinal microbial communities based on unweighted UniFrac and weighted UniFrac distances were also confirmed to have statistical differences. In the taxonomic composition of intestinal microbiomes, carnivores were also significantly different compared to the others groups (Figure 18). In carnivores, besides Vibrionaceae and Thiotrichales incertae sedis, Flavobacteraceae were detected more often than in the other two feeding groups. On the other hand, Enterobacteriaceae, Entomoplasmates incertae sedis, Flavobacteriacea, Mycoplasmaceae and Rhodobacteraceae were more dominant in deposit-feeders and detritivores. Peptococcaceae was also found uniquely in the microbiomes of deposit-feeders.

Functional profile analysis was also performed based on the feeding behavior. A total of 199 functional profiles satisfying statistical significance were identified. Among

them, a total of 57 profiles were associated with glycolysis, TCA cycle, protein metabolism, carbohydrate metabolism, nucleic acid metabolism, and nitrogen metabolism (Figure 19 and Table 15). The relative frequency of predicted functional profiles tended to be divided into carnivore and non-carnivore (e.g., deposit feeder and detritivore). In carnivores, the functional profiles related to the TCA cycle and protein metabolism were predicted more frequently compared to in the other two feeding groups. Meanwhile, glycolysis, carbohydrate metabolism, nucleic acid metabolism, and nitrogen metabolism were more frequently detected in deposit-feeders and detritivorers compared to carnivores.

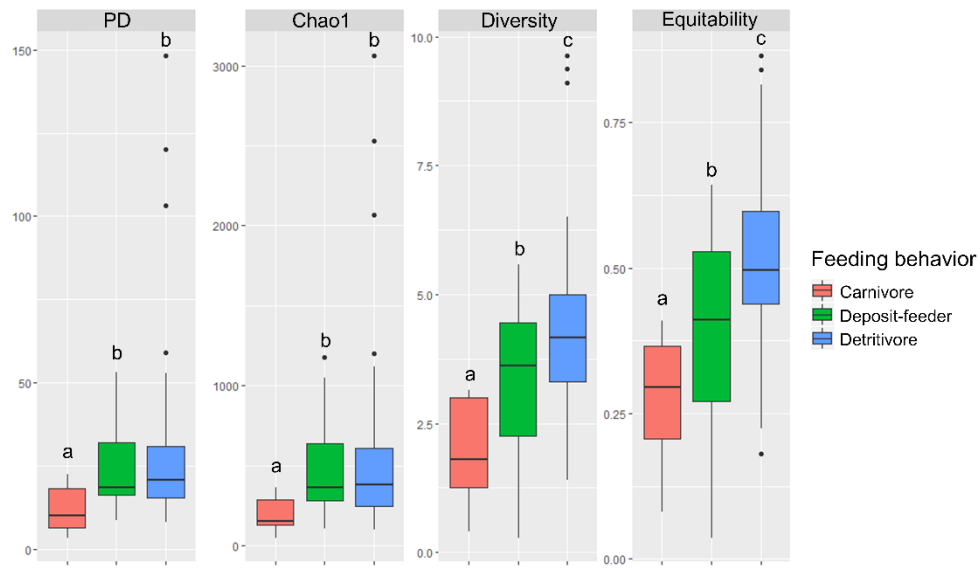

Figure 16. Biodiversity indices for the intestinal microbiomes according to the feeding behavior. Statistical differences of the biodiversity indices according to the feeding behavior were marked in alphabet, and groups sharing the same alphabet were not significantly different from each other. More detailed statistical values were given in Table 13.

Table 13. Statistical differences in intestinal microbial biodiversity according to the feeding behavior. Statistical significances among feeding behaviors were calculated with Kruskal-Wallis and pairwise comparisons were performed using Dunn's test, as a post hoc test. All P-value adjustments were applied as False Discovery Rate (FDR) suggested by Benjamini-Hochberg. (**: P < 0.01, *: P < 0.05, N.S.: no significance)

Biodiversity index	Pairwise comparison	adjusted *P*	Significance
Phylogenetic distance ($P < 0.05$)	Carnivore - Deposit-feeder	0.015	*
	Carnivore - Detritivore	0.017	*
	Deposit-feeder - Detritivore	0.454	N.S.
Chao1 ($P < 0.05$)	Carnivore - Deposit-feeder	0.001	*
	Carnivore – Detritivore	0.010	*
	Deposit-feeder - Detritivore	0.497	N.S.
Shannon's diversity ($P < 0.01$)	Carnivore - Deposit-feeder	0.020	*
	Carnivore – Detritivore	0.001	**
	Deposit-feeder - Detritivore	0.021	*
equitability ($P < 0.01$)	Carnivore - Deposit-feeder	0.027	*
	Carnivore - Detritivore	0.001	**
	Deposit-feeder - Detritivore	0.012	*

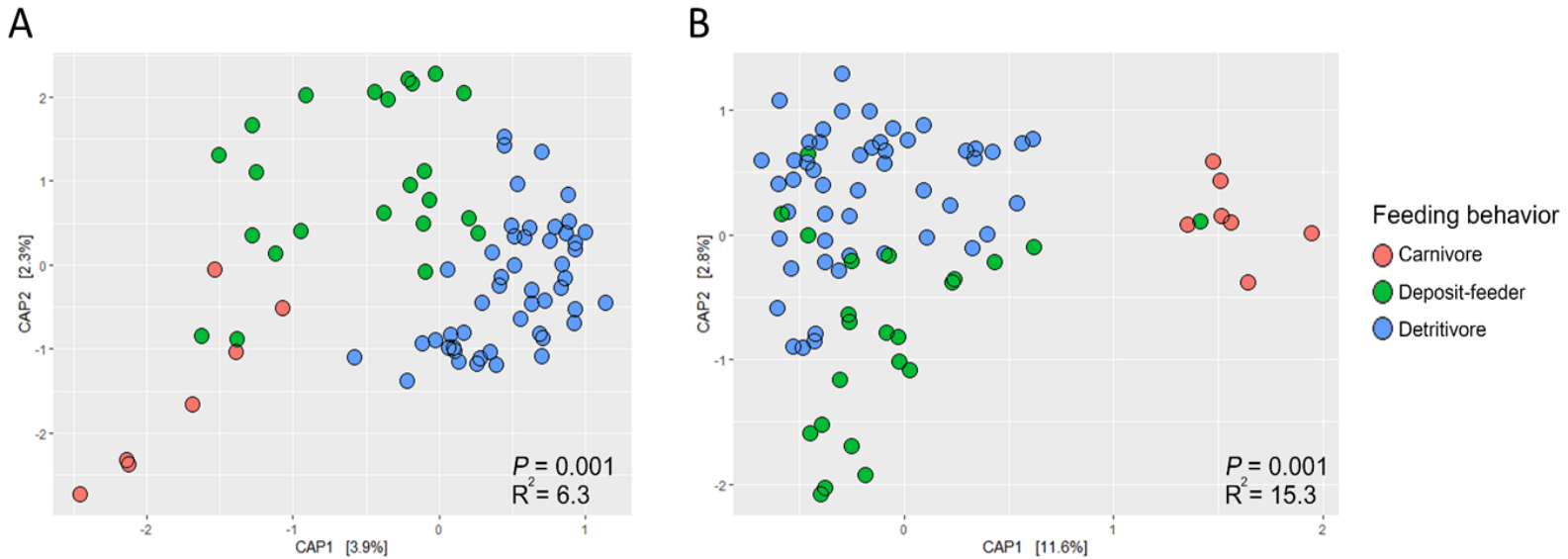

Figure 17. Intestinal microbial communities of crab samples according to the feeding behavior. CAP analysis for intestinal microbial communities based on (A) unweighted UniFrac and weighted UniFrac distances.

Table 14. Statistical differences in intestinal microbial communities based on unweighted UniFrac and weighted UniFrac distances according to the feeding behavior. Statistical significance by feeding groups was calculated with Kruskal-Wallis and pairwise comparisons were performed using Dunn's test, as a post hoc test. All P-value adjustments were applied as False Discovery Rate (FDR) suggested by Benjamini-Hochberg. (**: $P < 0.01$, *: $P < 0.05$, N.S.: no significance)

Distance	Pairwise comparison	adjusted *P*	Significance
unweighted UniFrac distance	Carnivore – Deposit-feeder	0.003	**
	Carnivore – Detritivore	0.002	**
	Deposit-feeder – Detritivore	0.002	**
weighted UniFrac distance	Carnivore - Deposit-feeder	0.002	**
	Carnivore – Detritivore	0.002	**
	Deposit-feeder - Detritivore	0.005	**

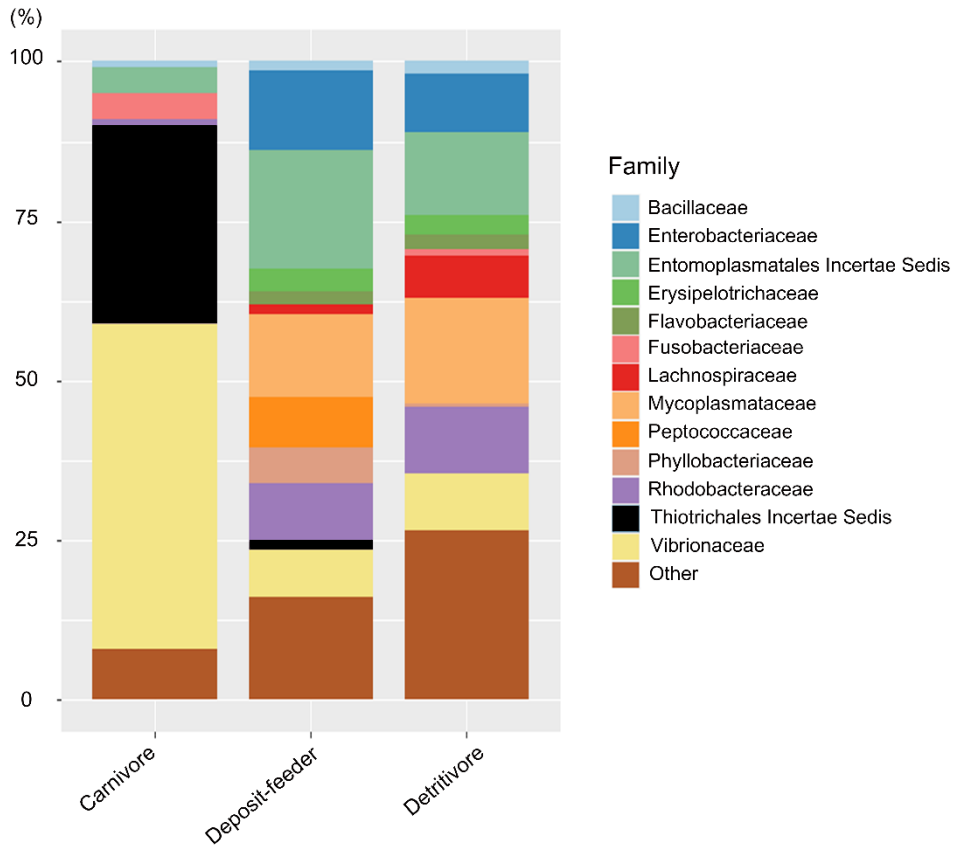

Figure 18. The relative abundance of intestinal microbiomes according to the feeding behavior. Bar plots of bacterial family level proportions according to the feeding behavior.

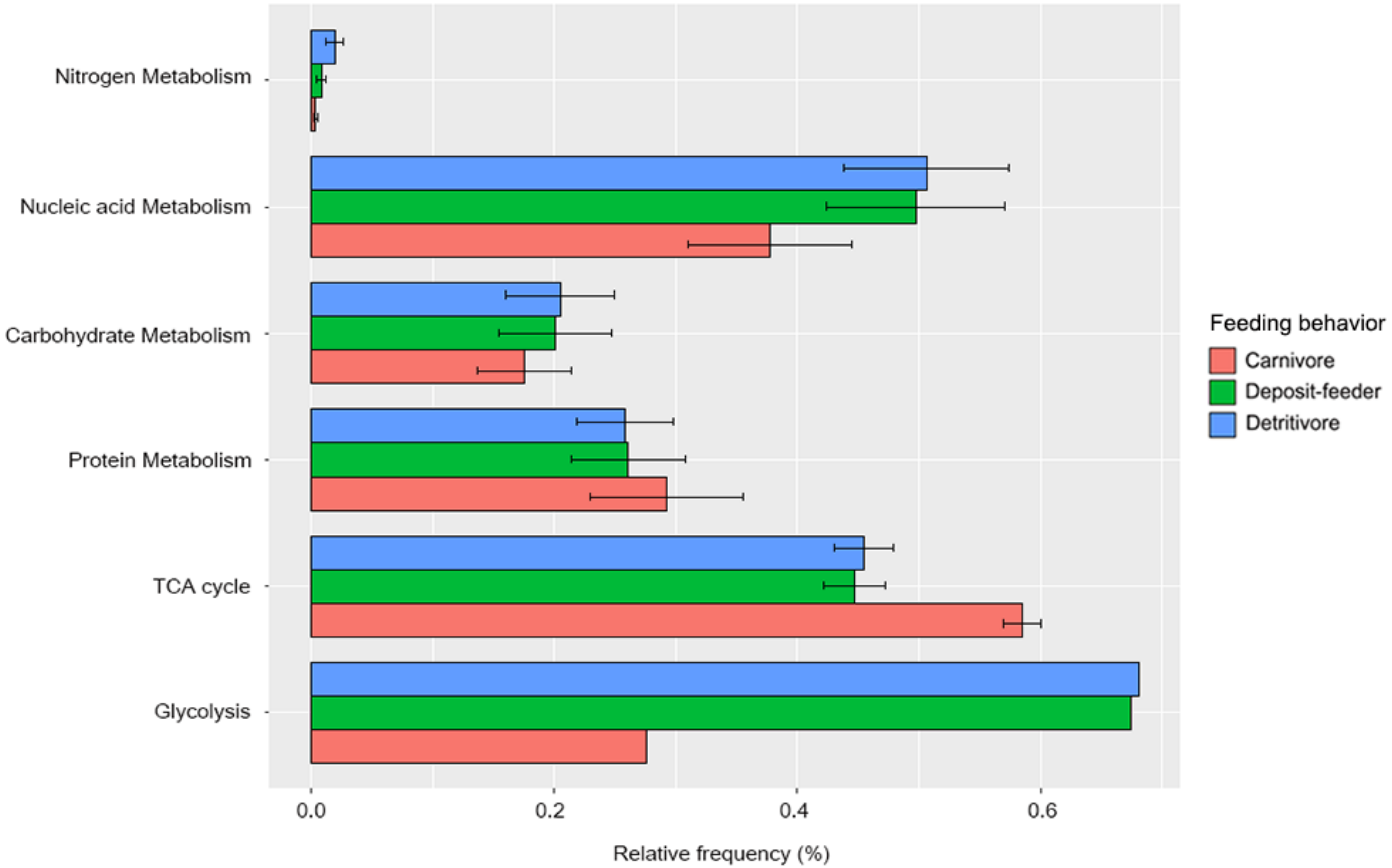

Figure 19. Comparison of predicted pathway classes of intestinal microbiomes according to the feeding behavior. Error bars indicate standard errors.

Table 15. List of functional profiles of intestinal microbiomes that were significant different according to the feeding behavior

Class	Pathway	Putative function	adjusted *P*	Effect size
Glycolysis	ANAGLYCOLYSIS-PWY	glycolysis III	0.001	0.333
TCA cycle	PWY-5913	TCA cycle VI	0.001	0.138
	PWY-6969	TCA cycle V	0.017	0.007
	P105-PWY	TCA cycle IV	< 0.001	0.167
	TCA	TCA cycle I	0.039	0.049
Amino acid metabolism	PWY-6629	superpathway of L-tryptophan biosynthesis	0.002	0.066
	SER-GLYSYN-PWY	superpathway of L-serine and glycine biosynthesis I	0.044	0.083
	PWY-5345	superpathway of L-methionine biosynthesis	0.001	0.202
	PWY0-1061	superpathway of L-alanine biosynthesis	0.009	0.119
	TRPSYN-PWY	L-tryptophan biosynthesis	0.021	0.076
	GLUTORN-PWY	L-ornithine biosynthesis	0.007	0.11
	PWY-2941	L-lysine biosynthesis II	0.008	0.089
	PWY-5505	L-glutamate and L-glutamine biosynthesis	< 0.001	0.129
	PWY-7400	L-arginine biosynthesis IV	0.013	0.085
	PWY-5154	L-arginine biosynthesis III	0.002	0.138
	ARGSYNBSUB-PWY	L-arginine biosynthesis II	0.004	0.113
	ARGSYN-PWY	L-arginine biosynthesis I	0.012	0.085
	THREOCAT-PWY	superpathway of L-threonine metabolism	0.038	0.049

Table 15. Continued

Class	Pathway	Putative function	adjusted *P*	Effect size
Amino acid metabolism	ARGDEG-PWY	superpathway of L-arginine, putrescine, and 4-aminobutanoate degradation	0.003	0.042
	ORNARGDEG-PWY	superpathway of L-arginine and L-ornithine degradation	0.003	0.042
	PWY-5651	L-tryptophan degradation to 2-amino-3 carboxymuconate semialdehyde	0.031	0.02
	P163-PWY	L-lysine fermentation to acetate and butanoate	0.001	0.046
	ARGORNPROST-PWY	arginine, ornithine and proline interconversion	0.001	0.127
Carbohydrate metabolism	PWY-7090	UDP-2,3-diacetamido-2,3-dideoxy-α-D-mannuronate biosynthesis	< 0.001	0.084
	PWY-7332	superpathway of UDP-N-acetylglucosamine-derived O-antigen building blocks biosynthesis	0.002	0.05
	PWY-7328	superpathway of UDP-glucose-derived O-antigen building blocks biosynthesis	< 0.001	0.395
	PWY-7323	superpathway of GDP-mannose-derived O-antigen building blocks biosynthesis	0.001	0.206
	PWY-7347	sucrose biosynthesis III	0.048	0.395
	SUCSYN-PWY	sucrose biosynthesis I	0.049	0.346
	OANTIGEN-PWY	O-antigen building blocks biosynthesis	< 0.001	0.284
	GLYCOGENSYNTH-PWY	glycogen biosynthesis I	0.033	0.088
	PWY-6478	GDP-D-glycero-α-D-manno-heptose biosynthesis	0.001	0.087
	DTDPRHAMSYN-PWY	dTDP-L-rhamnose biosynthesis I	0.002	0.174
	COLANSYN-PWY	colanic acid building blocks biosynthesis	0.001	0.237
	PWY-1269	CMP-3-deoxy-D-manno-octulosonate biosynthesis I	0.005	0.102

Table 15. Continued

Class	Pathway	Putative function	adjusted *P*	Effect size
Carbohydrate metabolism	CALVIN-PWY	Calvin-Benson-Bassham cycle	0.009	0.074
	PWY-6901	superpathway of glucose and xylose degradation	< 0.001	0.294
	PWY-621	sucrose degradation III	0.011	0.068
	PWY-3801	sucrose degradation II	0.014	0.241
	RHAMCAT-PWY	L-rhamnose degradation I	0.005	0.046
	GLUCOSE1PMETAB-PWY	glucose and glucose-1-phosphate degradation	< 0.001	0.355
	FUCCAT-PWY	fucose degradation	0.007	0.392
	PWY-6572	chondroitin sulfate degradation I	0.001	0.04
	PWY-6906	chitin derivatives degradation	0.014	0.195
	PWY-6992	1,5-anhydrofructose degradation	0.029	0.085
Nucleotide metabolism	PWY-5686	UMP biosynthesis	0.048	0.05
	PWY-6277	superpathway of 5-aminoimidazole ribonucleotide biosynthesis	0.026	0.075
	PWY-6545	pyrimidine deoxyribonucleotides de novo biosynthesis III	0.002	0.102
	PWY-7187	pyrimidine deoxyribonucleotides de novo biosynthesis II	0.002	0.108
	PWY-7197	pyrimidine deoxyribonucleotide phosphorylation	0.026	0.07
	PWY-7199	pyrimidine deoxyribonucleosides salvage	0.012	0.13
	PWY-7221	guanosine ribonucleotides de novo biosynthesis	0.03	0.061
	PWY-6122	5-aminoimidazole ribonucleotide biosynthesis II	0.026	0.075
	PWY-6121	5-aminoimidazole ribonucleotide biosynthesis I	0.037	0.054
Nitrogen Metabolism	PWY490-3	nitrate reduction VI	0.009	0.078
	DENITRIFICATION-PWY	nitrate reduction I	< 0.001	0.138

2.4 Discussion

Relationship between Ocypodoidea and Grapsoidea observed using intestinal microbiome

Host symbiotic microbes may potentially alter the phenotype, fitness, and function of the host in response to changes in the marine environment. If this pattern is transmitted vertically to the offspring and persists, it becomes a heritable characteristic of the host (Wilkins *et al.*, 2019). Based on the 16S ribosomal DNA metadata of the intestinal microbiomes of the crab samples, this study confirmed the possibility of how intestinal microbiomes contribute to divergence. The controversial phylogenetic relationship of two superfamilies, Ocypodoidea and Grapsoidea, was interpreted from a new perspective using the intestinal microbiome. Consistent with other molecular phylogenetic studies, the results were able to more clearly explain the clustering of intestinal microbiomes when the two superfamilies are in different clades. Considering cases in which the intestinal microbiome reflects its phylogenetic relationship (Easson and Thacker, 2014; Tzeng *et al.*, 2015), these results indirectly support the previous hypotheses that the two superfamilies are not one monophyletic clade (Table 11).

Proteobacteria, conserved intestinal microbes in crabs

Using the ClaaTU algorithm, it was confirmed that all conserved intestinal microbes were included in the phylum Proteobacteria (Figure 12). Proteobacteria is the most diverse and abundant bacteria taxa on the Earth. Although widely known as a pathogen, it is also easy

to find in various marine environments ranging from the surface to the deep oceans (Cottrell and Kirchman, 2000; Tanner *et al.*, 2000; Buijs *et al.*, 2019; Nimnoi and Pongsilp, 2020). These extensive habitats of Proteobacteria imply that they have also been able to adapt well in the intestines of crabs that inhabit and dominate various marine environments. Through PICRUSt analysis, the functions of these microbes were predicted to be related to various biosynthesis metabolisms (e.g., nucleoside and nucleotide biosynthesis, amino acid biosynthesis, fatty acid and lipid biosynthesis, carbohydrate biosynthesis, and cofactor, carrier, and vitamin biosynthesis). While further studies are necessary to establish the exact interactions between these microbes and crabs, it can be assumed that the products of these biosynthesis pathways are involved not only in the growth of these microbes but also in the health and survival of the crabs.

Mycoplasmataceae, intestinal microbes in crabs

Several families of crabs have specific Mycoplasmataceae OTUs, which seem to be associated with the divergence of crabs (Figures 13 and 14). Most Mycoplasmataceae OTUs potentially related to the phylogeny of crabs in intestinal microbiomes were identified by BLAST as *Candidatus* Bacilloplasma. *Candidatus* Bacilloplasma is a symbiotic microbe that was first discovered in the hindgut of the terrestrial isopod *Porcelio scaber*. This symbiotic microbe, which has a structure that sticks well to the wall of the gut, can adapt well to the intestinal environment (Štrus and Avguštin, 2007). Several studies have confirmed that *Candidatus* Bacilloplasma and its relatives have been found in marine crustaceans (e.g., crabs and shrimps) as well as in terrestrial isopods, which have been

suspected to be related to the evolution of Malacostraca (Durand *et al.*, 2009; Zhang *et al.*, 2014; Chen *et al.*, 2015; Bouchon *et al.*, 2016; Zhang *et al.*, 2016; Sun *et al.*, 2020). The unique detection of these microbial OTUs has verified the possibility that these microbes are related to the evolution of Malacostraca. The Mycoplasmataceae OTUs were predicted to be involved in nucleic acid metabolism, lipid metabolism, and pentose phosphate pathways (Figure 15 and Table 12). Further studies are needed to investigate the link between these microbial functions and the evolution of Malacostraca. However, *Candidatus* Bacilloplasma OTUs were not found in the intestines of the *Philyra pisum* and *Scopimera longidactyla*, collected at Yeongjongdo Island. The samples collected from Yeongjongdo Island found to have higer numbers of Thiotrichales incertae sedis and Vibrionaceae than samples from other locations. The order Thiotrichales contains sulfur-oxidizing bacteria that inhabit aquatic sediment surfaces (Lenk *et al.*, 2011; Lenk *et al.*, 2012). Sulfur-oxidizing bacteria have recently been used as bioindicators to detect pollution in aquatic environments (Van Ginkel *et al.*, 2011; Hassan *et al.*, 2019). The unique detection of Thiotrichales incertae sedis in the intestinal microbiomes of crab samples collected in Yeongjongdo Island indicates that this sampling site is much more polluted than the other sampling locations. Also, the predominance of Vibrionaceae in the intestines of *Philyra pisum* is presumed to be due to the outbreak of disease due to contaminated environments. It may therefore be inferred that the Candidatus *Bacilloplasma* OTUs have the potential to have lower or hidden abundances depending on the host health status and the degree of pollution in the surrounding marine environment.

High intestinal microbial biodiversity of detritivorous crabs

Feeding behavior has been found to be factor that controls intestinal microbial diversity and community structure (Ley *et al.*, 2008; Yun *et al.*, 2014). In this study, it was confirmed that all biodiversity indices of intestinal microbiome for detritivores was higher than those of carnivores (Figure 16 and Table 13). It can be inferred that this biodiversity pattern is due to the fact that detritivores consume more types of food than carnivores. Plant detritus, the main source of food for the detritivores, lacks nitrogen. Detritivorous crabs cannot obtain enough nutrients by consuming only protein-poor plant detritus and they replenish nitrogen by selectively eating small tissues from other organisms or from scavenging carrion (Quensen III and S Woodruff, 1997; Kneib *et al.*, 1999; Thongtham and Kristensen, 2005; López-Victoria and Werding, 2008; Lee, 2015). The carnivorous *Pyrhila pisum* prefers small benthic organisms or bivalves as sources of food (Kobayashi, 2013). Yun *et al.* (2014), who conducted gut microbiome research in insects, also reported that omnivorous insects have higher gut diversity than insects that consume limited food sources, such as carnivores and herbivores. This makes it clearer that high intestinal microbial diversity is related to the number of food types available to hosts.

Differences in the function of intestinal microbiomes in carnivores and non-carnivores

The difference between the functional profiles of carnivores and non-carnivores (e.g., deposit-feeders and detritivores) was also clearly apparent (Figure 19). This may be due to

the differences in the nutritional characteristics of the main food sources of each feeding group. Carnivores obtain nutrients from small aquatic animals, making it relatively easier for them to consume animal protein than the other two feeding groups. Plant detritus, the main source of food for deposit-feeders and detritivores, is relatively rich in cellulose and lignin, but lacks protein (Mann, 1988; Zimmer, 2008; Lee, 2015). In this study, non-carnivores were more frequently detected in the functional profiles associated with carbohydrate metabolism and glycolysis; whereas, in the case of carnivores, the functional profiles associated with protein metabolism and TCA cycle were detected more frequently. Previous studies have confirmed that the metabolic processes in fishe depend on the nutrient content of the diet. Fish that ingested high protein / low carbohydrate diets were found to have increased activities associated with the TCA cycle along with protein metabolism, while fish that ingested low protein / high carbohydrate diets were found to have increased activities in enzyme synthesis and pathways related to carbohydrate metabolism and the glycolysis process (Shimeno, 1974; Shimeno *et al.*, 1981; Hilton and Atkinson, 1982; Walton, 1986). This implies that the functional profiles of the intestinal microbiomes of aquatic organisms, including fishes and crabs, reflect the nutritional characteristics of their main food sources.

Chapter 3

Preliminary study on microeukaryotic community analysis using DNA metabaracoding to determine postmortem submersion interval (PMSI) in the drowned pig

3.1 Introduction

Drowning is one of the major causes of unnatural death in Korea. According to 2015 autopsy statistics provided by the National Forensic Service, the number of drowning cases was 427, accounting for 12.8% of unnatural deaths in Korea (Park *et al.*, 2016). However, it is difficult to determine the cause of death and estimate postmortem submersion interval (PMSI) when a drowned or abandoned corpse is found in water. To solve these drowning cases, investigators and forensic scientists have suggested several parameters. In terms of forensic taphonomy, accumulated degree-days (ADD) based on a morphological state of decomposition has been used to determine PMSI (Megyesi *et al.*, 2005; Heaton *et al.*, 2010). However, using ADD as evidence for PMSI has several limitations. The decomposition of a corpse in an aquatic environment is poorly studied and the biological decomposition process in water is easily affected by environmental factors (Piette and Els, 2006; Dickson *et al.*, 2011). In addition, the use of ADD can lead to a lack of objectivity because these standards related to the decomposition process are judged subjectively by individual researchers. To complement these flaws, aquatic organisms such as bacteria, fungi, algae, diatoms, and aquatic insects from a corpse have been used as biological indicators to estimate PMSI (Merritt and Wallace, 2001; Zimmerman and Wallace, 2008; Wallace, 2015). However, unlike the frequent use of insects from a corpse in terrestrial cases (Amendt *et al.*, 2004; Oliveira-Costa and Mello-Patiu, 2004; Sukontason *et al.*, 2005; Sukontason *et al.*, 2007; Bugelli *et al.*, 2018), studies on appearances of aquatic organisms in drowning cases have not been sufficiently conducted. In addition, morphological identification of these organisms requires a high level of expertise and a lot of time.

As mentioned in the General introduction, DNA metabarcoding, also known as high-throughput sequencing, can produce massive amounts of sequences and the means to identify multiple taxa from environmental samples. With these advantages, it has been widely applied in ecological and environmental studies to monitor biodiversity and detect several organisms from terrestrial or aquatic environmental samples (Taberlet *et al.*, 2012a; Thomsen *et al.*, 2012; Yoccoz *et al.*, 2012; Valentini *et al.*, 2016). DNA metabarcoding has also been applied to forensic fields (Weber-Lehmann *et al.*, 2014). Biological samples obtained from the scene of an incident often contain mixed samples. Thus, DNA metabarcoding can be used to detect several organisms from biological samples at one time (Yang *et al.,* 2014). However, forensic studies using DNA metabarcoding have been focused on terrestrial cases. Based on different bacterial biodiversity and community structures, several researchers have estimated time since death in terrestrial cases through DNA metabarcoding from both soil and corpses (Hyde *et al.*, 2013; Metcalf *et al.*, 2013; Pechal *et al.*, 2014; Metcalf *et al.*, 2016; Hyde *et al.*, 2017). Studies on the biodiversity and community structures of microeukaryotes related to drowning cases are very limited.

Therefore, this study investigated biodiversity and microeukaryotic community structures of car bonnet and pig carcass to determine the applicability of DNA metabarcoding in the drowning case. Pig carcass was used to simulate the decomposing process of drowning bodies. As a control, car bonnet was used to confirm the general process of succession occurring in an aquatic environment. The objectives of this chapter are the followings: (1) to confirm the correlation between decomposition and biodiversity; (2) to detect aquatic organisms related to decomposition; (3) to identify potential indicator

organisms for determining PMSI through changes in the relative abundance of taxa depending on decomposition period.

3.2 Materials and Methods

Sample collection for sequencing

A drowning experiment was conducted in a reservoir located in Gimje-si (35°88'25.86"N 126°96'38.01"E) from June 24, 2016, to August 21, 2016. After obtaining approval from the Institutional Animal Care and Use Committee of the Korean Police Investigation Academy (approval number: KPIA 16-02), the drowning experiment was performed. The pH, dissolved oxygen, biochemical oxygen demand, and chemical oxygen demand of the reservoir was measured as 8.1, 10.2 mg/L, 2.9 mg/L, and 9.0 mg/L, respectively. During the experiment, the average temperature of the surface of the reservoir was 28.3 ℃ and the average temperature of the bottom of the reservoir was 15.3 ℃. A pig was sacrificed in water and placed on a stainless tray and fixed on the bottom of the reservoir with a depth of 5 meters. At 20 meters from the pig, a car bonnet, as an abiotic control object was also placed on the bottom of the reservoir.

Samples for sequencing were collected by a SCUBA diver scraping the surfaces of the car bonnet and pig carcass with sterile swabs (Figure 20). The sampling areas were set to be 10 cm × 10 cm, and different sections were swabbed for each sampling. Samplings for two sample types (car bonnet samples and pig carcass samples) were performed every day from the first week to the fourth week (from June 25, 2016, to July 16, 2016) and then every three days from the fifth week to the ninth week (from July 19, 2016, to August 21, 2016). After collections, swab samples from car bonnet and pig carcass were immediately frozen and stored at -80°C.

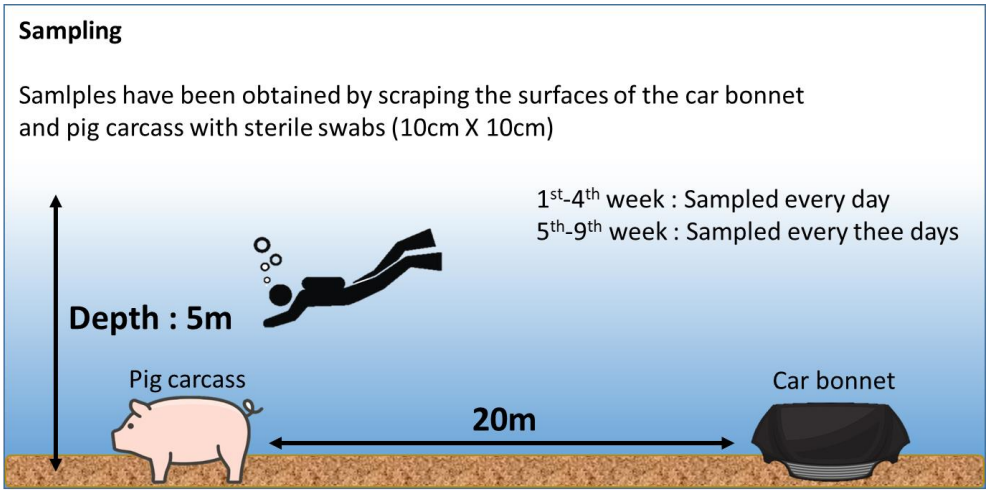

Figure 20. Schematic diagram of the sampling procedure in the drowning experiment.

DNA extraction, PCR amplification, and Illumina MiSeq sequencing

Genomic DNA was extracted from car bonnet samples or pig carcass samples using a PowerSoil DNA Isolation kit (MoBio, USA). The 18S ribosomal DNA (rDNA) V1-V2 variable region was amplified using a primer set SSU_F04/SSU_R22 (Blaxter *et al.*, 1998). PCR-amplified conditions were an initial denaturation at 95 °C for 2 min, 35 cycles of denaturation at 95 °C for 1 min, annealing at 57 °C for 45 s, and extension at 72 °C for 3 min, and a final extension at 72 °C for 10 min. All PCR products were confirmed by gel electrophoresis and purified using the QIAquick PCR Purification Kit (QIAGEN, Germany). Paired-end Illumina MiSeq sequencing (2 × 300 bp) was performed at Macrogen Inc. (Seoul, Korea).

Data analysis

Raw data from Illumina sequencing were analyzed with the custom python script "DNA_metabarcoding_analysis.py" based on the Querial Insights Into Microbial Ecology (QIIME) v 1.9.1. (Caporaso *et al.*, 2010) (Appendix 1). Forward and reverse reads were assembled into single contigs. Low-quality assembled contigs (Q < 30) were excluded from data analysis. After filtering reads for quality, operational taxonomic unit (OTU) clustering was performed using Usearch (Edgar, 2010). All OTUs were determined using a cut-off value of 97% similarity. Taxonomic categorical rank was assigned based on the most abundant sequence in each OTU using BLAST against the eukaryotic 18S rDNA database in NCBI. Information from the databases such as accession IDs, sequences, and taxonomic categorical ranks were parsed using Biopython (http://www.biopython.org). Sequences of pig, chimeric reads, and singleton OTUs were removed. To avoid biases of biodiversity data generated by the number of sequences, rarefaction was performed at a sequencing depth of 10,000 reads. Biodiversity indices were calculated by richness (the number of OTUs and Chao1), Shannon's diversity, and equitability. Constrained analysis of principal coordinates (CAP) using Bray-Curtis dissimilarities was performed to see changes in microeukaryotic community structures according to sample type and decomposition period for each sample type. Decomposition periods of the two sample types were determined according to the decomposition period suggested by Anderson and Hobischak (2004) [Fresh period (n = 10) : 0–9 days, Bloat period (n = 19): 9-35 days, and Active period (n = 6): 35+ days] because it was difficult to discern decomposition period morphologically due to adipocere formation of the carcass. I tested for the statistical significance of the CAP analysis using ANOVA with 999 random permutations. Taxonomic composition of

microeukaryotic community structures were analyzed by major kingdom (Animalia, Chromista, Fungi, Plantae, and the others) and major genus (10 most abundant taxonomic genera in the two sample types).

Statistical analysis

To compare biodiversity and community structures of microeukaryotes between sample types and between decomposition periods for each sample type, statistical analysis was performed. A pairwise Wilcoxon rank sum test was used to test significant differences in biodiversity and community structures of microeukaryotes between sample types. Significant differences in biodiversity and community structures according to the decomposition period for each sample type were checked by the Kruskal-Wallis test. To determine significant differences in biodiversity and relative abundances of the major kingdom and genus, pairwise comparisons were conducted using the Wilcoxon rank sum between two of three decomposition periods (Fresh-Bloat, Bloat-Active, and Fresh-Active period). All statistical calculations were performed using R v. 3.3.0. and results were visualized by plots with ggplot2 and Phyloseq in the R package (McMurdie and Holmes, 2013; Team, 2014; Wickham, 2016). Calculated *P* values were revised using the false discovery rate (FDR) by the Benjamini-Hochberg procedure (Benjamini and Hochberg, 1995).

3.3 Results

The results of Illumina MiSeq sequencing

Using Illumina sequencing, a total of 8,149,316 and 8,756,022 sequences were produced from car bonnet and pig carcass, respectively. After trimming and filtering, 2,787,156 and 2,869,242 reads remained for car bonnet and pig carcass, respectively. The numbers of OTUs in the car bonnet and pig carcass were 351 and 275 OTUs, respectively. A total of 212 OTUs were shared between the two sample types. All Good's coverage values in both samples were over 0.98, indicating that the number of reads was enough to analyze biodiversity in both samples. In terms of taxonomic categorical ranks, car bonnet samples consisted of 32 phyla, 81 classes, 151 orders, 191 families, and 241 genera while pig carcass samples consisted of 32 phyla, 68 classes, 121 orders, 154 families, and 195 genera. Thirty phyla, 54 classes, 94 orders, 115 families, and 145 genera were shared by both samples.

Comparison of biodiversity and community structures between sample types

When comparing biodiversity indices between the two sample types, all biodiversity indices [richness (the number of OTUs and Chao1), Shannon's diversity, and equitability] were significantly higher in car bonnet than those in the pig carcass ($P < 0.001$ for all indices) (Figure 21A).

CAP analysis based on Bray-Curtis dissimilarities indicated that sample types had a significant effect on the formation of microeukaryotic community structures ($P = 0.001$, 41.2% explanatory power) (Figure 21B). In addition, the taxonomic composition of the

microeukaryotic community differed significantly between sample types. At the kingdom level, Animalia was dominant in car bonnet. However, relative abundances of Plantae, Fungi, and Chromista were higher in pig carcass (Figure 22A). At the genus level, relative abundances of *Acartia* ($P < 0.001$), *Laxus* ($P < 0.001$), *Membranipora* ($P < 0.001$), and *Metacyclopina* ($P < 0.001$) were higher in car bonnet, while those of *Achlya* ($P < 0.001$), *Hydrodictyon* ($P < 0.001$), and *Saprolegnia* ($P < 0.001$) were significantly higher in pig carcass (Figure 22B). However, relative abundances of *Filobasidium*, *Lobosphaera,* or *Scenedesmus* were not different between the two sample types ($P = 0.131$, $P = 0.274$, and $P = 0.161$, respectively).

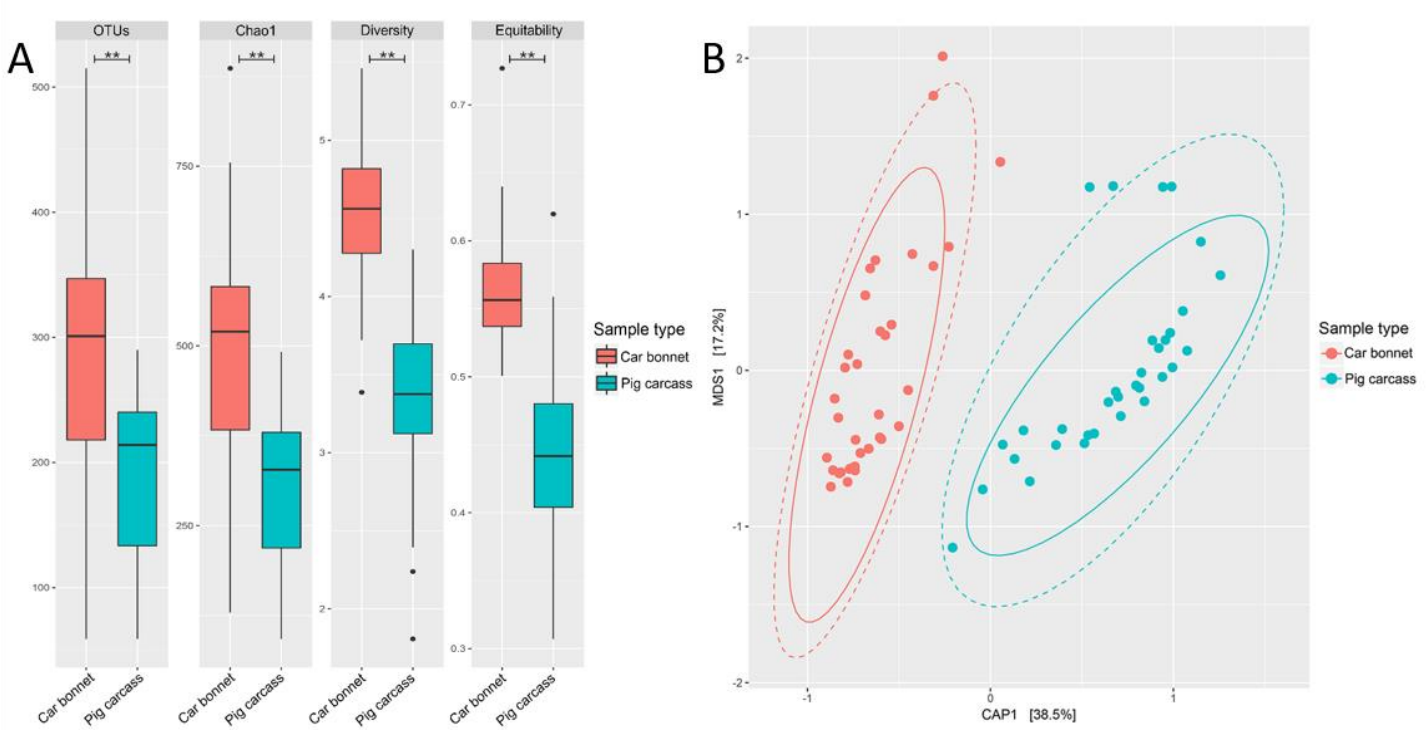

Figure 21. Biodiversity and microeukaryotic communities between car bonnet and pig carcass. (A) Biodiversity indices of two sample types. All indices of biodiversity were compared between sample types using the Wilcoxon rank sum test. All P values were adjusted using the false discovery rate (FDR) presented by Benjamini and Hochberg (** $P < 0.01$). (B) CAP plots for microeukaryotic communities between sample types.

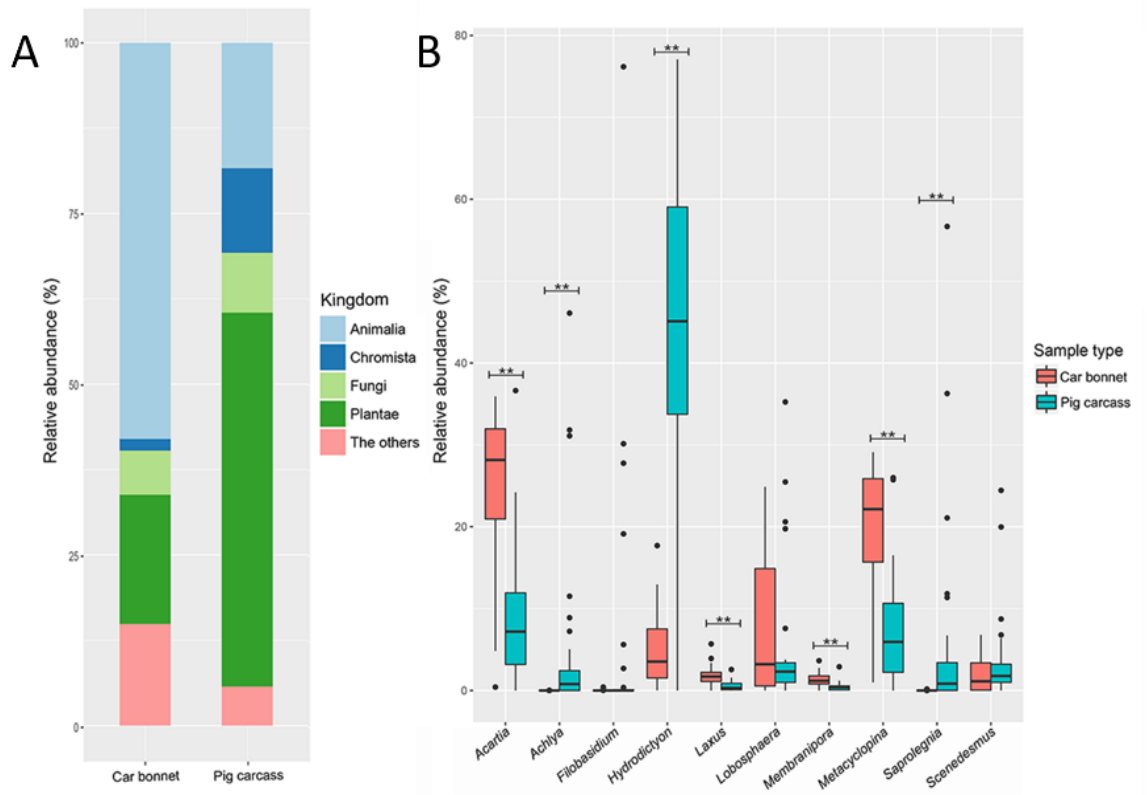

Figure 22. Relative abundances of the major (A) kingdom and (B) genus levels in car bonnet and pig carcass. The significant difference in relative abundances between sample types was calculated using the pairwise Wilcoxon rank sum test. All P values were adjusted using the false discovery rate (FDR) presented by Benjamini and Hochberg (** $P < 0.01$)

Comparison of biodiversity and community structures between decomposition periods in each sample type

Richness indices (the number of OTUs and Chao1) in car bonnet were not significantly different between the Fresh and Bloat periods and were decreased in the Active period (Figure 23). This change pattern was similar to that of pig carcass. However, the change pattern of Shannon's diversity index and the equitability index in the two sample types were different from each other according to decomposition periods.

To determine changes in microeukaryotic community structures according to the decomposition period, CAP analysis was conducted based on Bray-Curtis dissimilarities. Microeukaryotic community structures were significantly separated according to the decomposition period in both car bonnet (P = 0.001, 28.4% explanatory power) and pig carcass (P = 0.001, 31.4% explanatory power) (Figure 24). The taxonomic composition of the microeukaryotic community according to the decomposition period differed between the two sample types (Figure 25, Tables 16 and 17). In case of car bonnet, the relative abundances of Animalia and Plantae were significantly different between the Fresh and Bloat periods. *Laxus* (included in Animalia) was detected less in the Bloat period than that in the Fresh period while *Lobosphaera* and *Scenedesmus* (included in Plantae) were detected more in the Bloat period than those in the Fresh period. Compared to the relative abundance of the major kingdom in the Bloat and Active period, relative abundances of all major kingdoms (Animalia, Chromista, Fungi, and Plantae) were not significantly different between the two periods ($P = 0.199$, $P = 1.000$, $P = 0.376$, and $P = 0.820$, respectively). At

the genus level, *Hydrodictyon, Membranipora,* and *Scenedesmus* were less detected in the Active period than those in the Bloat period.

In case of pig carcass, Fungi (*Filobasidium*) were outstandingly detected in the Fresh period but hardly detected in the Bloat period (Figure 25, Tables 16 and 17). Relative abundances of Animalia (*Acartia*, *Laxus*, *Membranipora*, and *Metacyclopina*) and Chromista (*Achlya* and *Saprolegnia*) were significantly decreased in the Active period compared to those in the Bloat period. Besides differences in the relative abundance of Fungi, Animalia and Chromista, the relative abundance of Plantae (*Lobosphaera*, *Hydrodictyon*, and *Scenedesmus*) increased according to the decomposition period. The relative abundance of *Lobosphaera* was significantly different among decomposition periods (between the Fresh and Bloat periods and between the Bloat and Active periods). The increase in relative abundance of *Lobosphaera* was greater in the Bloat-Active period compared to that of the Fresh-Bloat period. The relative abundance of *Hydrodictyon* was significantly different in the Fresh-Bloat period. In case of *Scenedesmus*, the relative abundance differed statistically at the Bloat-Active period.

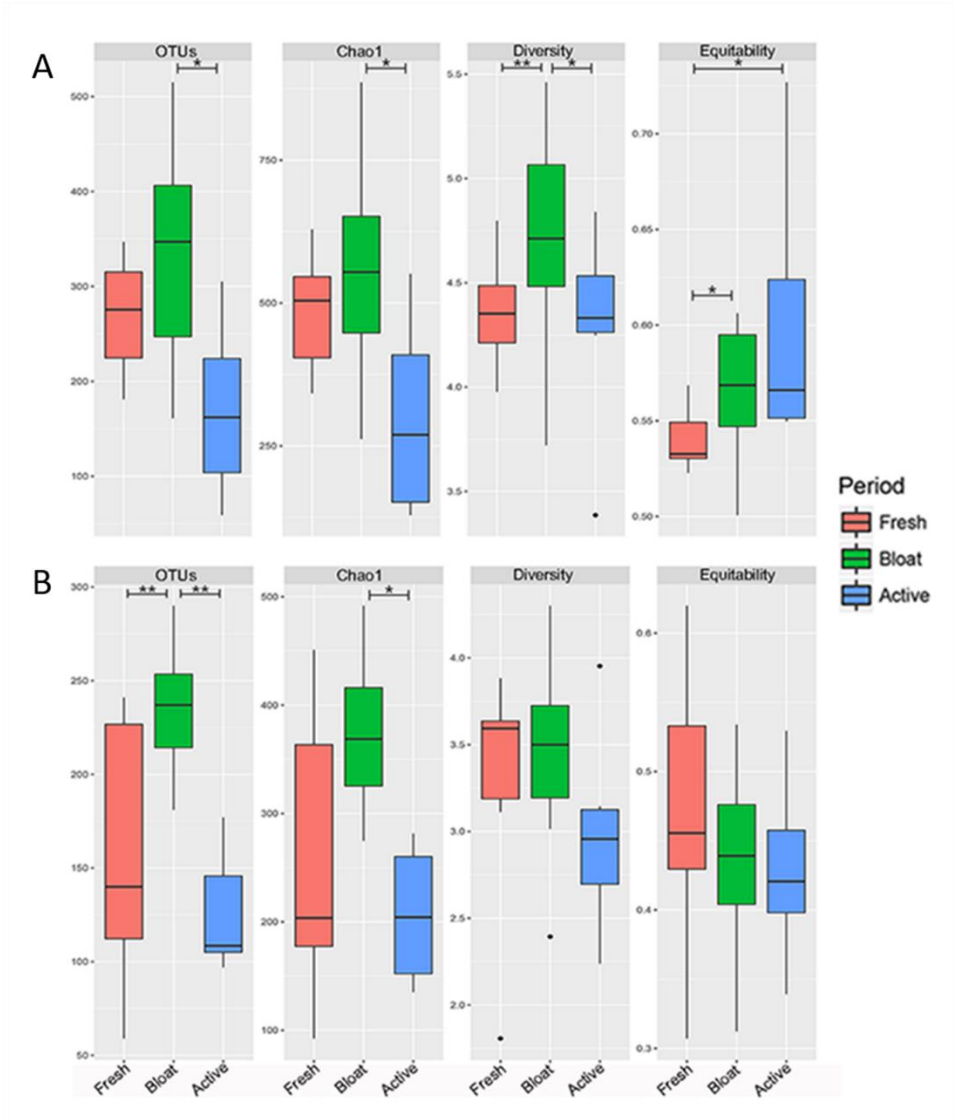

Figure 23. Biodiversity indices of (A) car bonnet and (B) pig carcass according to the decomposition period. The significance of diversity indices between decomposition periods in each sample type was calculated using the Kruskal-Wallis test. As a post hoc test, pairwise comparisons were conducted using the Wilcoxon rank sum test to check for significant differences between decomposition periods. All P values were adjusted using the false discovery rate (FDR) presented by Benjamini and Hochberg (**: $P < 0.01$, *: $P < 0.05$, N.S.: no significance).

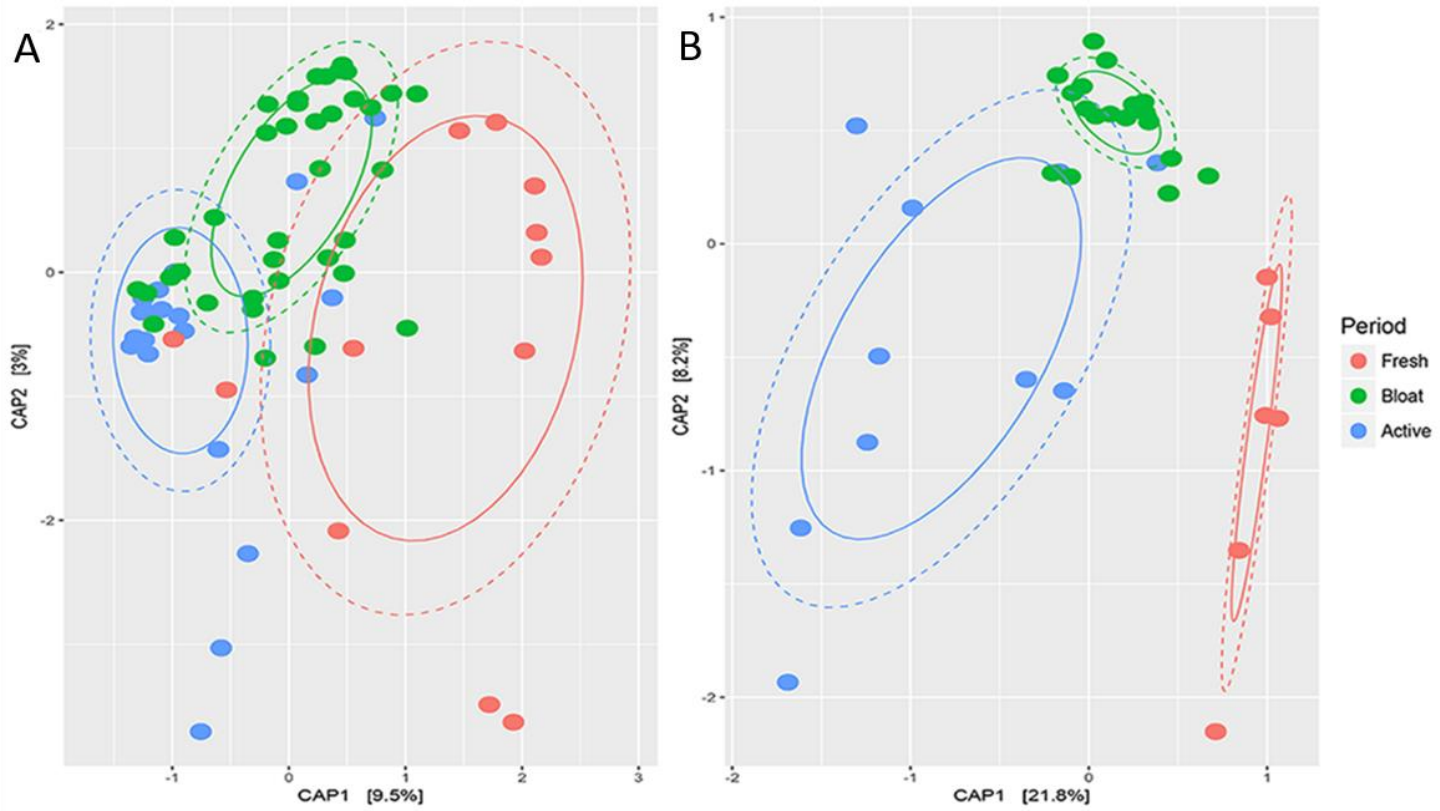

Figure 24. CAP plots for microeukaryotic communities of (A) car bonnet and (B) pig carcass according to the decomposition period.

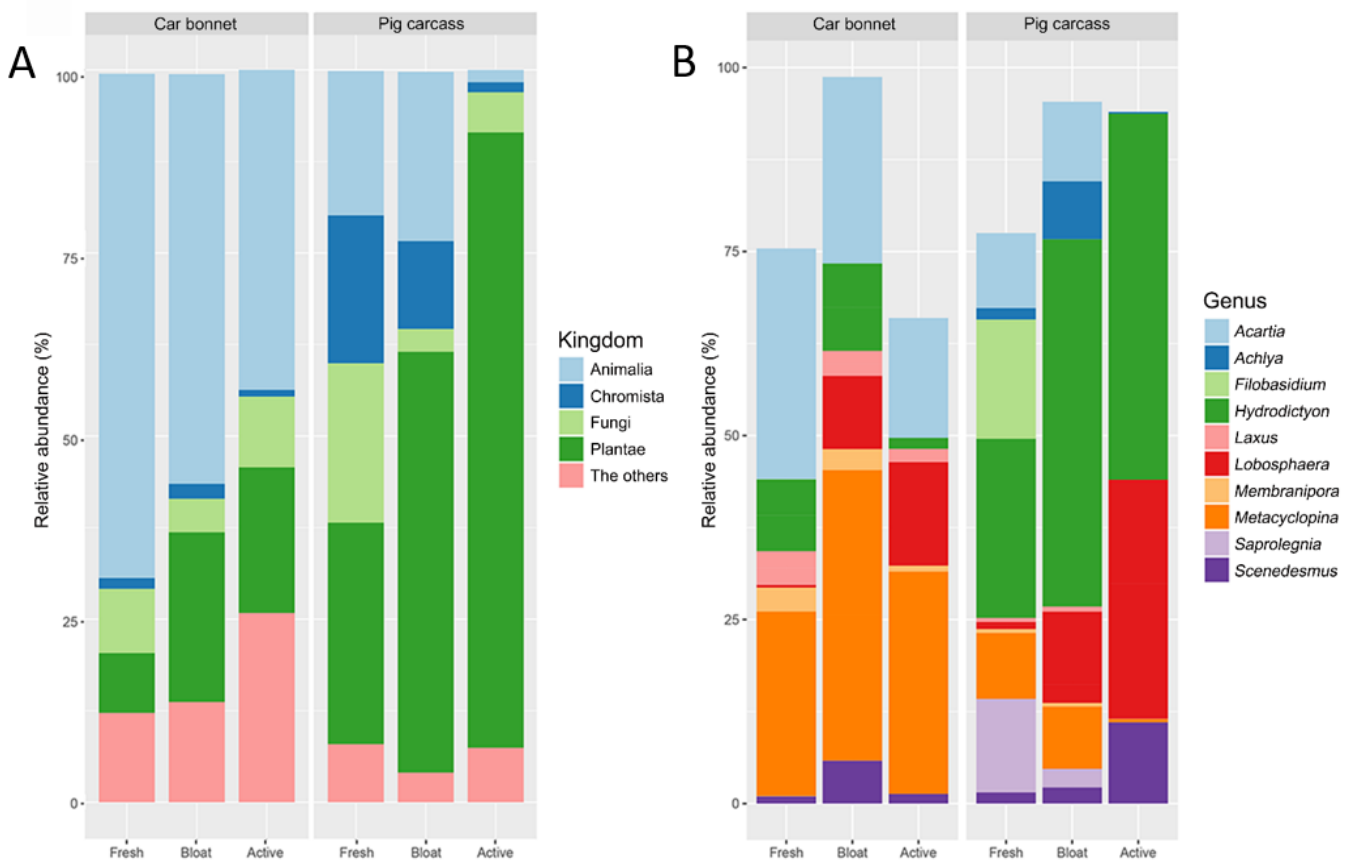

Figure 25. Relative abundances of the major (A) kingdom and (B) genus levels by the decomposition period.

Table 16. Average proportions (%) of the major kingdom by the decomposition period. Standard errors of average proportions of major kingdom according to the decomposition period in each sample type are shown in brackets. The significance of average proportions of the major kingdom between decomposition periods in each sample type was calculated using the Kruskal-Wallis test. Names in bold indicate that the p-value is below 0.05. As a post hoc test, pairwise comparisons were conducted using the Wilcoxon rank sum test to check for significant differences between decomposition periods. All P values were adjusted using the false discovery rate (FDR) presented by Benjamini-Hochberg (**: $P < 0.01$, *: $P < 0.05$, N.S.: no significance).

Sample type	Kingdom	Decomposition period			Post hoc test		
		Fresh	Bloat	Active	Fresh- Bloat	Bloat-Active	Fresh-Active
Car bonnet	**Animalia**	69.08 (2.21)	57.06 (3.65)	38.68 (10.21)	*	N.S.	*
	Chromista	3.14 (0.29)	3.88 (0.41)	4.53 (1.94)	N.S.	N.S.	N.S.
	Fungi	8.85 (1.82)	4.56 (0.52)	11.12 (4.16)	N.S.	N.S.	N.S.
	Plantae	8.65 (1.34)	22.90 (3.40)	21.59 (5.37)	**	N.S.	N.S.
	The others	10.28 (0.81)	11.59 (0.76)	24.09 (5.02)	**	N.S.	**
Pig carcass	**Animalia**	23.43 (4.03)	22.57 (3.10)	1.59 (0.34)	N.S.	**	**
	Chromista	19.42 (5.33)	12.11 (3.50)	5.56 (3.94)	N.S.	**	N.S.
	Fungi	20.87 (0.45)	3.14 (0.31)	5.81 (2.57)	**	N.S.	N.S.
	Plantae	28.57 (4.68)	59.15 (3.57)	82.87 (4.65)	**	**	**
	The others	7.70 (0.58)	3.04 (0.38)	4.17 (1.82)	N.S.	N.S.	N.S.

Table 17. Average proportions (%) of the major genus by decomposition period. Standard errors of average proportions of major genus level according to decomposition period are shown in brackets. The significance of average proportions of major genus level between decomposition periods was calculated using the Kruskal-Wallis test. Names in bold indicated that the p-value is below 0.05. As a post hoc test, pairwise comparisons were conducted using the Wilcoxon rank sum test to check for significant differences between decomposition periods. All P values were adjusted using the false discovery rate (FDR) presented by Benjamini-Hochberg (**: $P < 0.01$, *: $P < 0.05$, N.S.: no significance).

Sample type	Genus	Decomposition period			Post hoc test		
		Fresh	Bloat	Active	Fresh- Bloat	Bloat-Active	Fresh-Active
Car bonnet	***Acartia***	31.34 (0.80)	25.7 (1.77)	13.42 (4.97)	N.S.	N.S.	**
	Achlya	0.00 (0.00)	0.00 (0.00)	0.00 (0.00)	N.S.	N.S.	N.S.
	Filobasidium	0.06 (0.04)	0.01 (0.01)	0.00 (0.00)	N.S.	N.S.	N.S.
	Hydrodictyon	4.87 (1.23)	5.87 (1.17)	0.88 (0.49)	N.S.	**	**
	Laxus	2.29 (0.17)	1.77 (0.28)	0.65 (0.44)	*	N.S.	N.S.
	Lobosphaera	0.36 (0.17)	9.58 (1.86)	16.30 (2.97)	**	N.S.	**
	Membranipora	1.62 (0.19)	1.38 (0.21)	0.40 (0.24)	N.S.	*	*
	Metacyclopina	25.09 (0.97)	20.09 (1.38)	12.71 (4.59)	N.S.	N.S.	N.S.
	Saprolegnia	0.02 (0.02)	0.01 (0.01)	0.00 (0.00)	N.S.	N.S.	N.S.
	Scenedesmus	0.49 (0.20)	2.88 (0.49)	0.71 (0.70)	**	**	N.S.

Table 17. Continued.

Sample type	Genus	Decomposition period			Post hoc test		
		Fresh	Bloat	Active	Fresh- Bloat	Bloat-Active	Fresh-Active
Pig carcass	***Acartia***	10.18 (3.21)	10.23 (1.50)	0.00 (0.00)	N.S.	**	**
	Achlya	1.56 (1.12)	7.54 (3.06)	0.00 (0.00)	N.S.	**	N.S.
	Filobasidium	16.20 (7.65)	0.01 (0.01)	0.00 (0.00)	**	N.S.	**
	Hydrodictyon	24.34 (7.04)	50.41(3.02)	47.67 (7.00)	**	N.S.	**
	Laxus	0.56 (0.17)	0.64 (0.14)	0.00 (0.00)	N.S.	**	**
	Lobosphaera	0.60 (0.32)	2.76 (0.33)	20.59 (5.44)	**	**	**
	Membranipora	0.54 (0.27)	0.48 (0.07)	0.06 (0.06)	N.S.	**	N.S.
	Metacyclopina	8.95 (2.98)	8.07 (0.99)	0.22 (0.16)	N.S.	**	**
	Saprolegnia	12.70 (5.98)	2.37 (1.11)	0.02 (0.02)	N.S.	*	**
	Scenedesmus	1.52 (0.68)	3.14 (0.99)	9.25 (3.98)	N.S.	*	*

3.4 Discussion

As a preliminary study, I used DNA metabarcoding to investigate biodiversity and community structures of microeukaryotes associated with decomposition of pig carcass drowned in a reservoir using a submerged car bonnet as a control. The results of this study showed that biodiversity and community structures of the microeukaryotes were significantly differed depending on the two sample types. In addition, I found that *Achyla*, *Hydrodictyon,* and *Saprolegnia* were detected more in pig carcass than those in car bonnet. Unlike the taxonomic composition of car bonnet, relative abundances of fungi, water molds, and algae in pig carcass were discriminatively different according to decomposition period.

The correlation between biodiversity and decomposition of drowned pig

All biodiversity indices (the number of OTUs, Chao1, Shannon's diversity, and equitability) were significantly lower in pig carcass than those in the car bonnet (Figure 21A). This may be due to decomposition of pig carcass as a result of environmental changes. A decaying pig carcass is a specific habitat for certain organisms (Braig and Perotti, 2009; Gennard, 2012). The richness of car bonnet was relatively higher than that of pig carcass because organisms living in the freshwater environment can attach themselves to the car bonnet. Conversely, the low richness found in pig carcass might reflect the changing environmental conditions associated with decomposition that might be only favorable to specific organisms. Unlike car bonnet, only a small number of organisms such as decomposers, producers, and scavengers seemed to settle down successfully on decaying pig carcass

tissue. The relatively low equitability index of pig carcass showed that only some kinds of organisms were dominant on the surface of pig carcass.

In general, biodiversity is known to have an inverse relationship with the decomposition process. Previous studies have found that taxon richness decreases as decomposition progresses (Zimmerman and Wallace, 2008; Pechal *et al.*, 2014). On the other hand, this study showed that the number of OTUs in pig carcass slightly increased in the Bloat period (9-35 days) than in the Fresh period (0-9 days) (Figure 23B). Similar to this study, the number of species in soil communities in buried cadavers was increased slightly during the period from 0-3 months to 4-6 months in a previous study (Finley *et al.*, 2016). These study may suggest that richness does not always decrease as decomposition progresses. In addition, richness indices in car bonnet and pig carcass had similar change pattern according to the decomposition period. Species richness is affected by complex environmental factors such as temperature, salinity, and organic matter (Gough *et al.*, 1994; Jetz and Rahbek, 2002). This implies that the change pattern of microeukaryotic richness indices in this study might be influenced by other factors (e.g., temperature) more than just the decomposition process. Given these results, it seems difficult to determine PMSI solely based on richness.

Characteristics of microeukaryotes related to the decomposition of drowned pig

Microeukaryotic community structures were clearly different between the two sample types (Figure 21B). Relative abundances of *Acartia*, *Laxus, Membranipora,* and *Metacyclopina* (included in Animalia) were higher in car bonnet than those in pig carcass (Figure 22). Copepods, bryozoans, and nematodes included in these taxa are known to be dominant in

a natural Freshwater environment (Heip *et al.*, 1985; Okamura and Hatton-Ellis, 1995; Boxshall and Defaye, 2007). These taxa might have directly attached to the surface of car bonnet. In contrast to car bonnet, *Achlya, Saprolegnia* (included in Chromista), and *Hydrodictyon* (included in Plantae) were significantly more abundant in pig carcass. These dominant taxa are associated with decomposition and known to play a significant role in the nutrient cycle in aquatic environments (Bitton and Dutka, 1983; Rabalais, 2002; Strauss and Lamberti, 2002). For example, decomposers such as bacteria, fungi, and other microeukaryotes can convert nitrogen compounds back to amino acids, ammonia, and other nitrogenous forms (Newell *et al.*, 1995; Gessner *et al.*, 2007). Genera *Achlya* and *Saprolegnia* are classified as water mold. The family Saprolegniaceae (containing *Achlya* and *Saprolegnia*) is widely distributed in freshwater environments. Freshwater water molds can grow on decaying organic matter. They play an important role as decomposers (Ward, 1883). Inorganic nutrients produced by decomposers such as water molds are linked to the dominance of *Hydrodictyon* in pig carcass. *Hydrodictyon* is a green alga known as "water net". This water net requires a large amount of nitrogen to survive (Lelkova and Pouličkova, 2004; Volodina and Gerb, 2013). The relative abundance of *Hydrodictyon* was much higher in pig carcass than that in car bonnet. It could be inferred that *Hydrodictyon* was dominant in pig carcass because *Hydrodictyon* needed nutrients (e.g., nitrogen) produced by the decomposers present on decaying pig tissue.

Characteristics of microeukaryotes according to decomposition period in drowned pig

Microeukaryotic community structures in pig carcass were significantly different according to the decomposition period (Figure 24B). Such differences of the taxonomic composition in communities between decomposition periods might be linked to nutrients released from pig carcass. Community structure is influenced by many factors, including the availability of nutrients (e.g., nitrogen and phosphorous) and environmental parameters (e.g., sunlight levels, temperature, season, and salinity) (Deswati, 2018). The detection of *Filobasidium* in the Fresh period might be related to nitrogen released from pig carcass (Figure 25B, Tables 16 and 17). Nitrogen is abundant in the soft tissues of a corpse. The release of nitrogen from carcass occurs during a relatively early period of decomposition compared to other nutrients (Parmenter and Lamarra, 1991). Freshwater fungi serve as decomposers in a freshwater environment. They are known as early successional taxa (Gessner and Van Ryckegem, 2003; Tsui *et al.*, 2016). Fungi are dominant when there is a high proportion of nitrogen (Wardle *et al.*, 2004; Güsewell and Gessner, 2009). In contrast to the Fresh period, *Filobasidium* was hardly detected in the Bloat period. These can be explained that *Filobasidium* needs a high proportion of nitrogen to live and the concentration of nitrogen may be different between the Fresh and Bloat periods. Therefore, *Filobasidium* is regarded as a good indicator for the Fresh period of decomposition. Although water molds perform the same role as fungi, *Achlya* and *Saprolegnia* existed until the Bloat period. Considering these results, water molds (*Achlya* and *Saprolegnia*) can act as decomposers longer than fungi (*Filobasidium*), and they are less sensitive to the release of nitrogen than fungi.

The dominance of algae in the decomposition process might also be associated with nutrients released from pig carcass (Figure 25A, Tables 16 and 17). In this study, the relative abundance of algae (included in Plantae) in pig carcass was increased as decomposition progressed, consistent with previous studies showing that the chlorophyll *a* concentration of algae in drowning pigs increased according to the time period (Haefner *et al.*, 2004). This might be due to the activities of decomposers during decomposition. Decomposers such as bacteria and fungi play important roles in the decomposition process by breaking down organic compounds into large amounts of nutrients such as nitrogen, carbon, and phosphorous. Producers such as plants and algae can acquire these inorganic nutrients (Zak and Grigal, 1991; Kaye and Hart, 1997; Grattan and Suberkropp, 2001; Niyogi *et al.*, 2003). A sufficient supply of nutrients by decomposer activities will lead to an increase in the number of algae. In this study, the average proportion of algae (included in Plantae) reached 84% when the decomposition period was changed from the Bloat period to Active period (Figure 26A). On the contrary, the average proportions of Animalia, Chromista, and Fungi plummeted in the Bloat-Active period. These results seemed to be caused by the depletion of dissolved oxygen due to the activities of decomposers. When a corpse decomposes in the water, the decayed organic matter becomes food sources for decomposers. Increasing the number of decomposers and their activities on decayed tissues will lead to depletion of dissolved oxygen, resulting in the death of other aquatic organisms except for algae.

The relative abundance of algae (included in Plantae) increased at different decomposition periods depending on the genus (Figure 26B). This might be associated with a change in the proportion of nutrients released from pig carcass according to the time of

decomposition. While a corpse decomposes, nitrogen is first released from soft tissues (Figure 27). Fatty tissues such as internal organs and the face also break down into fatty acids. When bones of the corpse are exposed via decomposition, components of bones such as phosphorus, calcium, and magnesium are released (Parmenter and Lamarra, 1991; Ueland *et al.*, 2014). Given these results, the proportion of nutrients released from the corpse is initially rich in nitrogen. As decomposition progresses, the proportions of other nutrients (e.g., carbon and phosphate) released from the corpse increase. Alga has its distinct optimal nutritional ratios. It has different growth rates according to nutrient levels (e.g., nitrogen, phosphorus, carbon, and silica) in water (Lund, 1972; Tilman *et al.*, 1982; Stelzer and Lamberti, 2001). In this study, the relative abundances of *Hydrodictyon*, *Lobosphaera*, and *Scenedesmus* increased at different periods (Figure 26B). It might be related to changes in the proportion of nutrients according to the decomposition period in water. When the decomposition period changed from the Fresh period to the Bloat period, the relative abundance of *Hydrodictyon* was significantly increased. It seems that *Hydrodictyon* has a higher growth rate when nitrogen content is high compared to *Lobosphaera* and *Scenedesmus*. Thus, the growth of *Hydrodictyon* might be useful as a good indicator to distinguish the Fresh period and the Bloat period. Compared to the Fresh period, relative abundances of *Lobosphaera* and *Scenedesmus* were significantly increased in the Bloat-Active period. These results suggest that *Lobosphaera* and *Scenedesmus* may prefer other nutrients rather than nitrogen. *Lobosphaera* and *Scenedesmus* are also green algae like *Hydrodictyon*. Although studies on the growth of *Lobosphaera* and optimal nutritional ratio for *Lobosphaera* are insufficient, the growth of *Scenedesmus* is known to

need polyphosphates (Rhee, 1972; Rhee, 1973). These results suggest that the growth of these algae is more affected by other nutrients than nitrogen.

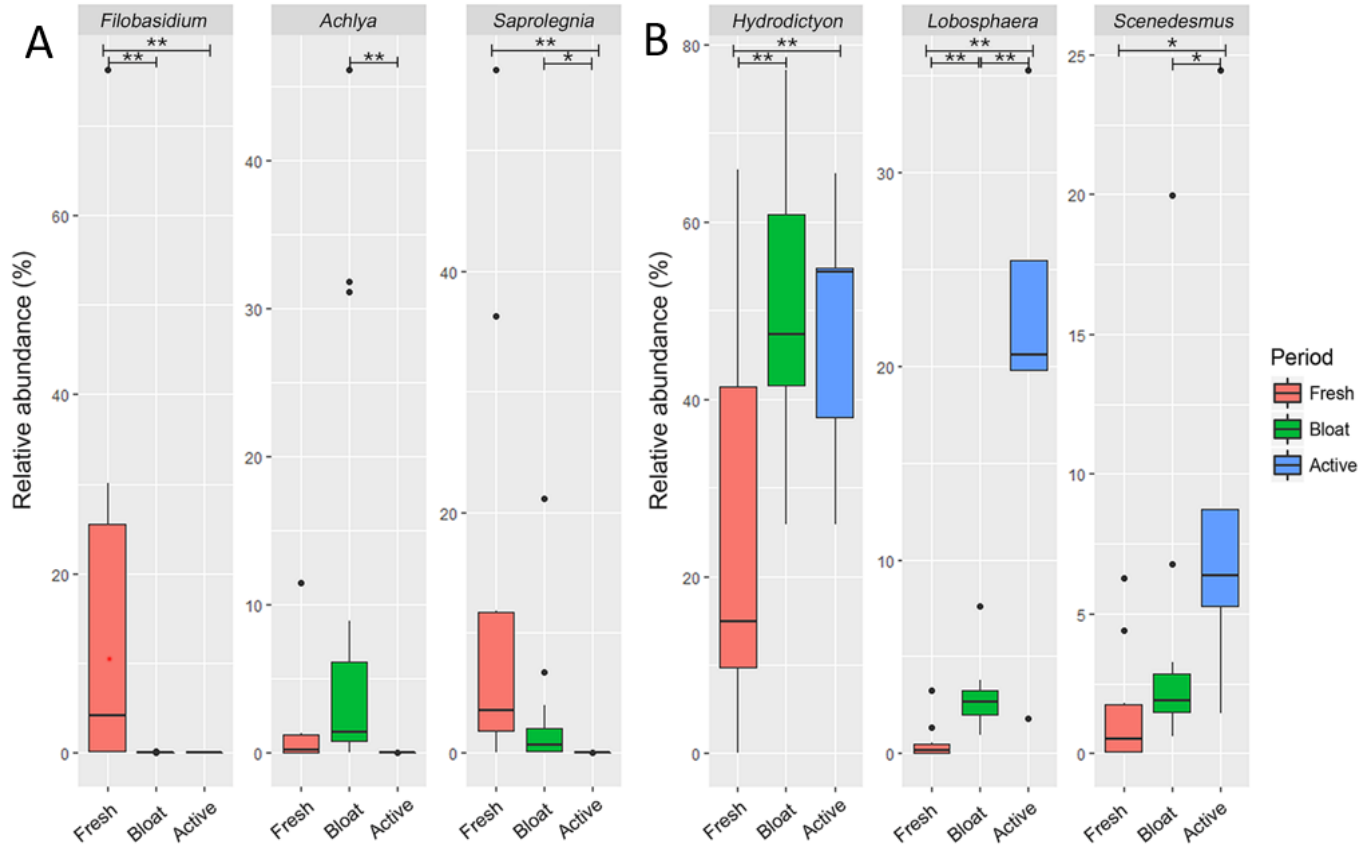

Figure 26. Relative abundances of the (A) decomposers and (B) algae in pig carcass according to the decomposition period.

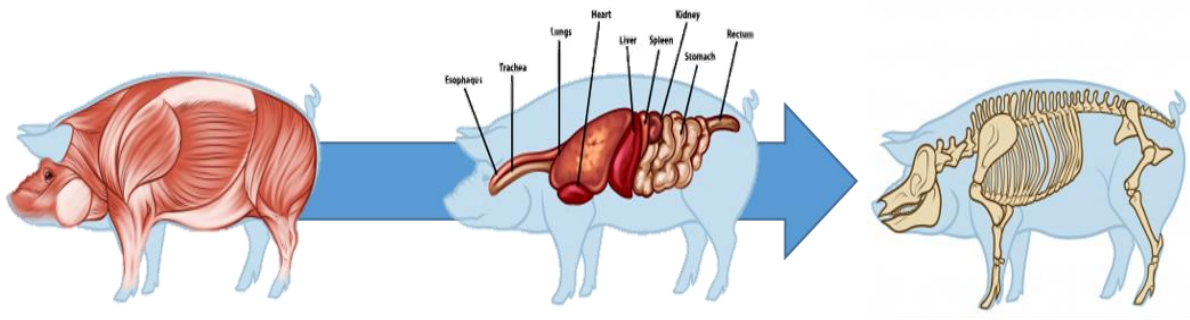

Decomposition site	Soft tissues	Internal organs, face	Bones
Released nutrients	**Nitrogen↑**	Fatty acid	**Phosphorus, Calcium ↑** **Nitrogen ↓**
The proportion of nutrients	**Rich in nitrogen**		**Rich in phosphorus and calcium**

Figure 27. The mechanism of decomposition.

Conclusions

Conclusions

In this dissertation, I applied the DNA metabarcoding approach to various case studies in aquatic environments and drawn some meaningful results. In Chapter 1, DNA metabarcoding was used to establish an efficient survey and research method for mesozooplankton community analysis in the Marine and Coastal National Parks of Korea. In Chapter 2, the relationship between the family of crabs and feeding behaviors on intestinal microbiomes of Korean crabs was confirmed through DNA metabarcoding. In Chapter 3, as a case study, I investigated microeukaryotic biodiversity and community structures of car bonnet and pig carcass to determine the applicability of DNA metabarcoding in drowning case.

These results have revealed the strength of DNA metabarcoding: 1) DNA metabarcoding enables efficient identification of biotic communities in aquatic environments. The use of DNA metabarcoding is efficient in terms of time and labor for large scale community surveys in large areas such as the Marine and Coastal National Parks of Korea. Given 2 % of microbes on Earth are culturable, it is also essential to use DNA metabarcoding for the study of symbiotic microbiomes. DNA metabarcoding is also effective in the community analysis of aquatic organisms associated with drowning cases that are difficult to study due to physical constraints; 2) DNA metabarcoding has the ability to detect indicator taxa that enable identify and represent change pattern in biotic communities due to changes in external factors. These taxa are believed to be useful in determining abnormal climates in marine ecosystems (e.g., global warming) and the decomposition periods of drowned bodies; 3) DNA metabarcoding can also be used as a

tool to identify taxa with high research value in future studies, such as the phylum Rotifera (see Chapter 1) and the family Mycoplasmataceae in Chapter 2. However, the improvements about the technical biases shown in Chapter 1 must be considered in order for DNA metabarcoding to be more widely used in the future. Also, further studies under various conditions (e.g., additional sampling and primer sets, extensions of target organisms, and application in various environments and situations) are also required.

I believe that the results of this dissertation will serve as background data for various studies of aquatic environments using DNA metabarcoding. The establishment of a monitoring system using DNA metabarcoding according to the method proposed in Chapter 1 will help identify the mid- to long-term patterns of changes in the zooplankton community and changes in the bioindicator taxa due to changes in the environment, making it an effective tool for the management of marine ecosystems in the Marine and Coastal National Parks. The results shown in Chapter 2, provide the first evidence to detect the host-intestinal microbiome patterns of crab hosts, in tandem with discovering the relationship between the evolutionary history and feeding behavior found in vertebrates, and expect to be used as a backbone data for symbiotic microbiome studies in aquatic organisms. Although further studies are needed, the results of Chapter 3 suggest that the DNA metabarcoding approach to microeukaryotic community structure could be applied to estimate PMSI in the forensic investigations of drowning cases.

References

Abad, D., Albaina, A., Aguirre, M., and Estonba, A. 2017. 18S V9 metabarcoding correctly depicts plankton estuarine community drivers. *Marine Ecology Progress Series* **584**, 31-43.

Adamowicz, S.J., Boatwright, J.S., Chain, F., Fisher, B.L., Hogg, I.D., Leese, F., Lijtmaer, D.A., Mwale, M., Naaum, A.M., and Pochon, X. 2019. Trends in DNA barcoding and metabarcoding. *Genome* **62**, v-viii.

Albaina, A., Aguirre, M., Abad, D., Santos, M., and Estonba, A. 2016. 18S rRNA V9 metabarcoding for diet characterization: a critical evaluation with two sympatric zooplanktivorous fish species. *Ecology and Evolution* **6**, 1809-1824.

Amaral-Zettler, L.A., McCliment, E.A., Ducklow, H.W., and Huse, S.M. 2009. A method for studying protistan diversity using massively parallel sequencing of V9 hypervariable regions of small-subunit ribosomal RNA genes. *PloS one* **4**.

Amendt, J., Krettek, R., and Zehner, R. 2004. Forensic entomology. *Naturwissenschaften* **91**, 51-65.

Anderson, G., and Hobischak, N. 2004. Decomposition of carrion in the marine environment in British Columbia, Canada. *International journal of legal medicine* **118**, 206-209.

Andruszkiewicz, E.A., Starks, H.A., Chavez, F.P., Sassoubre, L.M., Block, B.A., and Boehm, A.B. 2017. Biomonitoring of marine vertebrates in Monterey Bay using eDNA metabarcoding. *PLoS One* **12**, e0176343.

Apprill, A., McNally, S., Parsons, R., and Weber, L. 2015. Minor revision to V4 region

SSU rRNA 806R gene primer greatly increases detection of SAR11 bacterioplankton. *Aquatic Microbial Ecology* **75**, 129-137.

Araujo, H.M.P. 2006. Distribution of Paracalanidae species (Copepoda, Crustacea) in the continental shelf off Sergipe and Alagoas states, Northeast Brazil. *Brazilian Journal of Oceanography* **54**, 173-181.

Aylagas, E., Borja, Á., Irigoien, X., and Rodríguez-Ezpeleta, N. 2016. Benchmarking DNA metabarcoding for biodiversity-based monitoring and assessment. *Frontiers in Marine Science* **3**, 96.

Baek, S.H., Kim, D., Choi, H.-W., and Kim, Y.O. 2013. Hydrographical and Bio-ecological Characteristics of Heterotrophic Red Tide Dinoflagellate Noctiluca scintillans in Semi-enclosed Gwangyang Bay, Korea. *Korean Journal of Environmental Biology* **31**, 308-321.

Benjamini, Y., and Hochberg, Y. 1995. Controlling the false discovery rate: a practical and powerful approach to multiple testing. *Journal of the royal statistical society. Series B (Methodological)*, 289-300.

Bertini, G., Fransozo, A., and de Melo, G.A. 2004. Biodiversity of brachyuran crabs (Crustacea: Decapoda) from non-consolidated sublittoral bottom on the northern coast of São Paulo State, Brazil. *Biodiversity & Conservation* **13**, 2185-2207.

Bitton, G., and Dutka, B. 1983. Bacterial and biochemical tests for assessing chemical toxicity in the aquatic environment: A review. *Critical Reviews in Environmental Science and Technology* **13**, 51-67.

Blackett, M., Licandro, P., Coombs, S.H., and Lucas, C.H. 2014. Long-term variability of the siphonophores Muggiaea atlantica and M. kochi in the Western

English Channel. *Progress in Oceanography* **128**, 1-14.

Blaxter, M.L., De Ley, P., Garey, J.R., Liu, L.X., Scheldeman, P., Vierstraete, A., Vanfleteren, J.R., Mackey, L.Y., Dorris, M., and Frisse, L.M. 1998. A molecular evolutionary framework for the phylum Nematoda. *Nature* **392**, 71.

Bongers, T., and Ferris, H. 1999. Nematode community structure as a bioindicator in environmental monitoring. *Trends in Ecology & Evolution* **14**, 224-228.

Borrell, Y.J., Miralles, L., Do Huu, H., Mohammed-Geba, K., and Garcia-Vazquez, E. 2017. DNA in a bottle—Rapid metabarcoding survey for early alerts of invasive species in ports. *PloS one* **12**, e0183347.

Bortone, S., Davis, W., and Bundrick, C.M. 1989. Morphological and behavioral characters in mosquitofish as potential bioindication of exposure to kraft mill effluent. *Bulletin of environmental contamination and toxicology* **43**, 370-377.

Bouchon, D., Zimmer, M., and Dittmer, J. 2016. The terrestrial isopod microbiome: an all-in-one toolbox for animal–microbe interactions of ecological relevance. *Frontiers in microbiology* **7**, 1472.

Boxshall, G.A., and Defaye, D. 2007. Global diversity of copepods (Crustacea: Copepoda) in freshwater. In *Freshwater Animal Diversity Assessment*. Springer, 195-207.

Braig, H.R., and Perotti, M.A. 2009. Carcases and mites. *Experimental and Applied Acarology* **49**, 45-84.

Buck, T.L., Breed, G.A., Pennings, S.C., Chase, M.E., Zimmer, M., and Carefoot, T.H. 2003. Diet choice in an omnivorous salt-marsh crab: different food types, body size, and habitat complexity. *Journal of Experimental Marine Biology and*

Ecology **292**, 103-116.

Bucklin, A., Lindeque, P.K., Rodriguez-Ezpeleta, N., Albaina, A., and Lehtiniemi, M. 2016. Metabarcoding of marine zooplankton: prospects, progress and pitfalls. *Journal of Plankton Research* **38**, 393-400.

Buecher, E. 1999. Appearance of Chelophyes appendiculata and Abylopsis tetragona (Cnidaria, Siphonophora) in the Bay of Villefranche, northwestern Mediterranean. *Journal of sea research* **41**, 295-307.

Bugelli, V., Gherardi, M., Focardi, M., Pinchi, V., Vanin, S., and Campobasso, C.P. 2018. Decomposition pattern and insect colonization in two cases of suicide by hanging. *Forensic Sciences Research* **3**, 94-102.

Buijs, Y., Bech, P.K., Vazquez-Albacete, D., Bentzon-Tilia, M., Sonnenschein, E.C., Gram, L., and Zhang, S.-D. 2019. Marine Proteobacteria as a source of natural products: advances in molecular tools and strategies. *Natural product reports* **36**, 1333-1350.

Caporaso, J.G., Kuczynski, J., Stombaugh, J., Bittinger, K., Bushman, F.D., Costello, E.K., Fierer, N., Pena, A.G., Goodrich, J.K., and Gordon, J.I. 2010. QIIME allows analysis of high-throughput community sequencing data. *Nature methods* **7**, 335.

Caporaso, J.G., Lauber, C.L., Walters, W.A., Berg-Lyons, D., Huntley, J., Fierer, N., Owens, S.M., Betley, J., Fraser, L., and Bauer, M. 2012. Ultra-high-throughput microbial community analysis on the Illumina HiSeq and MiSeq platforms. *The ISME journal* **6**, 1621.

Casé, M., Leça, E.E., Leitão, S.N., Sant, E.E., Schwamborn, R., and de Moraes

Junior, A.T. 2008. Plankton community as an indicator of water quality in tropical shrimp culture ponds. *Marine Pollution Bulletin* **56**, 1343-1352.

Caspi, R., Foerster, H., Fulcher, C.A., Kaipa, P., Krummenacker, M., Latendresse, M., Paley, S., Rhee, S.Y., Shearer, A.G., and Tissier, C. 2007. The MetaCyc Database of metabolic pathways and enzymes and the BioCyc collection of Pathway/Genome Databases. *Nucleic acids research* **36**, D623-D631.

Chen, H., and Liu, G. 2015. Zooplankton community structure in the Yellow Sea and East China Sea in autumn. *Brazilian Journal of Oceanography* **63**, 455-468.

Chen, H., Qi, Y., and Liu, G. 2011. Spatial and temporal variations of macro-and mesozooplankton community in the Huanghai Sea (Yellow Sea) and East China Sea in summer and winter. *Acta Oceanologica Sinica* **30**, 84-95.

Chen, J., Xing, Y., Yao, W., Zhang, C., Zhang, Z., Jiang, G., and Ding, Z. 2018. Characterization of four new mitogenomes from Ocypodoidea & Grapsoidea, and phylomitogenomic insights into thoracotreme evolution. *Gene* **675**, 27-35.

Chen, X., Di, P., Wang, H., Li, B., Pan, Y., Yan, S., and Wang, Y. 2015. Bacterial community associated with the intestinal tract of Chinese mitten crab (Eriocheir sinensis) farmed in Lake Tai, China. *PloS one* **10**, e0123990.

Cheng, P., Gao, S., and Bokuniewicz, H. 2004. Net sediment transport patterns over the Bohai Strait based on grain size trend analysis. *Estuarine, Coastal and Shelf Science* **60**, 203-212.

Clare, E.L., Chain, F.J., Littlefair, J.E., and Cristescu, M.E. 2016. The effects of parameter choice on defining molecular operational taxonomic units and resulting ecological analyses of metabarcoding data. *Genome* **59**, 981-990.

Clayton, J.B., Gomez, A., Amato, K., Knights, D., Travis, D.A., Blekhman, R., Knight, R., Leigh, S., Stumpf, R., and Wolf, T. 2018. The gut microbiome of nonhuman primates: Lessons in ecology and evolution. *American journal of primatology* **80**, e22867.

Coissac, E., Riaz, T., and Puillandre, N. 2012. Bioinformatic challenges for DNA metabarcoding of plants and animals. *Molecular ecology* **21**, 1834-1847.

Comtet, T., Sandionigi, A., Viard, F., and Casiraghi, M. 2015. DNA (meta) barcoding of biological invasions: a powerful tool to elucidate invasion processes and help managing aliens. *Biological Invasions* **17**, 905-922.

Cottrell, M.T., and Kirchman, D.L. 2000. Natural assemblages of marine proteobacteria and members of the Cytophaga-Flavobacter cluster consuming low-and high-molecular-weight dissolved organic matter. *Appl. Environ. Microbiol.* **66**, 1692-1697.

Cowart, D.A., Pinheiro, M., Mouchel, O., Maguer, M., Grall, J., Miné, J., and Arnaud-Haond, S. 2015. Metabarcoding is powerful yet still blind: a comparative analysis of morphological and molecular surveys of seagrass communities. *PloS one* **10**.

Cristescu, M.E. 2014. From barcoding single individuals to metabarcoding biological communities: towards an integrative approach to the study of global biodiversity. *Trends in ecology & evolution* **29**, 566-571.

De Vargas, C., Audic, S., Henry, N., Decelle, J., Mahé, F., Logares, R., Lara, E., Berney, C., Le Bescot, N., and Probert, I. 2015. Eukaryotic plankton diversity in the sunlit ocean. *Science* **348**, 1261605.

Decaëns, T., Porco, D., Rougerie, R., Brown, G.G., and James, S.W. 2013. Potential of DNA barcoding for earthworm research in taxonomy and ecology. *Applied Soil Ecology* **65**, 35-42.

Dela-Cruz, J., Middleton, J.H., and Suthers, I.M. 2003. Population growth and transport of the red tide dinoflagellate, Noctiluca scintillans, in the coastal waters off Sydney Australia, using cell diameter as a tracer. *Limnology and Oceanography* **48**, 656-674.

Deswati, L. 2018 Community structure, phytoplankton density and physical-chemical factor of batang palangki waters of sijunjung regency, west sumatera. *IOP Conference Series: Earth and Environmental Science*. IOP Publishing, 130, 012023.

Dickson, G.C., Poulter, R.T., Maas, E.W., Probert, P.K., and Kieser, J.A. 2011. Marine bacterial succession as a potential indicator of postmortem submersion interval. *Forensic science international* **209**, 1-10.

Dinno, A., and Dinno, M.A. 2017. Package 'dunn. test'. *CRAN Repos. doi* **10**.

Djurhuus, A., Pitz, K., Sawaya, N.A., Rojas-Márquez, J., Michaud, B., Montes, E., Muller-Karger, F., and Breitbart, M. 2018. Evaluation of marine zooplankton community structure through environmental DNA metabarcoding. *Limnology and Oceanography: Methods* **16**, 209-221.

Doi, H., Fukaya, K., Oka, S.-i., Sato, K., Kondoh, M., and Miya, M. 2019. Evaluation of detection probabilities at the water-filtering and initial PCR steps in environmental DNA metabarcoding using a multispecies site occupancy model. *Scientific reports* **9**, 3581.

Dormontt, E., Van Dijk, K.-j., Bell, K., Biffin, E., Breed, M., Byrne, M., Caddy-Retalic, S., Encinas-Viso, F., Nevill, P., and Shapcott, A. 2018. Advancing DNA barcoding and metabarcoding applications for plants requires systematic analysis of herbarium collections-an Australian perspective.

Douglas, G.M., Maffei, V.J., Zaneveld, J.R., Yurgel, S.N., Brown, J.R., Taylor, C.M., Huttenhower, C., and Langille, M.G. 2020. PICRUSt2 for prediction of metagenome functions. *Nature Biotechnology*, 1-5.

Dray, S., Dufour, A.B., and Chessel, D. 2007. The ade4 package-II: Two-table and K-table methods. *R news* **7**, 47-52.

Durand, L., Zbinden, M., Cueff-Gauchard, V., Duperron, S., Roussel, E.G., Shillito, B., and Cambon-Bonavita, M.-A. 2009. Microbial diversity associated with the hydrothermal shrimp Rimicaris exoculata gut and occurrence of a resident microbial community. *FEMS microbiology ecology* **71**, 291-303.

Easson, C.G., and Thacker, R.W. 2014. Phylogenetic signal in the community structure of host-specific microbiomes of tropical marine sponges. *Frontiers in microbiology* **5**, 532.

Edgar, R.C. 2010. Search and clustering orders of magnitude faster than BLAST. *Bioinformatics* **26**, 2460-2461.

Faith, J.J., McNulty, N.P., Rey, F.E., and Gordon, J.I. 2011. Predicting a human gut microbiota's response to diet in gnotobiotic mice. *Science* **333**, 101-104.

Finley, S.J., Pechal, J.L., Benbow, M.E., Robertson, B., and Javan, G.T. 2016. Microbial signatures of cadaver gravesoil during decomposition. *Microbial ecology* **71**, 524-529.

Gabaldón, C., Fontaneto, D., Carmona, M., Montero-Pau, J., and Serra, M. 2017. Ecological differentiation in cryptic rotifer species: what we can learn from the Brachionus plicatilis complex. *Hydrobiologia* **796**, 7-18.

Gao, Q., Xu, Z., and Zhuang, P. 2008. The relation between distribution of zooplankton and salinity in the Changjiang Estuary. *Chinese Journal of Oceanology and Limnology* **26**, 178-185.

Gaulke, C.A., Arnold, H.K., Humphreys, I.R., Kembel, S.W., O'Dwyer, J.P., and Sharpton, T.J. 2018. Ecophylogenetics clarifies the evolutionary association between mammals and their gut microbiota. *MBio* **9**, e01348-01318.

Gennard, D. 2012 *Forensic entomology: an introduction*. John Wiley & Sons.

Gessner, M., Gulis, V., Kuehn, K., Chauvet, E., and Suberkropp, K. 2007. 17 Fungal Decomposers of Plant Litter in Aquatic Ecosystems. *Environmental and microbial relationships* **4**, 301.

Gessner, M.O., and Van Ryckegem, G. 2003. Water fungi as decomposers in freshwater ecosystems. *Encyclopedia of environmental microbiology*.

Gevers, D., Knight, R., Petrosino, J.F., Huang, K., McGuire, A.L., Birren, B.W., Nelson, K.E., White, O., Methé, B.A., and Huttenhower, C. 2012. The Human Microbiome Project: a community resource for the healthy human microbiome. *PLoS biology* **10**.

Gilbert, J.A., Jansson, J.K., and Knight, R. 2014. The Earth Microbiome project: successes and aspirations. *BMC biology* **12**, 69.

Go, W.-J., Kim, S.-W., and Jang, L.-H. 2009. Relationship between ocean-meteorological factors and snowfall in the western coastal region of Korea in

winter. *Journal of the Korean Society of Marine Environment & Safety* **15**, 17-24.

Gough, L., Grace, J.B., and Taylor, K.L. 1994. The relationship between species richness and community biomass: the importance of environmental variables. *Oikos* **70**, 271-279.

Grattan, R.M., and Suberkropp, K. 2001. Effects of nutrient enrichment on yellow poplar leaf decomposition and fungal activity in streams. *Journal of the North American Benthological Society* **20**, 33-43.

Grossmann, M.M., and Lindsay, D.J. 2013. Diversity and distribution of the Siphonophora (Cnidaria) in Sagami Bay, Japan, and their association with tropical and subarctic water masses. *Journal of oceanography* **69**, 395-411.

Group, C.P.W., Hollingsworth, P.M., Forrest, L.L., Spouge, J.L., Hajibabaei, M., Ratnasingham, S., van der Bank, M., Chase, M.W., Cowan, R.S., and Erickson, D.L. 2009. A DNA barcode for land plants. *Proceedings of the National Academy of Sciences* **106**, 12794-12797.

Groussin, M., Mazel, F., Sanders, J.G., Smillie, C.S., Lavergne, S., Thuiller, W., and Alm, E.J. 2017. Unraveling the processes shaping mammalian gut microbiomes over evolutionary time. *Nature Communications* **8**, 1-12.

Güsewell, S., and Gessner, M.O. 2009. N: P ratios influence litter decomposition and colonization by fungi and bacteria in microcosms. *Functional Ecology* **23**, 211-219.

Haefner, J.N., Wallace, J.R., and Merritt, R.W. 2004. Pig decomposition in lotic aquatic systems: the potential use of algal growth in establishing a postmortem submersion interval (PMSI). *Journal of Forensic Science* **49**, 1-7.

Hassan, S.H., Gurung, A., Kang, W.-c., Shin, B.-S., Rahimnejad, M., Jeon, B.-H., Kim, J.R., and Oh, S.-E. 2019. Real-time monitoring of water quality of stream water using sulfur-oxidizing bacteria as bio-indicator. *Chemosphere* **223**, 58-63.

Heaton, V., Lagden, A., Moffatt, C., and Simmons, T. 2010. Predicting the postmortem submersion interval for human remains recovered from UK waterways. *Journal of forensic sciences* **55**, 302-307.

Hebert, P.D., Cywinska, A., Ball, S.L., and Dewaard, J.R. 2003. Biological identifications through DNA barcodes. *Proceedings of the Royal Society of London. Series B: Biological Sciences* **270**, 313-321.

Heeren, T., and Mitchell, B. 1997. Morphology of the mouthparts, gastric mill and digestive tract of the giant crab, Pseudocarcinus gigas (Milne Edwards)(Decapoda: Oziidae). *Marine and freshwater research* **48**, 7-18.

Heimeier, D., Lavery, S., and Sewell, M.A. 2010. Using DNA barcoding and phylogenetics to identify Antarctic invertebrate larvae: lessons from a large scale study. *Marine genomics* **3**, 165-177.

Heip, C., Vincx, M., and Vranken, G. 1985. *The ecology of marine nematodes*. Aberdeen University Press.

Hilton, J., and Atkinson, J. 1982. Response of rainbow trout (Salmo gairdneri) to increased levels of available carbohydrate in practical trout diets. *British Journal of Nutrition* **47**, 597-607.

Hsieh, C.-h.H., Chiu, T.-S., and Shih, C.-t. 2004. Copepod diversity and composition as indicators of intrusion of the Kuroshio Branch Current into the Northern Taiwan Strait in Spring 2000.

Hyde, E.R., Haarmann, D.P., Lynne, A.M., Bucheli, S.R., and Petrosino, J.F. 2013. The living dead: bacterial community structure of a cadaver at the onset and end of the bloat stage of decomposition. *PloS one* **8**, e77733.

Hyde, E.R., Metcalf, J.L., Bucheli, S.R., Lynne, A.M., and Knight, R. 2017. Microbial communities associated with decomposing corpses. *Forensic Microbiology*, 245.

Ivanova, N.V., Zemlak, T.S., Hanner, R.H., and Hebert, P.D. 2007. Universal primer cocktails for fish DNA barcoding. *Molecular Ecology Notes* **7**, 544-548.

Jang, M.-C., Baek, S.-H., Jang, P.-G., Lee, W.-J., and Shin, K.-S. 2012. Patterns of zooplankton distribution as related to water masses in the Korea Strait during winter and summer. *Ocean and Polar Research* **34**, 37-51.

Janzen, D.H., Hallwachs, W., Blandin, P., Burns, J.M., CADIOU, J.M., Chacon, I., Dapkey, T., Deans, A.R., Epstein, M.E., and Espinoza, B. 2009. Integration of DNA barcoding into an ongoing inventory of complex tropical biodiversity. *Molecular Ecology Resources* **9**, 1-26.

Jetz, W., and Rahbek, C. 2002. Geographic range size and determinants of avian species richness. *Science* **297**, 1548-1551.

Ji, Y.-K., Wang, A., Lu, X.-L., Song, D.-H., Jin, Y.-H., Lu, J.-J., and Sun, H.-Y. 2014. Mitochondrial genomes of two brachyuran crabs (Crustacea: Decapoda) and phylogenetic analysis. *Journal of Crustacean Biology* **34**, 494-503.

Johnson, T.B., and Terazaki, M. 2003. Species composition and depth distribution of chaetognaths in a Kuroshio warm-core ring and Oyashio water. *Journal of plankton research* **25**, 1279-1289.

Ju, F., and Zhang, T. 2015. 16S rRNA gene high-throughput sequencing data mining of

microbial diversity and interactions. *Applied microbiology and biotechnology* **99**, 4119-4129.

Kang, J.-H. 2010. Distributional Characteristics and Carrying Capacity of the Potentially Risky Species Noctiluca scintillans at International Korean Seaports. *Ocean and Polar Research* **32**, 449-462.

Kang, J.-H., and Kim, W.-S. 2008. Spring dominant copepods and their distribution pattern in the Yellow Sea. *Ocean Science Journal* **43**, 67-79.

Kang, Y.-S. 1996. Redescription of Paracalanus parvus and P. indicus (Copepoda: Paracalanidae) recorded in the Korean waters. *Korean Journal of Fisheries and Aquatic Sciences* **29**, 409-413.

Katoh, K., and Standley, D.M. 2013. MAFFT multiple sequence alignment software version 7: improvements in performance and usability. *Molecular biology and evolution* **30**, 772-780.

Kaye, J.P., and Hart, S.C. 1997. Competition for nitrogen between plants and soil microorganisms. *Trends in Ecology & Evolution* **12**, 139-143.

Kim, D.-K., Park, K., Jo, H., and Kwak, I.-S. 2019. Comparison of Water Sampling between Environmental DNA Metabarcoding and Conventional Microscopic Identification: A Case Study in Gwangyang Bay, South Korea. *Applied Sciences* **9**, 3272.

Kitaura, J., Wada, K., and Nishida, M. 2002. Molecular phylogeny of grapsoid and ocypodoid crabs with special reference to the genera Metaplax and Macrophthalmus. *Journal of Crustacean Biology* **22**, 682-693.

Kneib, R., Lee, S., and Kneib, J. 1999. Adult–juvenile interactions in the crabs Sesarma

(Perisesarma) bidens and S.(Holometopus) dehaani (Decapoda: Grapsidae) from intertidal mangrove habitats in Hong Kong. *Journal of Experimental Marine Biology and Ecology* **234**, 255-273.

Kobayashi, S. 2013. Feeding habits of the Leucosiid Crab Pyrhila pisum (De Haan) observed on a sandy tidal flat in Hakata bay, Fukuoka, Japan. *Japanese Journal of Benthology* **68**, 37-41.

Kodama, T., Hirai, J., Tamura, S., Takahashi, T., Tanaka, Y., Ishihara, T., Tawa, A., Morimoto, H., and Ohshimo, S. 2017. Diet composition and feeding habits of larval Pacific bluefin tuna Thunnus orientalis in the Sea of Japan: integrated morphological and metagenetic analysis. *Marine Ecology Progress Series* **583**, 211-226.

Kress, W.J., García-Robledo, C., Uriarte, M., and Erickson, D.L. 2015. DNA barcodes for ecology, evolution, and conservation. *Trends in ecology & evolution* **30**, 25-35.

Korea National Park Service. *http://www.knps.or.kr*.

Kuklina, I., Kouba, A., and Kozák, P. 2013. Real-time monitoring of water quality using fish and crayfish as bio-indicators: a review. *Environmental monitoring and assessment* **185**, 5043-5053.

Lacoursière-Roussel, A., Howland, K., Normandeau, E., Grey, E.K., Archambault, P., Deiner, K., Lodge, D.M., Hernandez, C., Leduc, N., and Bernatchez, L. 2018. eDNA metabarcoding as a new surveillance approach for coastal Arctic biodiversity. *Ecology and evolution* **8**, 7763-7777.

Lamb, P.D., Hunter, E., Pinnegar, J.K., Creer, S., Davies, R.G., and Taylor, M.I.

2019. How quantitative is metabarcoding: A meta-analytical approach. *Molecular ecology* **28**, 420-430.

Lee, C.-R., Kang, H.-K., and Noh, J.-H. 2009. Temporal and Spatial Variation of Zooplankton Community Structure Post Construction of Saemangeum Dyke *Ocean and Polar Research* **31**, 327-338.

Lee, C., Kim, S., Lee, B., Noh, H., Jeong, J., Song, S., and Kim, T. 2011. Hydrographical characteristics and distribution of mesozooplankton in the Chilbal is. and the Yeoseo is. *Dadohaehaesang national park in oct*, 64-74.

Lee, C.E., Remfert, J.L., and Gelembiuk, G.W. 2003. Evolution of physiological tolerance and performance during freshwater invasions. *Integrative and Comparative Biology* **43**, 439-449.

Lee, S. 2015. Ecology of Brachyura. In *Treatise on Zoology-Anatomy, Taxonomy, Biology. The Crustacea, 9, Part C (2)*. BRILL, 469-541.

Lelkova, E., and Pouličkova, A. 2004. The influence of Hydrodictyon reticulatum (L.) LAGERH. on diurnal changes in environmental variables in a shallow pool. *Czech phycology* **4**, 103-109.

Lenk, S., Arnds, J., Zerjatke, K., Musat, N., Amann, R., and Mußmann, M. 2011. Novel groups of Gammaproteobacteria catalyse sulfur oxidation and carbon fixation in a coastal, intertidal sediment. *Environmental microbiology* **13**, 758-774.

Lenk, S., Moraru, C., Hahnke, S., Arnds, J., Richter, M., Kube, M., Reinhardt, R., Brinkhoff, T., Harder, J., and Amann, R. 2012. Roseobacter clade bacteria are abundant in coastal sediments and encode a novel combination of sulfur

oxidation genes. *The ISME journal* **6**, 2178.

Ley, R.E., Hamady, M., Lozupone, C., Turnbaugh, P.J., Ramey, R.R., Bircher, J.S., Schlegel, M.L., Tucker, T.A., Schrenzel, M.D., and Knight, R. 2008. Evolution of mammals and their gut microbes. *Science* **320**, 1647-1651.

Li, X., Yu, Y., Feng, W., Yan, Q., and Gong, Y. 2012. Host species as a strong determinant of the intestinal microbiota of fish larvae. *The Journal of Microbiology* **50**, 29-37.

Lie, H.-J., and Cho, C.-H. 2016. Seasonal circulation patterns of the Yellow and East China Seas derived from satellite-tracked drifter trajectories and hydrographic observations. *Progress in Oceanography* **146**, 121-141.

Littman, R.A., Willis, B.L., Pfeffer, C., and Bourne, D.G. 2009. Diversities of coral-associated bacteria differ with location, but not species, for three acroporid corals on the Great Barrier Reef. *FEMS microbiology ecology* **68**, 152-163.

López-Victoria, M., and Werding, B. 2008. Ecology of the Endemic Land Crab Johngarthia malpilensis (Decapoda: Brachyura: Gecarcinidae), a Poorly Known Species from the Tropical Eastern Pacific1. *Pacific Science* **62**, 483-494.

Lund, J. 1972. Changes in the biomass of blue-green and other algae in an English lake from 1945-1969. *International Symposium on Taxonomy and Biology of Bluegreen Algae, 1st, Madras, 1970. Papers*.

Mackie, G., Pugh, P., and Purcell, J. 1988. Siphonophore biology. In *Advances in Marine biology*. Elsevier, **24**, 97-262.

Mangiafico, S., and Mangiafico, M.S. 2017. Package 'rcompanion'. *Cran Repos*, 1-71.

Mann, K. 1988. Production and use of detritus in various freshwater, estuarine, and

coastal marine ecosystems. *Limnology and Oceanography* **33**, 910-930.

Martinez Arbizu, P. 2017. pairwiseAdonis: Pairwise multilevel comparison using adonis. *R package version 0.0* **1**.

McFall-Ngai, M. 2008. Hawaiian bobtail squid. *Current Biology* **18**, R1043-R1044.

McMurdie, P.J., and Holmes, S. 2013. phyloseq: an R package for reproducible interactive analysis and graphics of microbiome census data. *PloS one* **8**, e61217.

Megyesi, M.S., Nawrocki, S.P., and Haskell, N.H. 2005. Using accumulated degree-days to estimate the postmortem interval from decomposed human remains. *Journal of Forensic Science* **50**, 1-9.

Merritt, R.W., and Wallace, J.R. 2001. The role of aquatic insects in forensic investigations. *Forensic Entomology: The utility of arthropods in legal investigations*, 177-222.

Metcalf, J.L., Parfrey, L.W., Gonzalez, A., Lauber, C.L., Knights, D., Ackermann, G., Humphrey, G.C., Gebert, M.J., Van Treuren, W., and Berg-Lyons, D. 2013. A microbial clock provides an accurate estimate of the postmortem interval in a mouse model system. *elife* **2**, e01104.

Metcalf, J.L., Xu, Z.Z., Weiss, S., Lax, S., Van Treuren, W., Hyde, E.R., Song, S.J., Amir, A., Larsen, P., and Sangwan, N. 2016. Microbial community assembly and metabolic function during mammalian corpse decomposition. *Science* **351**, 158-162.

Miyaguchi, H., Fujiki, T., Kikuchi, T., Kuwahara, V.S., and Toda, T. 2006. Relationship between the bloom of Noctiluca scintillans and environmental factors in the coastal waters of Sagami Bay, Japan. *Journal of Plankton Research*

28, 313-324.

Miyake, S., Ngugi, D.K., and Stingl, U. 2015. Diet strongly influences the gut microbiota of surgeonfishes. *Molecular ecology* **24**, 656-672.

Moeller, A.H., Peeters, M., Ndjango, J.-B., Li, Y., Hahn, B.H., and Ochman, H. 2013. Sympatric chimpanzees and gorillas harbor convergent gut microbial communities. *Genome research* **23**, 1715-1720.

Moon, S.-Y., Seo, M.-H., Shin, Y.-S., and Soh, H.-Y. 2012. Seasonal variation of mesozooplankton communities in the semi-enclosed Muan Bay, Korea. *Ocean and Polar Research* **34**, 1-18.

Mora, C., Tittensor, D.P., Adl, S., Simpson, A.G., and Worm, B. 2011. How many species are there on Earth and in the ocean? *PLoS biology* **9**.

Newell, S., Moran, M., Wicks, R., and Hodson, R. 1995. Productivities of microbial decomposers during early stages of decomposition of leaves of a freshwater sedge. *Freshwater Biology* **34**, 135-148.

Nimnoi, P., and Pongsilp, N. 2020. Marine bacterial communities in the upper gulf of Thailand assessed by Illumina next-generation sequencing platform. *BMC microbiology* **20**, 19.

Niyogi, D.K., Simon, K.S., and Townsend, C.R. 2003. Breakdown of tussock grass in streams along a gradient of agricultural development in New Zealand. *Freshwater Biology* **48**, 1698-1708.

Noblezada, M.M.P., and Campos, W.L. 2008. Spatial distribution of chaetognaths off the northern Bicol Shelf, Philippines (Pacific coast). *ICES Journal of Marine Science* **65**, 484-494.

O'Brien, P.A., Webster, N.S., Miller, D.J., and Bourne, D.G. 2019. Host-microbe coevolution: applying evidence from model systems to complex marine invertebrate holobionts. *MBio* **10**, e02241-02218.

Oh, H.-J., Krogh, P.H., Jeong, H.-G., Joo, G.-J., Kwak, I.-S., Hwang, S.-J., Gim, J.-S., Chang, K.-H., and Jo, H. 2020. Pretreatment Method for DNA Barcoding to Analyze Gut Contents of Rotifers. *Applied Sciences* **10**, 1064.

Okamura, B., and Hatton-Ellis, T. 1995. Population biology of bryozoans: correlates of sessile, colonial life histories in freshwater habitats. *Experientia* **51**, 510-525.

Oksanen, J., Blanchet, F.G., Kindt, R., Legendre, P., O'hara, R., Simpson, G.L., Solymos, P., Stevens, M.H.H., and Wagner, H. 2010. Vegan: community ecology package. R package version 1.17-4. *http://CRAN.R-project.org/package=vegan*.

Oksanen, J., Kindt, R., Legendre, P., O'Hara, B., Stevens, M.H.H., Oksanen, M.J., and Suggests, M. 2007. The vegan package. *Community ecology package* **10**, 631-637.

Oliveira-Costa, J., and Mello-Patiu, C.A. 2004. Application of forensic entomology to estimate of the postmortem interval (PMI) in homicide investigations by the Rio de Janeiro Police Department in Brazil. *Aggrawal's Internet Journal of Forensic Medicine and Toxicology* **5**, 40-44.

Oscar, K. 1982. Satellite observations and the annual cycle of surface circulation in the Yellow Sea, East China Sea and Korea Strait. *La mer* **20**, 210-222.

Põllupüü, M., Simm, M., and Ojaveer, H. 2010. Life history and population dynamics of the marine cladoceran Pleopis polyphemoides (Leuckart)(Cladocera,

Crustacea) in a shallow temperate Pärnu Bay (Baltic Sea). *Journal of plankton research* **32**, 1459-1469.

Pang, I.-C., and Hyun, K.-H. 1998. Seasonal variation of water mass distributions in the eastern Yellow Sea and the Yellow Sea Warm Current. *Journal of the korean society of oceanography* **33**, 41-52.

Parada, A.E., Needham, D.M., and Fuhrman, J.A. 2016. Every base matters: assessing small subunit rRNA primers for marine microbiomes with mock communities, time series and global field samples. *Environmental microbiology* **18**, 1403-1414.

Park, J.H., Na, J.-Y., Lee, B.W., Chung, N.E., and Choi, Y.S. 2016. A statistical analysis on forensic autopsies performed in Korea in 2015. *Korean Journal of Legal Medicine* **40**, 104-118.

Parks, D.H., Tyson, G.W., Hugenholtz, P., and Beiko, R.G. 2014. STAMP: statistical analysis of taxonomic and functional profiles. *Bioinformatics* **30**, 3123-3124.

Parmar, T.K., Rawtani, D., and Agrawal, Y. 2016. Bioindicators: the natural indicator of environmental pollution. *Frontiers in life science* **9**, 110-118.

Parmenter, R.R., and Lamarra, V.A. 1991. Nutrient cycling in a freshwater marsh: the decomposition of fish and waterfowl carrion. *Limnology and Oceanography* **36**, 976-987.

Paturej, E., and Gutkowska, A. 2015. The effect of salinity levels on the structure of zooplankton communities. *Arch. Biol. Sci* **67**, 483-492.

Pearman, J.K., El-Sherbiny, M.M., Lanzén, A., Al-Aidaroos, A.M., and Irigoien, X. 2014. Zooplankton diversity across three Red Sea reefs using pyrosequencing. *Frontiers in Marine Science* **1**, 27.

Pechal, J.L., Crippen, T.L., Benbow, M.E., Tarone, A.M., Dowd, S., and Tomberlin, J.K. 2014. The potential use of bacterial community succession in forensics as described by high throughput metagenomic sequencing. *International Journal of Legal Medicine* **128**, 193-205.

Piette, M.H., and Els, A. 2006. Drowning: still a difficult autopsy diagnosis. *Forensic science international* **163**, 1-9.

Pochon, X., Bott, N.J., Smith, K.F., and Wood, S.A. 2013. Evaluating detection limits of next-generation sequencing for the surveillance and monitoring of international marine pests. *PloS one* **8**, e73935.

Polz, M.F., and Cavanaugh, C.M. 1998. Bias in template-to-product ratios in multitemplate PCR. *Appl. Environ. Microbiol.* **64**, 3724-3730.

Purushothama, R., Sayeswara, H., Goudar, M.A., and Harishkumar, K. 2011. Physicochemical profile and zooplankton community composition in Brahmana Kalasi Tank, Sagar, Karnataka, India. *Ecoscan* **5**, 99-103.

Quensen III, J., and S Woodruff, D. 1997. Associations between shell morphology and land crab predation in the land snail Cerion. *Functional Ecology* **11**, 464-471.

Rabalais, N.N. 2002. Nitrogen in aquatic ecosystems. *AMBIO: A Journal of the Human Environment* **31**, 102-112.

Rader, B.A., and Nyholm, S.V. 2012. Host/microbe interactions revealed through "omics" in the symbiosis between the Hawaiian bobtail squid Euprymna scolopes and the bioluminescent bacterium Vibrio fischeri. *The Biological Bulletin* **223**, 103-111.

Radulovici, A.E., SAINTE-MARIE, B., and Dufresne, F. 2009. DNA barcoding of

marine crustaceans from the Estuary and Gulf of St Lawrence: a regional-scale approach. *Molecular ecology resources* **9**, 181-187.

Ratnasingham, S., and Hebert, P.D. 2007. BOLD: The Barcode of Life Data System (http://www.barcodinglife. org). *Molecular ecology notes* **7**, 355-364.

Rhee, G.Y. 1972. Competition Between AN Alga and AN Aquatic Bacterium for PHOSPHATE1. *Limnology and Oceanography* **17**, 505-514.

Rhee, G.Y. 1973. A continuous culture study of phosphate uptake, growth rate and polyphosphate in Scenedesmus sp. 1. *Journal of Phycology* **9**, 495-506.

Richardson, A.J. 2008. In hot water: zooplankton and climate change. *ICES Journal of Marine Science* **65**, 279-295.

Rognes, T., Flouri, T., Nichols, B., Quince, C., and Mahé, F. 2016. VSEARCH: a versatile open source tool for metagenomics. *PeerJ* **4**, e2584.

Ruppert, K.M., Kline, R.J., and Rahman, M.S. 2019. Past, present, and future perspectives of environmental DNA (eDNA) metabarcoding: A systematic review in methods, monitoring, and applications of global eDNA. *Global Ecology and Conservation*, e00547.

Rusch, D.B., Halpern, A.L., Sutton, G., Heidelberg, K.B., Williamson, S., Yooseph, S., Wu, D., Eisen, J.A., Hoffman, J.M., and Remington, K. 2007. The Sorcerer II global ocean sampling expedition: northwest Atlantic through eastern tropical Pacific. *PLoS biology* **5**, e77.

Sabatés, A., Gili, J., and Pages, F. 1989. Relationship between zooplankton distribution, geographic characteristics and hydrographic patterns off the Catalan coast (Western Mediterranean). *Marine Biology* **103**, 153-159.

Sánchez, E., Soto, J., Garcia, P., López-Lefebre, L., Rivero, R., Ruiz, J., and Romero, L. 2000. Phenolic and oxidative metabolism as bioindicators of nitrogen deficiency in french bean plants (Phaseolus vulgaris L. cv. Strike). *Plant Biology* **2**, 272-277.

Sawaya, N.A., Djurhuus, A., Closek, C.J., Hepner, M., Olesin, E., Visser, L., Kelble, C., Hubbard, K., and Breitbart, M. 2019. Assessing eukaryotic biodiversity in the Florida Keys National Marine Sanctuary through environmental DNA metabarcoding. *Ecology and evolution* **9**, 1029-1040.

Schenk, S.C., and Wainwright, P.C. 2001. Dimorphism and the functional basis of claw strength in six brachyuran crabs. *Journal of Zoology* **255**, 105-119.

Schiebelhut, L.M., Abboud, S.S., Gómez Daglio, L.E., Swift, H.F., and Dawson, M.N. 2017. A comparison of DNA extraction methods for high-throughput DNA analyses. *Molecular ecology resources* **17**, 721-729.

Schoch, C.L., Seifert, K.A., Huhndorf, S., Robert, V., Spouge, J.L., Levesque, C.A., Chen, W., and Consortium, F.B. 2012. Nuclear ribosomal internal transcribed spacer (ITS) region as a universal DNA barcode marker for Fungi. *Proceedings of the National Academy of Sciences* **109**, 6241-6246.

Segers, H. 2007. Global diversity of rotifers (Rotifera) in freshwater. In *Freshwater Animal Diversity Assessment*. Springer, 49-59.

Serrana, J.M., Miyake, Y., Gamboa, M., and Watanabe, K. 2019. Comparison of DNA metabarcoding and morphological identification for stream macroinvertebrate biodiversity assessment and monitoring. *Ecological Indicators* **101**, 963-972.

Shim, M.-B., and Choi, J.-K. 1996. A review on the microstructures and taxonomy of the Acartia bifilosa (Crustacea: Copepoda) in Kyeonggi Bay, Yellow Sea. *Ocean Science Journal* **31**, 37-42.

Shimeno, S. 1974. Studies on carbohydrate metabolism in fishes. *Rep. Fish. Res. Lab. Kochi Univ.* **2**, 1-107.

Shimeno, S., Takeda, M., Takayama, S., Fukui, A., Sasaki, H., and Kajiyama, H. 1981. Adaptation of hepatopancreatic enzymes to dietary carbohydrate in carp [Cyprinus carpio]. *Bulletin of the Japanese Society of Scientific Fisheries*.

Shokralla, S., Porter, T.M., Gibson, J.F., Dobosz, R., Janzen, D.H., Hallwachs, W., Golding, G.B., and Hajibabaei, M. 2015. Massively parallel multiplex DNA sequencing for specimen identification using an Illumina MiSeq platform. *Scientific reports* **5**, 9687.

Simon, C., Frati, F., Beckenbach, A., Crespi, B., Liu, H., and Flook, P. 1994. Evolution, weighting, and phylogenetic utility of mitochondrial gene sequences and a compilation of conserved polymerase chain reaction primers. *Annals of the entomological Society of America* **87**, 651-701.

Soh, H.Y., and Suh, H.-L. 2000. A new species of Acartia (Copepoda, Calanoida) from the Yellow Sea. *Journal of Plankton Research* **22**, 321-337.

Stamatakis, A. 2014. RAxML version 8: a tool for phylogenetic analysis and post-analysis of large phylogenies. *Bioinformatics* **30**, 1312-1313.

Stefanni, S., Stanković, D., Borme, D., de Olazabal, A., Juretić, T., Pallavicini, A., and Tirelli, V. 2018. Multi-marker metabarcoding approach to study mesozooplankton at basin scale. *Scientific reports* **8**, 1-13.

Stelzer, R.S., and Lamberti, G.A. 2001. Effects of N: P ratio and total nutrient concentration on stream periphyton community structure, biomass, and elemental composition. *Limnology and Oceanography* **46**, 356-367.

Strauss, E.A., and Lamberti, G.A. 2002. Effect of dissolved organic carbon quality on microbial decomposition and nitrification rates in stream sediments. *Freshwater Biology* **47**, 65-74.

Štrus, J., and Avguštin, G. 2007. "Candidatus Bacilloplasma," a novel lineage of Mollicutes associated with the hindgut wall of the terrestrial isopod Porcellio scaber (Crustacea: Isopoda). *Appl. Environ. Microbiol.* **73**, 5566-5573.

Sukontason, K., Narongchai, P., Kanchai, C., Vichairat, K., Sribanditmongkol, P., Bhoopat, T., Kurahashi, H., Chockjamsai, M., Piangjai, S., and Bunchu, N. 2007. Forensic entomology cases in Thailand: a review of cases from 2000 to 2006. *Parasitology Research* **101**, 1417.

Sukontason, K.L., Narongchai, P., Sukontason, K., Methanitikorn, R., and Piangjai, S. 2005. Forensically important fly maggots in a floating corpse: the first case report in Thailand. *JOURNAL-MEDICAL ASSOCIATION OF THAILAND* **88**, 1458.

Sullam, K.E., Rubin, B.E., Dalton, C.M., Kilham, S.S., Flecker, A.S., and Russell, J.A. 2015. Divergence across diet, time and populations rules out parallel evolution in the gut microbiomes of Trinidadian guppies. *The ISME journal* **9**, 1508.

Sun, Y., Han, W., Liu, J., Liu, F., and Cheng, Y. 2020. Microbiota comparison in the intestine of juvenile Chinese mitten crab Eriocheir sinensis fed different diets.

Aquaculture **515**, 734518.

Taberlet, P., Coissac, E., Hajibabaei, M., and Rieseberg, L.H. 2012a. Environmental DNA. *Molecular ecology* **21**, 1789-1793.

Taberlet, P., Coissac, E., Pompanon, F., Brochmann, C., and Willerslev, E. 2012b. Towards next-generation biodiversity assessment using DNA metabarcoding. *Molecular ecology* **21**, 2045-2050.

Talwar, C., Nagar, S., Lal, R., and Negi, R.K. 2018. Fish gut microbiome: current approaches and future perspectives. *Indian journal of microbiology* **58**, 397-414.

Tanner, M.A., Everett, C.L., Coleman, W.J., Yang, M.M., and Youvan, D.C. 2000. Complex microbial communities inhabiting sulfide-rich black mud from marine coastal environments. *Biotechnology et alia* **8**, 1-16.

Tarnecki, A.M., Burgos, F.A., Ray, C.L., and Arias, C.R. 2017. Fish intestinal microbiome: diversity and symbiosis unravelled by metagenomics. *Journal of applied microbiology* **123**, 2-17.

Team, R.C. 2014. R: A language and environment for statistical computing. Vienna, Austria: R Foundation for Statistical Computing; 2014.

Thierstein, H.R., Cortés, M.Y., and Haidar, A.T. 2004. Plankton community behavior on ecological and evolutionary time-scales: when models confront evidence. In *Coccolithophores*. Springer, 455-479.

Thomas, T., Moitinho-Silva, L., Lurgi, M., Björk, J.R., Easson, C., Astudillo-García, C., Olson, J.B., Erwin, P.M., López-Legentil, S., and Luter, H. 2016. Diversity, structure and convergent evolution of the global sponge microbiome. *Nature communications* **7**, 1-12.

Thomsen, P.F., Kielgast, J., Iversen, L.L., Wiuf, C., Rasmussen, M., Gilbert, M.T.P., Orlando, L., and Willerslev, E. 2012. Monitoring endangered freshwater biodiversity using environmental DNA. *Molecular ecology* **21**, 2565-2573.

Thongtham, N., and Kristensen, E. 2005. Carbon and nitrogen balance of leaf-eating sesarmid crabs (Neoepisesarma versicolor) offered different food sources. *Estuarine, Coastal and Shelf Science* **65**, 213-222.

Tilman, D., Kilham, S.S., and Kilham, P. 1982. Phytoplankton community ecology: the role of limiting nutrients. *Annual review of Ecology and Systematics* **13**, 349-372.

Tsang, L.M., Chan, B.K.K., SHIH, F.L., Chu, K.H., and ALLEN CHEN, C. 2009. Host-associated speciation in the coral barnacle Wanella milleporae (Cirripedia: Pyrgomatidae) inhabiting the Millepora coral. *Molecular Ecology* **18**, 1463-1475.

Tsang, L.M., Schubart, C.D., Ahyong, S.T., Lai, J.C., Au, E.Y., Chan, T.-Y., Ng, P.K., and Chu, K.H. 2014. Evolutionary history of true crabs (Crustacea: Decapoda: Brachyura) and the origin of freshwater crabs. *Molecular Biology and Evolution* **31**, 1173-1187.

Tsui, C.K., Baschien, C., and Goh, T.-K. 2016. Biology and ecology of freshwater fungi. In *Biology of Microfungi*. Springer, 285-313.

Tzeng, T.-D., Pao, Y.-Y., Chen, P.-C., Weng, F.C.-H., Jean, W.D., and Wang, D. 2015. Effects of host phylogeny and habitats on gut microbiomes of oriental river prawn (Macrobrachium nipponense). *PLoS One* **10**.

Ueda, H. 1982. Zooplankton investigations in Shijiki bay [Japan], 2: Zooplankton communities from September 1975 to April 1976, with special reference to distributional characteristics of inlet copepods. *Bulletin of the Seikai Regional*

Fisheries Research Laboratory (Japan).

Ueland, M., Breton, H.A., and Forbes, S.L. 2014. Bacterial populations associated with early-stage adipocere formation in lacustrine waters. *International journal of legal medicine* **128**, 379-387.

Unno, T. 2015. Bioinformatic suggestions on MiSeq-based microbial community analysis. *J Microbiol Biotechnol* **25**, 765-770.

Valentini, A., Taberlet, P., Miaud, C., Civade, R., Herder, J., Thomsen, P.F., Bellemain, E., Besnard, A., Coissac, E., and Boyer, F. 2016. Next-generation monitoring of aquatic biodiversity using environmental DNA metabarcoding. *Molecular Ecology* **25**, 929-942.

Van Ginkel, S.W., Hassan, S.H., Ok, Y.S., Yang, J.E., Kim, Y.-S., and Oh, S.-E. 2011. Detecting oxidized contaminants in water using sulfur-oxidizing bacteria. *Environmental science & technology* **45**, 3739-3745.

Van Houdt, J., Breman, F., Virgilio, M., and De Meyer, M. 2010. Recovering full DNA barcodes from natural history collections of Tephritid fruitflies (Tephritidae, Diptera) using mini barcodes. *Molecular ecology resources* **10**, 459-465.

Volodina, A., and Gerb, M. 2013. Findings of water net Hydrodictyon reticulatum (Hydrodictyaceae, Chlorophyta) in the Curonian Lagoon. *Botanica Lithuanica* **19**, 72-74.

Wallace, J.R. 2015. Aquatic vertebrate carrion decomposition. *Carrion Ecology, Evolution, and Their Applications; Benbow, ME, Tomberlin, JK, Tarone, AM, Eds*, 247-272.

Wallace, L.J., Boilard, S.M., Eagle, S.H., Spall, J.L., Shokralla, S., and Hajibabaei,

M. 2012. DNA barcodes for everyday life: routine authentication of natural health products. *Food Research International* **49**, 446-452.

Walton, M.J. 1986. Metabolic effects of feeding a high protein/low carbohydrate diet as compared to a low protein/high carbohydrate diet to rainbow troutSalmo gairdneri. *Fish physiology and biochemistry* **1**, 7-15.

Wang, J., Kalyan, S., Steck, N., Turner, L.M., Harr, B., Künzel, S., Vallier, M., Häsler, R., Franke, A., and Oberg, H.-H. 2015. Analysis of intestinal microbiota in hybrid house mice reveals evolutionary divergence in a vertebrate hologenome. *Nature communications* **6**, 1-10.

Wang, Z., Shi, X., Guo, H., Tang, D., Bai, Y., and Wang, Z. 2020. Characterization of the complete mitochondrial genome of Uca lacteus and comparison with other Brachyuran crabs. *Genomics* **112**, 10-19.

Ward, B.A., Dutkiewicz, S., Jahn, O., and Follows, M.J. 2012. A size-structured food-web model for the global ocean. *Limnology and Oceanography* **57**, 1877-1891.

Ward, M.M. 1883. Memoirs: Observations on Saprolegniæ. *Journal of Cell Science* **2**, 272-291.

Wardle, D.A., Walker, L.R., and Bardgett, R.D. 2004. Ecosystem properties and forest decline in contrasting long-term chronosequences. *Science* **305**, 509-513.

Warner, G.F., and Warner, G. 1977 *The biology of crabs*. Elek science London.

Weber-Lehmann, J., Schilling, E., Gradl, G., Richter, D.C., Wiehler, J., and Rolf, B. 2014. Finding the needle in the haystack: differentiating “identical” twins in paternity testing and forensics by ultra-deep next generation sequencing. *Forensic Science International: Genetics* **9**, 42-46.

Webster, N.S., and Thomas, T. 2016. The sponge hologenome. *MBio* **7**, e00135-00116.

Wickham, H. 2016. *ggplot2: elegant graphics for data analysis*. Springer.

Wilkins, L.G., Leray, M., O'Dea, A., Yuen, B., Peixoto, R.S., Pereira, T.J., Bik, H.M., Coil, D.A., Duffy, J.E., and Herre, E.A. 2019. Host-associated microbiomes drive structure and function of marine ecosystems. *PLoS biology* **17**.

Williams, W.D. 1998. Salinity as a determinant of the structure of biological communities in salt lakes. *Hydrobiologia* **381**, 191-201.

Wu, S., Xiong, J., and Yu, Y. 2015. Taxonomic resolutions based on 18S rRNA genes: a case study of subclass Copepoda. *PLoS One* **10**.

Wurzbacher, C., Attermeyer, K., Kettner, M.T., Flintrop, C., Warthmann, N., Hilt, S., Grossart, H.P., and Monaghan, M.T. 2017. DNA metabarcoding of unfractionated water samples relates phyto-, zoo-and bacterioplankton dynamics and reveals a single-taxon bacterial bloom. *Environmental microbiology reports* **9**, 383-388.

Xiong, W., Huang, X., Chen, Y., Fu, R., Du, X., Chen, X., and Zhan, A. 2020. Zooplankton biodiversity monitoring in polluted freshwater ecosystems: A technical review. *Environmental Science and Ecotechnology* **1**, 100008.

Yang, Y., Xie, B., and Yan, J. 2014. Application of next-generation sequencing technology in forensic science. *Genomics, proteomics & bioinformatics* **12**, 190-197.

Yoccoz, N., Bråthen, K., Gielly, L., Haile, J., Edwards, M., Goslar, T., Von Stedingk, H., Brysting, A., Coissac, E., and Pompanon, F. 2012. DNA from soil mirrors plant taxonomic and growth form diversity. *Molecular ecology* **21**, 3647-3655.

Yoo, J.-K., Jeong, J.-H., Nam, E.-J., Jeong, K.-M., Lee, S.-W., and Myung, C.-S. 2006. Zooplankton Community and Distribution in Relation to Water Quality in the Saemangeum Area, Korea: Change in Zooplankton Community by the Construction of Sea Dyke. *Ocean and Polar Research* **28**, 305-315.

Youngblut, N.D., Reischer, G.H., Walters, W., Schuster, N., Walzer, C., Stalder, G., Ley, R.E., and Farnleitner, A.H. 2019. Host diet and evolutionary history explain different aspects of gut microbiome diversity among vertebrate clades. *Nature communications* **10**, 1-15.

Yuan, J., Li, M., and Lin, S. 2015. An improved DNA extraction method for efficient and quantitative recovery of phytoplankton diversity in natural assemblages. *PLoS One* **10**.

Yun, J.-H., Roh, S.W., Whon, T.W., Jung, M.-J., Kim, M.-S., Park, D.-S., Yoon, C., Nam, Y.-D., Kim, Y.-J., and Choi, J.-H. 2014. Insect gut bacterial diversity determined by environmental habitat, diet, developmental stage, and phylogeny of host. *Appl. Environ. Microbiol.* **80**, 5254-5264.

Zak, D.R., and Grigal, D.F. 1991. Nitrogen mineralization, nitrification and denitrification in upland and wetland ecosystems. *Oecologia* **88**, 189-196.

Zhang, J., Kobert, K., Flouri, T., and Stamatakis, A. 2013. PEAR: a fast and accurate Illumina Paired-End reAd mergeR. *Bioinformatics* **30**, 614-620.

Zhang, M., Sun, Y., Chen, K., Yu, N., Zhou, Z., Chen, L., Du, Z., and Li, E. 2014. Characterization of the intestinal microbiota in Pacific white shrimp, Litopenaeus vannamei, fed diets with different lipid sources. *Aquaculture* **434**, 449-455.

Zhang, M., Sun, Y., Chen, L., Cai, C., Qiao, F., Du, Z., and Li, E. 2016. Symbiotic

bacteria in gills and guts of Chinese mitten crab (Eriocheir sinensis) differ from the free-living bacteria in water. *PloS one* **11**.

Zheng, Z., and Li, S. 1989 *Marine planktology*. China Ocean Press.

Zimmer, M. 2008. Detritus. *Encyclopedia of ecology. Oxford: Elsevier. p*, 903-911.

Zimmerman, K.A., and Wallace, J.R. 2008. The potential to determine a postmortem submersion interval based on algal/diatom diversity on decomposing mammalian carcasses in brackish ponds in Delaware. *Journal of forensic sciences* **53**, 935-941.

Zimmermann, J., Glöckner, G., Jahn, R., Enke, N., and Gemeinholzer, B. 2015. Metabarcoding vs. morphological identification to assess diatom diversity in environmental studies. *Molecular ecology resources* **15**, 526-542.

Abstract in Korean

NGS 기술의 발달로, 혼합된 샘플이나 환경샘플에서 많은 생물을 한번에 식별할 수 있는 DNA metabarcoding 이 등장하였다. 이러한 방법은 대량의 생물학적 데이터를 효율적으로 획득할 수 있으며, 생태계의 생물다양성과 군집구조를 평가할 수 있다. DNA metabarcoding 의 중요성을 일찍이 인지하고 이미 국외의 경우, 많은 연구프로젝트가 이미 활발히 진행되고 있다. 그러나 국외의 연구동향과 비교하였을 때, 국내의 DNA meteabarcoding 연구는 기초적이고 연구범위가 제한적이다. 본 학위논문은 이러한 국내 연구동향의 단점들을 보완하기 위해 수생환경에서의 세가지 사례연구에 DNA metabarcoding 을 적용하였다. 이 학위논문의 최종목표는 DNA metabarcoding 을 이용하여 생산된 DNA 메타데이터로 수생환경에서의 생명현상을 설명하고 이해하는 것이다. 본 학위논문의 각 장은 사례연구 별로 구성하였다.

제 1 장에서는 한국의 해상·해안국립공원 지역의 동물 플랑크톤군집의 조사 방법을 확립하기 위해 기존의 형태학적 식별과 함께 DNA metabarcoding 을 새롭게 적용하였다. 공원지역에서 출현하는 동물플랑크톤 군집을 대상으로 두 가지 식별 방법의 결과들을 비교하여 DNA metabarcoding 의 장, 단점을 확인하였다. 또한, DNA metabarcoding 의 민감한 탐지능력은 국립공원에서의 수온, 염도, 지형, 엽록소 농도와 같은 외부요인과 연관된 잠재적인 생물지표 분류군을 식별할 수 있게 하였다. 이를 기반으로 한국의 해상·해안국립공원 지역의 동물 플랑크톤군집을 효율적으로

조사하기 위해서는 DNA metabarcoding 을 사용한 잠재적인 생물지표 분류군을 모니터링을 할 것을 제안한다. 또한 DNA metabarcoding 은 이러한 국립 공원 지역에서 연구 가치가 높은 분류군을 지속적으로 탐색할 수 있는 도구로 이용 될 수 있다. DNA metabarcoding 을 이용한 이러한 접근 방법을 기반으로 한 지속적인 모니터링 시스템의 구축은 해상 · 해안 국립 공원의 해양 생태계 관리를 위한 효과적인 도구를 제공 할 수 있다.

제 2 장에서는 DNA metabarcoding 을 이용하여 조간대에서 서식하는 게 장내미생물 군집과 게의 과, 먹이습성간의 관계를 규명하였다. 게 장내미생물의 메타데이터를 기반으로 기존의 논란이 있었던 바위게상과와 달랑게상과간의 계통학적 관계를 새롭게 해석하였다. 게의 과 수준 에 따라 게 장내미생물의 군집이 서로 다른 것을 확인하였으며, 그 중 일부 게의 과에서 연갑류의 진화와 연관된 장내미생물 OTUs 를 발견하였다. 먹이습성에 따른 게 장내미생물의 생물다양성과 군집이 서로 다름을 확인하였으며, 이와 관련된 장내미생물의 기능과 역할을 예측하였다. 이러한 결과는 게의 섭취할 수 있는 먹이의 유형과 영양적인 특징과 연관이 있음이 유추되었다.

제 3 장에서는 사례연구로써, 익사사건에서의 DNA metabarcoding 의 적용가능성을 확인하고자 DNA metabarcoding 을 이용하여 자동차 보닛과 익사한 돼지의 미소진핵생물의 생물다양성과 군집구조를 조사하였다. 돼지 사체는 익사체의 부패과정을 가정하기 위해 사용하였다. 대조군으로써, 자동차 보닛은 수생환경에서 발생하는 일반적인 천이과정을 확인하기 위해 사용하였다. DNA

metabarcoding 을 사용함으로써 돼지사체의 미소진핵생물의 생물다양성은 자동차 보닛의 생물다양성보다 낮음을 확인하였다. 또한 부패와 연관이 있는 분류군들이 파악되었으며, 부패시기에 따라 상대적인 풍부도가 변화하는 것이 확인되었다. 이러한 변화패턴은 익사사건의 사후시간을 추정하기 위한 좋은 생물지표로 사용할 수 있을 것으로 기대된다.

본 학위논문 내용은 학위 과정 중 저널에 투고한 원고를 포함하였다.

주요어: DNA metabarcoding, 생물다양성, 군집구조, 동물플랑크톤, 생물지표, 게, 장내미생물, 사후시간, 익사

학번: 2016-27480

Appendix

Appendix 1. Custom python script for DNA metabarcoding analysis.

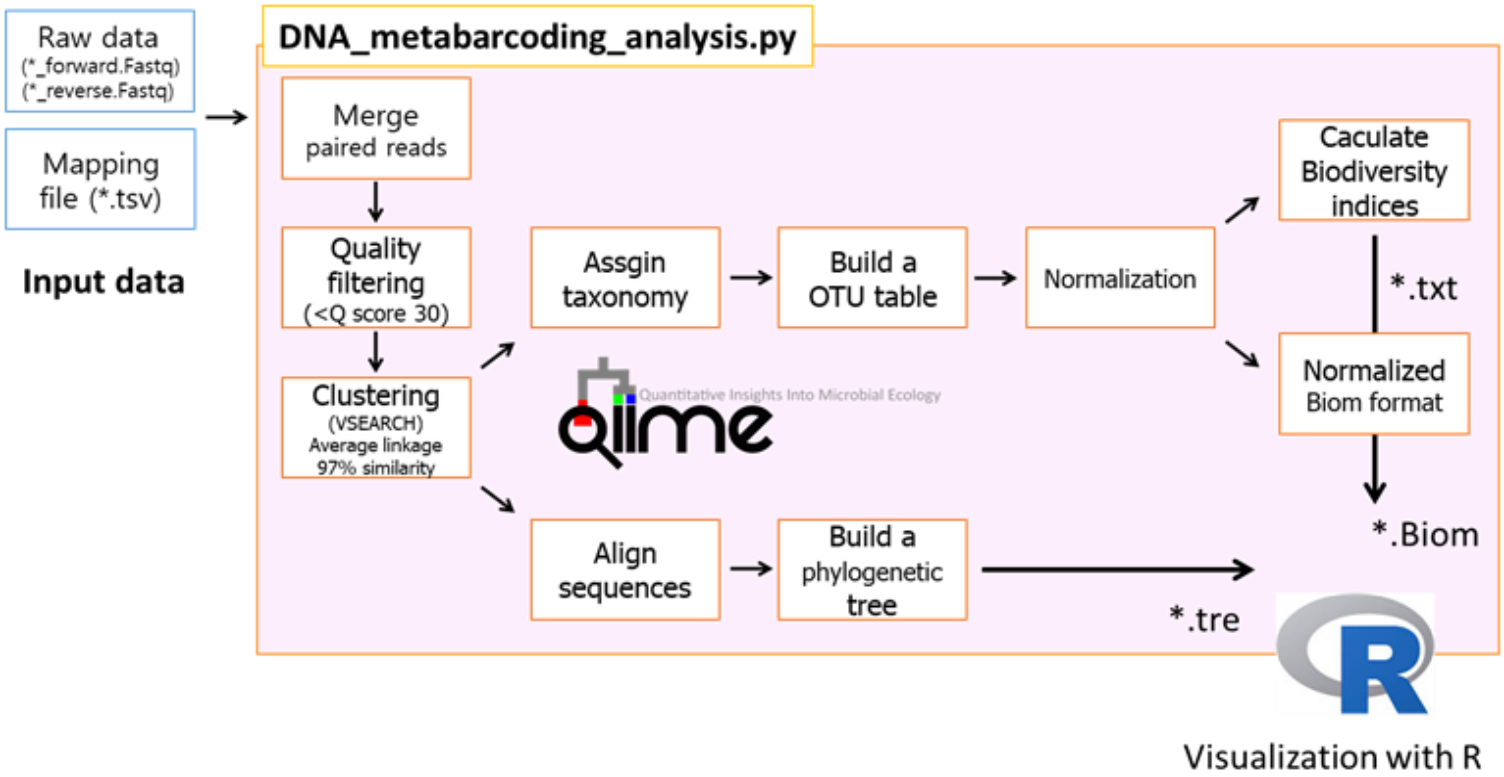

Appendix 2. Spatial and environmental variables for all sampling points in Marine and Coastal National Park areas of Korea.

Sampling station	Sea area	Location	Latitude	Longitude	Salinity	Temperature	Chlorophyll *a*
M1	Yellow Sea	Taean area	36.90417	126.2111	31.63952	11.30334	1.484
M2	Yellow Sea	Taean area	36.74917	126.0969	31.81364	10.75233	1.273
M3	Yellow Sea	Taean area	36.65	126.0472	31.84344	10.29685	1.265
M4	Yellow Sea	Taean area	36.55833	126.2211	31.8141	14.52748	2.92
M5	Yellow Sea	Taean area	36.43056	126.2972	31.87676	13.58758	2.91
Z31	Yellow Sea	Taean area	36.04694	126.3808	31.66443	15.15008	1.825
Z32	Yellow Sea	Taean area	36.32694	126.2508	31.73828	12.71909	1.064
Z34	Yellow Sea	Taean area	36.60722	125.9714	31.88391	10.33093	0.72
Z36	Yellow Sea	Taean area	36.91028	126.0661	31.82114	10.48061	0.644
L1	Yellow Sea	Byeonsan area	35.68528	126.4803	31.46371	16.13612	2.34
L2	Yellow Sea	Byeonsan area	35.64917	126.4358	31.4991	17.01695	5.87
Z29	Yellow Sea	Byeonsan area	35.77833	126.3853	31.67671	14.16165	2.472
Z28	Yellow Sea	Byeonsan area	35.67083	126.2861	31.61725	15.64086	3.58
Z26	Yellow Sea	Byeonsan area	35.29278	126.0639	31.94372	14.86546	2.311

Appendix 2. Continued.

Sampling station	Sea area	Location	Latitude	Longitude	Salinity	Temperature	Chlorophyll *a*
K2	Yellow Sea	Dadohae area	34.68889	125.8381	32.83549	12.29847	4.35
Z22	Yellow Sea	Dadohae area	34.70389	125.7008	32.48076	12.86635	2.43
N3	Yellow Sea	Dadohae area	34.71611	125.4319	32.65086	10.10711	3.49
N2	Yellow Sea	Dadohae area	34.67306	125.2519	32.36144	10.68672	0.29
N1	Yellow Sea	Dadohae area	34.66889	125.1906	31.97472	11.09514	0.566
K1	Yellow Sea	Dadohae area	34.56333	125.9747	33.33876	14.22606	0.499
K3	Yellow Sea	Dadohae area	34.54528	125.8322	32.87865	11.95711	1.062
Z20	Yellow Sea	Dadohae area	34.48278	125.8844	33.42463	15.12398	0.88
J2	Yellow Sea	Dadohae area	34.40194	125.9986	33.54583	13.78609	1.177
J3	Yellow Sea	Dadohae area	34.32111	125.8994	32.69453	13.87146	1.378
Z18	Yellow Sea	Dadohae area	34.21056	125.765	33.2777	13.26334	56.629
Z25	Yellow Sea	Dadohae area	34.10667	125.8353	31.10267	14.04976	13.26
J1	Yellow Sea	Dadohae area	34.24917	126.1219	33.75933	14.09021	23.788
Z15	Yellow Sea	Dadohae area	34.1775	126.2875	33.48714	14.56383	28.114

Appendix 2. **Continued.**

Sampling station	Sea area	Location	Latitude	Longitude	Salinity	Temperature	Chlorophyll *a*
Z16	Yellow Sea	Dadohae area	34.01639	126.1319	33.99401	15.36476	56.58
J4	Southern Sea of Korea	Dadohae area	34.22972	125.9044	33.63199	12.95987	32.91
I2	Southern Sea of Korea	Dadohae area	34.26944	126.7928	33.89583	14.69754	24.702
I3	Southern Sea of Korea	Dadohae area	34.15972	126.7675	31.45507	14.72244	38.84
I1	Southern Sea of Korea	Dadohae area	34.17806	126.9669	33.9329	14.92876	21.376
Z9	Southern Sea of Korea	Dadohae area	34.2375	127.1258	33.31888	16.71229	14.566
Z7	Southern Sea of Korea	Dadohae area	34.33361	127.3336	33.76433	18.19689	15.907
H2	Southern Sea of Korea	Dadohae area	34.4	127.4211	33.42112	20.56557	3.293
O4	Southern Sea of Korea	Dadohae area	34.04333	127.3039	31.7565	17.37853	10.301
H1	Southern Sea of Korea	Dadohae area	34.45833	127.5503	32.33773	19.49161	3.321
Z6	Southern Sea of Korea	Dadohae area	34.33389	127.6425	33.65231	18.4163	22.043
G2	Southern Sea of Korea	Dadohae area	34.48306	127.745	33.66514	18.30185	29.069
G1	Southern Sea of Korea	Dadohae area	34.55694	127.7925	33.62426	17.547	24.831
G3	Southern Sea of Korea	Dadohae area	34.4125	127.855	33.19473	17.18688	47.826

Appendix 2. **Continued.**

Sampling station	Sea area	Location	Latitude	Longitude	Salinity	Temperature	Chlorophyll *a*
F1	Southern Sea of Korea	Hallyeo area	34.76278	127.7953	33.13845	18.32025	11.755
E1	Southern Sea of Korea	Hallyeo area	34.92528	127.8456	32.81521	20.0442	9.348
D1	Southern Sea of Korea	Hallyeo area	34.68556	127.9606	33.16836	19.62185	20.574
C1	Southern Sea of Korea	Hallyeo area	34.88028	128.0892	33.53164	18.70349	9.981
B2	Southern Sea of Korea	Hallyeo area	34.76	128.3642	33.85471	17.96986	22.991
B1	Southern Sea of Korea	Hallyeo area	34.76917	128.4447	33.52345	17.71767	11.545
A2	Southern Sea of Korea	Hallyeo area	34.67806	128.5978	34.09864	16.19711	54.061
A1	Southern Sea of Korea	Hallyeo area	34.76778	128.73	33.69987	16.34718	45.141
Z1	Southern Sea of Korea	Hallyeo area	34.52194	128.7269	33.1068	16.58041	75.625

Appendix 3. List of zooplankton species identified by morphological identification and metabarcoding

Identification method	Phylum	Class	Order	Family	Genus	Species
Morphological identification	Annelida	Polychaeta	-	-	-	Polychaeta larva
	Arthropoda	Branchiopoda	Onychopoda	Podonidae	Evadne	*Evadne nordmanni*
	Arthropoda	Branchiopoda	Onychopoda	Podonidae	Pleopis	*Pleopis polyphaemoides*
	Arthropoda	Branchiopoda	Onychopoda	Podonidae	Podon	*Podon leuckarti*
	Arthropoda	Branchiopoda	Onychopoda	Podonidae	Pseudevadne	*Pseudevadne tergestina*
	Arthropoda	Hexanauplia	-	-	-	Cirripedia larva
	Arthropoda	Hexanauplia	Calanoida	Acartiidae	Acartia	*Acartia* sp.
	Arthropoda	Hexanauplia	Calanoida	Acartiidae	Acartia	*Acartia hongi*
	Arthropoda	Hexanauplia	Calanoida	Acartiidae	Acartia	*Acartia hudsonica*
	Arthropoda	Hexanauplia	Calanoida	Acartiidae	Acartia	*Acartia ohtsukai*
	Arthropoda	Hexanauplia	Calanoida	Acartiidae	Acartia	*Acartia omorii*
	Arthropoda	Hexanauplia	Calanoida	Calanidae	Calanus	*Calanus* sp.
	Arthropoda	Hexanauplia	Calanoida	Calanidae	Calanus	*Calanus sinicus*
	Arthropoda	Hexanauplia	Calanoida	Calanidae	Canthocalanus	*Canthocalanus pauper*
	Arthropoda	Hexanauplia	Calanoida	Calanidae	Mesocalanus	*Mesocalanus tenuicornis*

Appendix 3. Continued.

Identification method	Phylum	Class	Order	Family	Genus	Species
Morphological identification	Arthropoda	Hexanauplia	Calanoida	Candaciidae	Candacia	*Candacia bipinnata*
	Arthropoda	Hexanauplia	Calanoida	Candaciidae	Candacia	Candacia sp.
	Arthropoda	Hexanauplia	Calanoida	Centropagidae	Centropages	Centropages abdominalis
	Arthropoda	Hexanauplia	Calanoida	Centropagidae	Centropages	Centropages sp.
	Arthropoda	Hexanauplia	Calanoida	Clausocalanidae	Clausocalanus	*Clausocalanus arcuicornis*
	Arthropoda	Hexanauplia	Calanoida	Euchaetidae	Euchaeta	*Euchaeta* sp.
	Arthropoda	Hexanauplia	Calanoida	Euchaetidae	Paraeuchaeta	*Paraeuchaeta* sp.
	Arthropoda	Hexanauplia	Calanoida	Euchaetidae	Paraeuchaeta	*Paraeuchaeta russelli*
	Arthropoda	Hexanauplia	Calanoida	Paracalanidae	Paracalanus	*Paracalanus aculeatus*
	Arthropoda	Hexanauplia	Calanoida	Paracalanidae	Paracalanus	*Paracalanus* sp.
	Arthropoda	Hexanauplia	Calanoida	Paracalanidae	Paracalanus	*Paracalanus parvus*
	Arthropoda	Hexanauplia	Calanoida	Paracalanidae	Parvocalanus	*Parvocalanus crassirostris*
	Arthropoda	Hexanauplia	Calanoida	Pontellidae	Labidocera	*Labidocera* sp.
	Arthropoda	Hexanauplia	Calanoida	Pontellidae	Labidocera	*Labidocera euchaeta*
	Arthropoda	Hexanauplia	Calanoida	Pontellidae	Labidocera	*Labidocera rotunda*

Appendix 3. Continued.

Identification method	Phylum	Class	Order	Family	Genus	Species
Morphological identification	Arthropoda	Hexanauplia	Calanoida	Pseudodiaptomidae	Pseudodiaptomus	Pseudodiaptomus sp.
	Arthropoda	Hexanauplia	Calanoida	Pseudodiaptomidae	Pseudodiaptomus	*Pseudodiaptomus marinus*
	Arthropoda	Hexanauplia	Calanoida	Tortanidae	Tortanus	*Tortanus forcifatus*
	Arthropoda	Hexanauplia	Cyclopoida	Oithonidae	Oithona	Oithona sp.
	Arthropoda	Hexanauplia	Cyclopoida	Oithonidae	Oithona	*Oithona plumifera*
	Arthropoda	Hexanauplia	Cyclopoida	Oithonidae	Oithona	*Oithona similis*
	Arthropoda	Hexanauplia	Cyclopoida	Oncaeidae	Oncaea	*Oncaea clevei*
	Arthropoda	Hexanauplia	Cyclopoida	Oncaeidae	Oncaea	*Oncaea meditteranea*
	Arthropoda	Hexanauplia	Cyclopoida	Oncaeidae	Oncaea	*Oncaea venella*
	Arthropoda	Hexanauplia	Harpacticoida	Peltidiidae	Goniopsyllus	*Goniopsyllus rostrata*
	Arthropoda	Hexanauplia	Monstrilloida	Monstrillidae	Cymbasoma	*Cymbasoma longspinosum*
	Arthropoda	Hexanauplia	Poecilostomatoida	Corycaeidae	Corycaeus	*Corycaeus affinis*
	Arthropoda	Hexanauplia	Poecilostomatoida	Corycaeidae	Corycaeus	Corycaeus sp.
	Arthropoda	Harpacticoida	Hexanauplia	-	-	Unidentified Harpacticoida
	Arthropoda	Malacostraca	Amphipoda	-	-	Amphipoda larva

Appendix 3. Continued.

Identification method	Phylum	Class	Order	Family	Genus	Species
Morphological identification	Arthropoda	Malacostraca	Amphipoda	-	-	Tadpole larva
	Arthropoda	Malacostraca	Amphipoda	Gammaridae	-	Unidentified Gammaridae
	Arthropoda	Malacostraca	Cumacea	-	-	Unidentified Cumacea
	Arthropoda	Malacostraca	Decapoda	-	-	Decapoda larva
	Arthropoda	Malacostraca	Decapoda	Euphausiacea	Euphausiidae	Euphausid larva
	Arthropoda	Malacostraca	Decapoda	Porcellanidae	Porcellana	*Porcellana zoea*
	Arthropoda	Malacostraca	Isopoda	-	-	Unidentified Isopoda
	Arthropoda	Malacostraca	Mysida	Mysidae	-	Mycidacea larva
	Arthropoda	Ostracoda	Bythocytheridae	Sclerochilus	Cypris	Cypris larva
	Arthropoda	Ostracoda	Halocypridina	Halocyprididae	Conchoecia	*Conchoecia* sp.
	Asteroidea	-	-	-	-	Asteroidea larvae
	Bryozoa	Stenolaemata	Cyclostomatida	Tubuliporidae	Tubulipora	*Tubulipora* sp.
	Chaetognatha	Sagittoidea	Aphragmophora	Sagittidae	Sagitta	Sagitta larvae
	Chaetognatha	Sagittoidea	Aphragmophora	Sagittidae	Sagitta	*Sagitta crassa*
	Chaetognatha	Sagittoidea	Aphragmophora	Sagittidae	Sagitta	*Sagitta nagae*

Appendix 3. Continued.

Identification method	Phylum	Class	Order	Family	Genus	Species
Morphological identification	Chordata	Actinopterygii	Stomiiformes	Stomiidae	Photonectes	Lucifer sp.
	Chordata	Appendicularia	Copelata	Oikopleuridae	Oikopleura	*Oikopleura* spp.
	Chordata	Thaliacea	Salpida	Salpidae	Salpa	*Salpa* sp.
	Cnidaria	Hydrozoa	-	-	-	Unidentified Hydrozoa
	Cnidaria	Hydrozoa	Anthoathecata	Corymorphidae	Euphysa	*Euphysa aurata*
	Cnidaria	Hydrozoa	Anthoathecata	Rathkeidae	Rathkea	*Rathkea octopunctata*
	Cnidaria	Hydrozoa	Leptothecata	Phialellidae	Phialella	*Phialella* sp.
	Cnidaria	Hydrozoa	Narcomedusae	Solmundaeginidae	Solmundella	*Solmundella* sp.
	Cnidaria	Hydrozoa	Siphonophorae	Diphyidae	Diphyes	*Diphyes* spp.
	Cnidaria	Hydrozoa	Siphonophorae	Diphyidae	Muggiaea	*Muggiaea* spp.
	Echinodermata	-	-	-	-	Echinopluteus larva
	Echinodermata	Holothuroidea	Apodida	Synaptidae	Protankyra	Protankyra larva
	Echinodermata	Ophiuroidea	-	-	-	Ophiopluteus larva
	Mollusca	Bivalvia	-	-	-	Bivalve larva
	Mollusca	Cephalopoda	-	-	-	Cephalopoda larva

Appendix 3. Continued.

Identification method	Phylum	Class	Order	Family	Genus	Species
Morphological identification	Mollusca	Gastropoda	-	-	-	Gastropoda larva
	Mollusca	Gastropoda	Littorinimorpha	Cymatiidae	Cabestana	*Cabestana* sp.
	Mollusca	Gastropoda	Pteropoda	Creseidae	Creseis	*Creseis* spp.
	Myzozoa	Dinophyceae	Noctilucales	Noctilucaceae	Noctiluca	*Noctiluca scintillans*

Appendix 3. Continued.

Identification method	Phylum	Class	Order	Family	Genus	Species_OTU
DNA metabarcoding	Acanthocephala	Palaeacanthocephala	Echinorhynchida	Transvenidae	Pararhadinorhynchus	*Pararhadinorhynchus* sp. JYW-2010
	Acanthocephala	Palaeacanthocephala	Polymorphida	Centrorhynchidae	Centrorhynchus	*Centrorhynchus globirostris*
	Acanthocephala	Palaeacanthocephala	Polymorphida	Plagiorhynchidae	Plagiorhynchus	*Plagiorhynchus cylindraceus*
	Annelida	Polychaeta		Opheliidae	Ophelina	*Ophelina acuminata*
	Annelida	Polychaeta	Capitellida	Capitellidae	Heteromastus	*Heteromastus filiformis*
	Annelida	Polychaeta	Echiuroinea	Echiuridae	Thalassema	*Thalassema thalassemum*
	Annelida	Polychaeta	Phyllodocida	Alciopedidae	Torrea	*Torrea* sp. THS-2006
	Annelida	Polychaeta	Phyllodocida	Glyceridae	Glycera	*Glycera americana*
	Annelida	Polychaeta	Phyllodocida	Goniadidae	Glycinde	*Glycinde armigera*
	Annelida	Polychaeta	Phyllodocida	Hisionidae	Kefersteinia	*Kefersteinia cirrata*
	Annelida	Polychaeta	Phyllodocida	Nephtyidae	Nephtys	*Nephtys incisa*
	Annelida	Polychaeta	Phyllodocida	Phyllodocidae	Eteone	*Eteone longa*
	Annelida	Polychaeta	Phyllodocida	Polynoidae	Lepidonotus	*Lepidonotus sublevis*
	Annelida	Polychaeta	Phyllodocida	Sigalionidae	Sthenelanella	*Sthenelanella uniformis*
	Annelida	Polychaeta	Phyllodocida	Syllidae	Proceraea	*Proceraea misakiensis*

Appendix 3. Continued.

Identification method	Phylum	Class	Order	Family	Genus	Species_OTU
DNA metabarcoding	Annelida	Polychaeta	Phyllodocida	Syllidae	Syllides	*Syllides* sp. 2 MTA-2011
	Annelida	Polychaeta	Sabellida	Oweniidae	Owenia	*Owenia fusiformis*
	Annelida	Polychaeta	Sabellida	Sabellariidae	Idanthyrsus	*Idanthyrsus australiensis*
	Annelida	Polychaeta	Spionida	Chaetopteridae	Mesochaetopterus	*Mesochaetopterus taylori*
	Annelida	Polychaeta	Spionida	Chaetopteridae	Spiochaetopterus	*Spiochaetopterus bergensis*
	Annelida	Polychaeta	Spionida	Magelonidae	Magelona	*Magelona cincta*
	Annelida	Polychaeta	Spionida	Poecilochaetidae	Poecilochaetus	*Poecilochaetus serpens*
	Annelida	Polychaeta	Spionida	Spionidae	Boccardiella	*Boccardiella ligerica*
	Annelida	Polychaeta	Spionida	Spionidae	Laonice	*Laonice cirrata*
	Annelida	Polychaeta	Spionida	Spionidae	Polydora	*Polydora lingshuiensis*
	Annelida	Polychaeta	Spionida	Spionidae	Prionospio	*Prionospio cirrifera*
	Annelida	Polychaeta	Spionida	Spionidae	Prionospio	*Prionospio dubia*
	Annelida	Polychaeta	Spionida	Spionidae	Scolelepis	*Scolelepis chilensis*
	Annelida	Polychaeta	Spionida	Spionidae	Spio	*Spio* sp. LK-2011-1
	Annelida	Polychaeta	Terebellida	Pectinariidae	Pectinaria	*Pectinaria koreni*

Appendix 3. Continued.

Identification method	Phylum	Class	Order	Family	Genus	Species_OTU
DNA metabarcoding	Annelida	Polychaeta	Terebellida	Terebellidae	Lanice	*Lanice conchilega*
	Annelida	Polychaeta	Terebellida	Terebellidae	Lysilla	*Lysilla* sp. THS-2012
	Annelida	Polychaeta	Xenopneusta	Urechidae	Urechis	*Urechis* sp. RG-2015-1
	Arthropoda	Arachnida	Araneae	Pholcidae	Pholcus	*Pholcus manueli*
	Arthropoda	Arachnida	Trombidiformes	Eriophyidae	Calepitrimerus	*Calepitrimerus fopingi*
	Arthropoda	Arachnida	Trombidiformes	Microtrombidiidae	Microtrombidium	*Microtrombidium cooki*
	Arthropoda	Branchiopoda	Diplostraca	Podonidae	Evadne	*Evadne nordmanni*
	Arthropoda	Branchiopoda	Diplostraca	Podonidae	Evadne	*Evadne spinifera*
	Arthropoda	Branchiopoda	Diplostraca	Podonidae	Podon	*Podon* sp. pool 2
	Arthropoda	Branchiopoda	Diplostraca	Sididae	Sida	*Sida crystallina*
	Arthropoda	Hexanauplia	-	-	-	Unidentified Copepoda
	Arthropoda	Hexanauplia	Calanoida	Acartiidae	Acartia	*Acartia hongi*
	Arthropoda	Hexanauplia	Calanoida	Acartiidae	Acartia	*Acartia hudsonica*
	Arthropoda	Hexanauplia	Calanoida	Acartiidae	Acartia	*Acartia omorii*
	Arthropoda	Hexanauplia	Calanoida	Calanidae	-	Unidentified Calanidae

Appendix 3. Continued.

Identification method	Phylum	Class	Order	Family	Genus	Species_OTU
DNA metabarcoding	Arthropoda	Hexanauplia	Calanoida	Calanidae	Calanus	*Calanus finmarchicus*
	Arthropoda	Hexanauplia	Calanoida	Calanidae	Calanus	*Calanus helgolandicus*
	Arthropoda	Hexanauplia	Calanoida	Calanidae	Calanus	*Calanus sinicus*
	Arthropoda	Hexanauplia	Calanoida	Candaciidae	Candacia	*Candacia armata*
	Arthropoda	Hexanauplia	Calanoida	Centropagidae	Centropages	*Centropages abdominalis*
	Arthropoda	Hexanauplia	Calanoida	Centropagidae	Centropages	*Centropages typicus*
	Arthropoda	Hexanauplia	Calanoida	Centropagidae	Sinocalanus	*Sinocalanus sinensis*
	Arthropoda	Hexanauplia	Calanoida	Euchaetidae	Euchaeta	*Euchaeta indica*
	Arthropoda	Hexanauplia	Calanoida	Euchaetidae	Paraeuchaeta	*Paraeuchaeta gracilis*
	Arthropoda	Hexanauplia	Calanoida	Metridinidae	Pleuromamma	*Pleuromamma robusta*
	Arthropoda	Hexanauplia	Calanoida	Paracalanidae	-	Unidentified Paracalanidae
	Arthropoda	Hexanauplia	Calanoida	Pontellidae	Labidocera	*Labidocera euchaeta*
	Arthropoda	Hexanauplia	Calanoida	Pontellidae	Labidocera	*Labidocera japonica*
	Arthropoda	Hexanauplia	Calanoida	Pseudodiaptomidae	Pseudodiaptomus	*Pseudodiaptomus marinus*
	Arthropoda	Hexanauplia	Calanoida	Scolecitrichidae	Scolecithricella	*Scolecithricella longispinosa*

Appendix 3. Continued.

Identification method	Phylum	Class	Order	Family	Genus	Species_OTU
DNA metabarcoding	Arthropoda	Hexanauplia	Cyclopoida	Archinotodelphyidae	Archinotodelphys	*Archinotodelphys* sp. New Caledonia-RJH-2001
	Arthropoda	Hexanauplia	Cyclopoida	Cyclopidae	Ectocyclops	*Ectocyclops polyspinosus*
	Arthropoda	Hexanauplia	Cyclopoida	Cyclopinidae	Cyclopina	*Cyclopina gracilis*
	Arthropoda	Hexanauplia	Cyclopoida	Oithonidae	-	*Oithonidae* sp. DZMB624
	Arthropoda	Hexanauplia	Cyclopoida	Oithonidae	-	Oithonidae sp.
	Arthropoda	Hexanauplia	Harpacticoida	Canuellidae	Canuella	*Canuella perplexa*
	Arthropoda	Hexanauplia	Harpacticoida	Ectinosomatidae	Bradya	*Bradya* sp. Greenland-RJH-2004
	Arthropoda	Hexanauplia	Harpacticoida	Harpacticidae	Zausodes	*Zausodes arenicolus*
	Arthropoda	Hexanauplia	Harpacticoida	Laophontidae	Onychocamptus	*Onychocamptus bengalensis*
	Arthropoda	Hexanauplia	Harpacticoida	Miraciidae	Stenhelia	*Stenhelia* sp. *Greenland-RJH-2007*
	Arthropoda	Hexanauplia	Harpacticoida	Peltidiidae	Peltidium	*Peltidium sp. New Caledonia-RJH-2007*
	Arthropoda	Hexanauplia	Harpacticoida	Thalestridae	Paramenophia	*Paramenophia* sp. New Caledonia-RJH-2007
	Arthropoda	Hexanauplia	Harpacticoida	Tisbidae	Tisbe	*Tisbe* sp. JSL-2009
	Arthropoda	Hexanauplia	Kentrogonida	Sylonidae	Sylon	*Sylon hippolytes*
	Arthropoda	Hexanauplia	Monstrilloida	Monstrillidae	Monstrilla	*Monstrilla clavata*

Appendix 3. Continued.

Identification method	Phylum	Class	Order	Family	Genus	Species_OTU
DNA metabarcoding	Arthropoda	Hexanauplia	Monstrilloida	Monstrillidae	Monstrilla	*Monstrilla* sp. DZMB335
	Arthropoda	Hexanauplia	Poecilostomatoida	Clausidiidae	Hemicyclops	*Hemicyclops thalassius*
	Arthropoda	Hexanauplia	Poecilostomatoida	Corycaeidae	Corycaeus	*Corycaeus speciosus*
	Arthropoda	Hexanauplia	Poecilostomatoida	Oncaeidae	Oncaea	*Oncaea* sp. DZMB524
	Arthropoda	Hexanauplia	Pygophora	Lithoglyptidae	Berndtia	*Berndtia purpurea*
	Arthropoda	Ichthyostraca	Porocephalida	Armilliferidae	Armillifer	*Armillifer agkistrodontis*
	Arthropoda	Malacostraca	Amphipoda	Caprellidae	Perotripus	*Perotripus* sp. AI-2007-4
	Arthropoda	Malacostraca	Amphipoda	Caprellidae	Protogeton	*Protogeton* sp. AI-2007-3
	Arthropoda	Malacostraca	Amphipoda	Eusiridae	Eusirus	*Eusirus perdentatus*
	Arthropoda	Malacostraca	Amphipoda	Hyperiidae	Hyperietta	*Hyperietta sibaginis*
	Arthropoda	Malacostraca	Amphipoda	Hyperiidae	Themisto	*Themisto abyssorum*
	Arthropoda	Malacostraca	Amphipoda	Lysianassidae	Onisimus	*Onisimus nanseni*
	Arthropoda	Malacostraca	Amphipoda	Melphidippidae	Melphidippa	*Melphidippa antarctica*
	Arthropoda	Malacostraca	Amphipoda	Oedicerotidae	Arrhis	*Arrhis phyllonyx*
	Arthropoda	Malacostraca	Decapoda	Alpheidae	-	Alpheidae sp. BOLD:ACR8483

Appendix 3. Continued.

Identification method	Phylum	Class	Order	Family	Genus	Species_OTU
DNA metabarcoding	Arthropoda	Malacostraca	Decapoda	Alpheidae	Alpheus	*Alpheus packardii*
	Arthropoda	Malacostraca	Decapoda	Alpheidae	Athanas	*Athanas nitescens*
	Arthropoda	Malacostraca	Decapoda	Callianassidae	Neotrypaea	*Neotrypaea californiensis*
	Arthropoda	Malacostraca	Decapoda	Coenobitidae	Coenobita	*Coenobita compressus*
	Arthropoda	Malacostraca	Decapoda	Crangonidae	Crangon	*Crangon crangon*
	Arthropoda	Malacostraca	Decapoda	Diogenidae	Paguristes	*Paguristes tortugae*
	Arthropoda	Malacostraca	Decapoda	Galatheidae	Galathea	*Galathea rostrata*
	Arthropoda	Malacostraca	Decapoda	Hippolytidae	Eualus	*Eualus gaimardii*
	Arthropoda	Malacostraca	Decapoda	Hippolytidae	Latreutes	*Latreutes fucorum*
	Arthropoda	Malacostraca	Decapoda	Hippolytidae	Lysmata	*Lysmata* sp. BOLD:ACR4896
	Arthropoda	Malacostraca	Decapoda	Kiwaidae	Kiwa	*Kiwa* sp. n. Southwest Indian Ridge
	Arthropoda	Malacostraca	Decapoda	Mithracidae	Teleophrys	*Teleophrys cristulipes*
	Arthropoda	Malacostraca	Decapoda	Paguridae	Pagurus	*Pagurus pollicaris*
	Arthropoda	Malacostraca	Decapoda	Palaemonidae	Palaemon	*Palaemon serrifer*
	Arthropoda	Malacostraca	Decapoda	Palaemonidae	Urocaridella	*Urocaridella pulchella*

Appendix 3. Continued.

Identification method	Phylum	Class	Order	Family	Genus	Species_OTU
DNA metabarcoding	Arthropoda	Malacostraca	Decapoda	Parthenopidae	Parthenope	*Parthenope validus*
	Arthropoda	Malacostraca	Decapoda	Portunidae	Charybdis	*Charybdis japonica*
	Arthropoda	Malacostraca	Decapoda	Portunidae	Portunus	*Portunus sanguinolentus*
	Arthropoda	Malacostraca	Decapoda	Solenoceridae	Solenocera	*Solenocera necopina*
	Arthropoda	Malacostraca	Decapoda	Varunidae	Eriocheir	*Eriocheir sinensis*
	Arthropoda	Malacostraca	Euphausiacea	Euphausiidae	Meganyctiphanes	*Meganyctiphanes norvegica*
	Arthropoda	Malacostraca	Euphausiacea	Euphausiidae	Thysanopoda	*Thysanopoda pectinata*
	Arthropoda	Malacostraca	Isopoda	Bopyridae	Hemiarthrus	*Hemiarthrus abdominalis*
	Arthropoda	Malacostraca	Mysida	Mysidae	Gastrosaccus	*Gastrosaccus spinifer*
	Arthropoda	Malacostraca	Mysida	Mysidae	Neomysis	*Neomysis americana*
	Arthropoda	Ostracoda	Halocyprida	Halocyprididae	Conchoecia	*Conchoecia* sp. OC-2001
	Arthropoda	Ostracoda	Halocyprida	Halocyprididae	Conchoecia	*Conchoecia* sp. SN008
	Arthropoda	Ostracoda	Myodocopida	Cypridinidae	Vargula	*Vargula hilgendorfii*
	Arthropoda	Ostracoda	Myodocopida	Sarsiellidae	Eusarsiella	*Eusarsiella* sp. Belize
	Brachiopoda	-	-	Phoronidae	Phoronis	*Phoronis ijimai*

Appendix 3. Continued.

Identification method	Phylum	Class	Order	Family	Genus	Species_OTU
DNA metabarcoding	Brachiopoda	-	-	Phoronidae	Phoronis	*Phoronis* sp. 1 AS-2015
	Bryozoa	Gymnolaemata	Cheilostomatida	Membraniporidae	Membranipora	*Membranipora membranacea*
	Bryozoa	Gymnolaemata	Ctenostomatida	Alcyonidiidae	Alcyonidium	*Alcyonidium gelatinosum*
	Bryozoa	Gymnolaemata	Ctenostomatida	Nolellidae	Anguinella	*Anguinella palmata*
	Chaetognatha	Sagittoidea	Aphragmophora	Sagittidae	Aidanosagitta	*Aidanosagitta neglecta*
	Chaetognatha	Sagittoidea	Aphragmophora	Sagittidae	Decipisagitta	*Decipisagitta decipiens*
	Chaetognatha	Sagittoidea	Aphragmophora	Sagittidae	Pseudosagitta	*Pseudosagitta lyra*
	Chaetognatha	Sagittoidea	Aphragmophora	Sagittidae	Sagitta	*Sagitta elegans*
	Chaetognatha	Sagittoidea	Aphragmophora	Sagittidae	Sagitta	*Sagitta* sp. DP-2006
	Chlorophyta	Pedinophyceae	Marsupiomonadales	Marsupiomonadaceae	Protoeuglena	*Protoeuglena noctilucae*
	Chlorophyta	Trebouxiophyceae	Chlorellales	Oocystaceae	Oocystis	*Oocystis borgei*
	Chordata	Actinopteri	Blenniiformes	Gobiesocidae	Gouania	*Gouania willdenowi*
	Chordata	Actinopteri	Clupeiformes	Engraulidae	Engraulis	*Engraulis encrasicolus*
	Chordata	Actinopteri	Gadiformes	Gadidae	Gadus	*Gadus morhua*
	Chordata	Actinopteri	Pleuronectiformes	Pleuronectidae	Kareius	*Kareius bicoloratus*

Appendix 3. Continued.

Identification method	Phylum	Class	Order	Family	Genus	Species_OTU
DNA metabarcoding	Chordata	Actinopteri	Pleuronectiformes	Pleuronectidae	Pleuronichthys	*Pleuronichthys cornutus*
	Chordata	Actinopteri	Spariformes	Sparidae	Sparus	*Sparus aurata*
	Chordata	Actinopteri	Syngnathiformes	Mullidae	Mullus	*Mullus barbatus*
	Chordata	Ascidiacea	Enterogona	Ascidiidae	Phallusia	*Phallusia mammillata*
	Chordata	Ascidiacea	Enterogona	Ascidiidae	Phallusia	*Phallusia nigra*
	Chordata	Ascidiacea	Enterogona	Didemnidae	Didemnum	*Didemnum molle*
	Chordata	Ascidiacea	Enterogona	Didemnidae	Diplosoma	*Diplosoma simileguwa*
	Chordata	Ascidiacea	Stolidobranchia	Pyuridae	Halocynthia	*Halocynthia spinosa*
	Chordata	Thaliacea	Salpida	Salpidae	Salpa	*Salpa fusiformis*
	Cnidaria	Anthozoa	Actiniaria	Aiptasiidae	Aiptasia	*Aiptasia pulchella*
	Cnidaria	Anthozoa	Corallimorpharia	Discosomidae	Discosoma	*Discosoma* sp. TW019
	Cnidaria	Anthozoa	Corallimorpharia	Discosomidae	Rhodactis	*Rhodactis* sp. TW018
	Cnidaria	Anthozoa	Scleractinia	Acroporidae	Acropora	*Acropora granulosa*
	Cnidaria	Anthozoa	Scleractinia	Acroporidae	Montipora	*Montipora foliosa*
	Cnidaria	Anthozoa	Scleractinia	Acroporidae	Montipora	*Montipora venosa*

Appendix 3. Continued.

Identification method	Phylum	Class	Order	Family	Genus	Species_OTU
DNA metabarcoding	Cnidaria	Anthozoa	Scleractinia	Poritidae	Alveopora	*Alveopora spongiosa*
	Cnidaria	Hydrozoa	Anthoathecata	Bougainvilliidae	Bougainvillia	*Bougainvillia* sp. AGC-2001
	Cnidaria	Hydrozoa	Anthoathecata	Bougainvilliidae	Garveia	*Garveia* sp. CC-2005
	Cnidaria	Hydrozoa	Anthoathecata	Corymorphidae	Corymorpha	*Corymorpha bigelowi*
	Cnidaria	Hydrozoa	Anthoathecata	Corymorphidae	Corymorpha	*Corymorpha glacialis*
	Cnidaria	Hydrozoa	Anthoathecata	Corymorphidae	Euphysa	*Euphysa aurata*
	Cnidaria	Hydrozoa	Anthoathecata	Corymorphidae	Euphysa	*Euphysa tentaculata*
	Cnidaria	Hydrozoa	Anthoathecata	Cytaeididae	Cytaeis	*Cytaeis* sp. MAN-2015
	Cnidaria	Hydrozoa	Anthoathecata	Hydractiniidae	Podocoryna	*Podocoryna exigua*
	Cnidaria	Hydrozoa	Anthoathecata	Hydractiniidae	Solanderia	*Solanderia secunda*
	Cnidaria	Hydrozoa	Anthoathecata	Proboscidactylidae	Fabienna	*Fabienna sphaerica*
	Cnidaria	Hydrozoa	Anthoathecata	Tubulariidae	Ectopleura	*Ectopleura dumortierii*
	Cnidaria	Hydrozoa	Leptothecata	Blackfordiidae	Blackfordia	*Blackfordia virginica*
	Cnidaria	Hydrozoa	Leptothecata	Campanulariidae	Billardia	*Billardia subrufa*
	Cnidaria	Hydrozoa	Leptothecata	Campanulariidae	Clytia	*Clytia hemisphaerica*

Appendix 3. Continued.

Identification method	Phylum	Class	Order	Family	Genus	Species_OTU
DNA metabarcoding	Cnidaria	Hydrozoa	Leptothecata	Campanulariidae	Clytia	*Clytia* sp. AGC-2001
	Cnidaria	Hydrozoa	Leptothecata	Campanulariidae	Clytia	*Clytia xiamenensis*
	Cnidaria	Hydrozoa	Leptothecata	Campanulariidae	Obelia	*Obelia bidentata*
	Cnidaria	Hydrozoa	Leptothecata	Campanulariidae	Obelia	*Obelia dichotoma*
	Cnidaria	Hydrozoa	Leptothecata	Campanulariidae	Obelia	*Obelia longissima*
	Cnidaria	Hydrozoa	Leptothecata	Campanulariidae	Orthopyxis	*Orthopyxis crenata*
	Cnidaria	Hydrozoa	Leptothecata	Campanulariidae	Stegella	*Stegella lobata*
	Cnidaria	Hydrozoa	Leptothecata	Eirenidae	Helgicirrha	*Helgicirrha cari*
	Cnidaria	Hydrozoa	Leptothecata	Lafoeidae	Lafoea	*Lafoea dumosa*
	Cnidaria	Hydrozoa	Leptothecata	Laodiceidae	Melicertissa	*Melicertissa* sp. AGC-2001
	Cnidaria	Hydrozoa	Leptothecata	Melicertidae	Melicertum	*Melicertum octocostatum*
	Cnidaria	Hydrozoa	Narcomedusae	Aeginidae	Aegina	*Aegina citrea*
	Cnidaria	Hydrozoa	Siphonophorae	-	-	Calycophorae sp. LC-2017
	Cnidaria	Hydrozoa	Siphonophorae	Diphyidae	Muggiaea	*Muggiaea* sp. AGC-2001
	Cnidaria	Hydrozoa	Siphonophorae	Sphaeronectidae	Sphaeronectes	Sphaeronectes haddocki

Appendix 3. Continued.

Identification method	Phylum	Class	Order	Family	Genus	Species_OTU
DNA metabarcoding	Cnidaria	Scyphozoa	Rhizostomeae	Rhizostomatidae	Rhopilema	*Rhopilema esculentum*
	Cnidaria	Scyphozoa	Rhizostomeae	Rhizostomatidae	Stomolophus	*Stomolophus meleagris*
	Cnidaria	Scyphozoa	Semaeostomeae	Drymonematidae	Drymonema	*Drymonema larsoni*
	Cnidaria	Scyphozoa	Semaeostomeae	Ulmaridae	Aurelia	*Aurelia* sp. Incheon-2006
	Ctenophora	Tentaculata	Cydippida	Lampeidae	Lampea	*Lampea pancerina*
	Echinodermata	Asteroidea	Forcipulatida	Asteriidae	Pisaster	*Pisaster ochraceus*
	Echinodermata	Crinoidea	Bourgueticrinida	Bathycrinidae	Bathycrinus	*Bathycrinus* sp. D1425
	Echinodermata	Crinoidea	Isocrinida	-	Caledonicrinus	*Caledonicrinus vaubani*
	Echinodermata	Echinoidea	Echinoida	Echinidae	Sterechinus	*Sterechinus neumayeri*
	Echinodermata	Echinoidea	Temnopleuroida	Toxopneustidae	Lytechinus	*Lytechinus variegatus*
	Echinodermata	Holothuroidea	Apodida	Synaptidae	Oestergrenia	*Oestergrenia digitata*
	Echinodermata	Holothuroidea	Aspidochirotida	Synallactidae	Synallactes	*Synallactes* sp. AKM-2016
	Echinodermata	Holothuroidea	Dendrochirotida	Sclerodactylidae	Afrocucumis	*Afrocucumis africana*
	Echinodermata	Holothuroidea	Elasipodida	Deimatidae	Oneirophanta	*Oneirophanta setigera*
	Echinodermata	Ophiuroidea	Euryalida	Gorgonocephalidae	Gorgonocephalus	*Gorgonocephalus eucnemis*

Appendix 3. Continued.

Identification method	Phylum	Class	Order	Family	Genus	Species_OTU
DNA metabarcoding	Echinodermata	Ophiuroidea	Ophiurida	Amphiuridae	Amphipholis	*Amphipholis squamata*
	Entoprocta	-	-	Loxosomatidae	Loxosomella	*Loxosomella plakorticola*
	Entoprocta	-	-	Loxosomatidae	Loxosomella	*Loxosomella* sp. 2 JF-2010
	Hemichordata	Enteropneusta	-	-	-	Enteropneusta sp. extrawide-lipped
	Mollusca	Bivalvia	Arcoida	Arcidae	Barbatia	*Barbatia virescens*
	Mollusca	Bivalvia	Myoida	Hiatellidae	Hiatella	*Hiatella arctica*
	Mollusca	Bivalvia	Mytiloida	Mytilidae	Musculus	*Musculus lateralis*
	Mollusca	Bivalvia	Mytiloida	Mytilidae	Mytilus	*Mytilus trossulus*
	Mollusca	Bivalvia	Ostreoida	Ostreidae	Crassostrea	*Crassostrea gigas*
	Mollusca	Bivalvia	Ostreoida	Ostreidae	Ostrea	*Ostrea edulis*
	Mollusca	Bivalvia	Veneroida	Cardiidae	Cerastoderma	*Cerastoderma edule*
	Mollusca	Bivalvia	Veneroida	Galeommatidae	Galeomma	*Galeomma takii*
	Mollusca	Bivalvia	Veneroida	Lasaeidae	Platomysia	*Platomysia rugata*
	Mollusca	Bivalvia	Veneroida	Mactridae	Tresus	*Tresus nuttallii*
	Mollusca	Bivalvia	Veneroida	Montacutidae	Koreamya	*Koreamya setouchiensis*

Appendix 3. Continued.

Identification method	Phylum	Class	Order	Family	Genus	Species_OTU
DNA metabarcoding	Mollusca	Bivalvia	Veneroida	Pharidae	Ensis	*Ensis siliqua*
	Mollusca	Bivalvia	Veneroida	Psammobiidae	Soletellina	*Soletellina diphos*
	Mollusca	Bivalvia	Veneroida	Veneridae	Dosinia	*Dosinia corrugata*
	Mollusca	Bivalvia	Veneroida	Veneridae	Meretrix	*Meretrix lusoria*
	Mollusca	Gastropoda	-	Pyramidellidae	Pyrgisculus	*Pyrgisculus* sp. EED-Phy-920
	Mollusca	Gastropoda	-	Ringiculidae	Microglyphis	*Microglyphis* sp. YK-2016b
	Mollusca	Gastropoda	-	Siphonariidae	Siphonaria	*Siphonaria japonica*
	Mollusca	Gastropoda	Cephalaspidea	Aglajidae	Mariaglaja	*Mariaglaja inornata*
	Mollusca	Gastropoda	Cephalaspidea	Cylichnidae	Cylichna	*Cylichna cylindracea*
	Mollusca	Gastropoda	Littorinimorpha	Littorinidae	Echinolittorina	*Echinolittorina punctata*
	Mollusca	Gastropoda	Littorinimorpha	Littorinidae	Littorina	*Littorina saxatilis*
	Mollusca	Gastropoda	Littorinimorpha	Naticidae	Lunatia	*Lunatia gilva*
	Mollusca	Gastropoda	Littorinimorpha	Strombidae	Lambis	*Lambis lambis*
	Mollusca	Gastropoda	Neogastropoda	Buccinidae	Aeneator	*Aeneator recens*
	Mollusca	Gastropoda	Neogastropoda	Buccinidae	Cominella	*Cominella adspersa*

Appendix 3. Continued.

Identification method	Phylum	Class	Order	Family	Genus	Species_OTU
DNA metabarcoding	Mollusca	Gastropoda	Neogastropoda	Buccinidae	Kelletia	*Kelletia lischkei*
	Mollusca	Gastropoda	Neogastropoda	Fasciolariidae	Fusinus	*Fusinus longicaudus*
	Mollusca	Gastropoda	Neogastropoda	Nassariidae	Nassarius	*Nassarius festivus*
	Mollusca	Gastropoda	Nudibranchia	-	Triopha	*Triopha catalinae*
	Mollusca	Gastropoda	Nudibranchia	Dendrodorididae	Dendrodoris	*Dendrodoris fumata*
	Mollusca	Gastropoda	Nudibranchia	Discodorididae	Discodoris	*Discodoris concinna*
	Mollusca	Gastropoda	Nudibranchia	Tritoniidae	Tritoniopsis	*Tritoniopsis frydis*
	Mollusca	Gastropoda	Pleurobranchida	Pleurobranchidae	Pleurobranchaea	*Pleurobranchaea californica*
	Mollusca	Gastropoda	Siphonariida	Siphonariidae	Siphonaria	*Siphonaria japonica*
	Mollusca	Polyplacophora	Neoloricata	Mopaliidae	Katharina	*Katharina tunicata*
	Myzozoa	Dinophyceae	Noctilucales	Noctilucaceae	Noctiluca	*Noctiluca scintillans*
	Nematoda	Chromadorea	Chromadorida	Chromadoridae	Chromadorita	*Chromadorita leuckarti*
	Nematoda	Chromadorea	Rhabditida	Aphelenchoididae	Aphelenchoides	*Aphelenchoides* sp. FOFIFA-MG-2-1
	Nematoda	Enoplea	Enoplida	Phanodermatidae	Phanoderma	*Phanoderma* sp. 24S2F
	Nematoda	Enoplea	Enoplida	Trefusiidae	Trefusia	*Trefusia zostericola*

Appendix 3. Continued.

Identification method	Phylum	Class	Order	Family	Genus	Species_OTU
DNA metabarcoding	Nemertea	Palaeonemertea	-	Cephalothricidae	Cephalothrix	*Cephalothrix rufifrons*
	Nemertea	Palaeonemertea	-	Tubulanidae	-	Tubulanidae sp. MCZ IZ 45554
	Nemertea	Pilidiophora	-	Hubrechtidae	Hubrechtella	*Hubrechtella juliae*
	Nemertea	Pilidiophora	Heteronemertea	Cerebratulidae	Cerebratulus	*Cerebratulus lacteus*
	Nemertea	Pilidiophora	Heteronemertea	Lineidae	Kulikovia	*Kulikovia manchenkoi*
	Platyhelminthes	-	Polycladida	Leptoplanidae	Hoploplana	*Hoploplana californica*
	Platyhelminthes	-	Polycladida	Stylochidae	Stylochus	*Stylochus zebra*
	Platyhelminthes	Cestoda	Bothriocephalidea	Bothriocephalidae	Bothriocephalus	*Bothriocephalus claviceps*
	Platyhelminthes	Cestoda	Phyllobothriidea	Phyllobothriidae	Clistobothrium	*Clistobothrium* sp. JH-2016
	Platyhelminthes	Cestoda	Phyllobothriidea	Phyllobothriidae	Crossobothrium	*Crossobothrium* sp. PWK-2012
	Platyhelminthes	Monogenea	-	Ancyrocephalidae	Tetrancistrum	*Tetrancistrum nebulosi*
	Platyhelminthes	Trematoda	-	-	Prosorhynchoides	*Prosorhynchoides ovatus*
	Platyhelminthes	Trematoda	Azygiida	Derogenidae	Deropegus	*Deropegus aspina*
	Platyhelminthes	Trematoda	Azygiida	Hemiuridae	Aphanurus	*Aphanurus mugilus*
	Platyhelminthes	Trematoda	Azygiida	Lecithasteridae	Lecithaster	*Lecithaster gibbosus*

Appendix 3. Continued.

Identification method	Phylum	Class	Order	Family	Genus	Species_OTU
DNA metabarcoding	Platyhelminthes	Trematoda	Opisthorchiida	Heterophyidae	Apophallus	Apophallus donicus
	Platyhelminthes	Trematoda	Plagiorchiida	Nanophyetidae	Nanophyetus	*Nanophyetus* sp.
	Platyhelminthes	Trematoda	Plagiorchiida	Pleurogenidae	Pleurogenoides	*Pleurogenoides gastroporus*
	Rotifera	-	-	-	-	Rotifera sp.
	Rotifera	Monogononta	Ploima	Synchaetidae	Synchaeta	*Synchaeta tremuloida*
	Xenacoelomorpha	Acoela	-	Actinoposthiidae	Atriofronta	*Atriofronta polyvacuola*

Appendix 4. Publications

This dissertation includes manuscripts that prepared for publication in peer-reviewed journals or already published in Ph.D. course. The contents of each chapter in this dissertation were quoted as below. The title and authorship of the manuscripts can be changed during subsequent revisions.

*Co-first authorship

Chapter 1: **Heesoo Kim**, Chang-Rae Lee, Sang-kyu Lee, Seung-Yoon Oh and Won Kim. 2020. Biodiversity and community structure of mesozooplankton in the Marine and Coastal National Park areas of Korea, *MDPI diversity*, Published. (Impact Factor 2.047).

Chapter 2: **Heesoo Kim**, Sang-kyu Lee, Jin-hyup Jung, Seung-Yoon Oh and Won Kim. 2020. Influence of evolutionary history and feeding behavior on the intestinal microbiome in crabs living on the intertidal zone, in preparation.

Chapter 3: Cheol-ho Hyun*, **Heesoo Kim***, Seongho Ryu, and Won Kim. 2019. Preliminary study on microeukaryotic community analysis using NGS technology to determine postmortem submersion interval (PMSI) in the drowned pig. *Journal of Microbiology*, Published. (Impact Factor 2.319).